



Return period of low water periods in the river Rhine

**Saskia van Brenk
University of Twente**

**Master Thesis
November 2021**

Cover picture: imrose on Pinterest via <https://pin.it/6jrLggc>

Return period of low water periods in the river Rhine

Master Thesis

November, 2021

Author:

S.H. (Saskia) van Brenk

s.h.vanbrenk@alumnus.utwente.nl

Supervised by:

prof. dr. S.J.M.H. (Suzanne) Hulscher

dr. J.J. (Jord) Warmink

ir. L.R. (Lieke) Lokin

University of Twente,

Faculty of Engineering Technology,

Department of Civil Engineering,

Water Engineering & Management

Preface

Before you lies the final report to conclude my Master in Civil Engineering and Management at the University of Twente. I have enjoyed my (little over) six years in Enschede a lot. Although the last months might not have been my best here in Enschede due to the coronavirus, working on this report grew on me bit by bit. I would like to give my thanks to the people that helped and guided me during my study period and my thesis.

First of all, I would like to thank my supervisors from the University of Twente. I would like to thank Lieke for always being available to talk. The meetings we had were both helpful and pleasant. Furthermore, I would like to thank Jord, who pushed me to put the study into context, but also reminded me to not always go for the toughest route. Sometimes a step back helps you to find a way to overcome hurdles. Lastly, I would like to thank Suzanne for the time she invested in this study. Her sharp remarks made this a better report. Thank you all for the nice atmosphere during the (online) meetings!

This study would not have been possible without the provided data from the GRADE model. Therefore, I would like to thank Rita Lammersen from Rijkswaterstaat for allowing me to use the data and for her time and the meetings that we have had. Additionally, I would like to thank Mark Hegnauer from Deltares for providing me with the data and helping me to get started with it.

Furthermore, I want to thank Chris Geerse and Ruud Hurkmans from HKV Lijn in water. Chris helped me to get started in the tricky world of statistics. Ruud has helped me bridge the gap between the theoretical statistics and practical interpretation of droughts.

Lastly, I would like to thank my friends and family. Thank you to everyone who made the stay in Enschede wonderful. Connecting with you in real life and online has been important to me before my thesis, during my thesis, and hopefully after my thesis. And thank you to my family for all of their support and the faith they had in me.

I hope you will enjoy reading this thesis report.

Saskia van Brenk,

Enschede, November 2021

Samenvatting

Het jaar 2018 staat in de top 5 van droogste jaren sinds het begin van gereguleerde metingen in Nederland [Sprökkereef, 2019]. Het neerslagtekort van augustus 2018 was zelfs een paar dagen hoger dan in recordjaar 1976, volgens de Droogtemonitor [KNMI, 2021a]. Daarnaast is de gemeten waterstand in de Rijn bij Lobith nog nooit zo laag geweest als in 2018 [Sprökkereef, 2019]. Hoe extreem deze gebeurtenis was, is echter niet bekend. Laagwater herhalingstijden zijn belangrijk voor toepassingen in de scheepsvaart, risico-analyses voor waterbeschikbaarheid of het voorkomen van verzilting. Laagwater herhalingstijden hebben drie belangrijke aspecten: de afvoer, de duur en de onderlinge afhankelijkheid tussen laagwaters. Er is echter geen geschikte methode gevonden in de literatuur die met deze drie aspecten rekening houdt. Het doel van deze studie is om de herhalingstijden van het laagwater in 2018 te kwantificeren en om de effecten van klimaatverandering op de herhalingstijden van laagwater in de Rijn bij Lobith te bepalen.

De eerste stap in deze studie was het vinden van een geschikte methode om laagwater herhalings-tijden te bepalen. De blokmethode (in het Engels: block method) en de piek-onder-drempelwaarde methode (in het Engels: peak-under-threshold) zijn gebruikt om laagwater frequentie curves te maken, gebaseerd op de afvoeren, die gemeten zijn bij Lobith van 1901 tot en met 2020 [Rijkswaterstaat, 2021]. Deze methodes verschillen in hoe ze een gebeurtenis definiëren en er wordt een andere verdeling gefit. De blokmethode houdt met minder gebeurtenissen rekening dan de drempelwaarde methode, waardoor de drempelwaarde methode de voorkeur krijgt.

Echter, de blokmethode resulteerde in een betere fit voor de data, dan de drempelwaarde methode. Daarom is ervoor gekozen om de blokmethode verder te gebruiken in deze studie. Het grootste verschil tussen de twee methodes zit hem in de lagere herhalingstijden en hogere afvoeren. Hier geeft de drempelwaarde methode lagere afvoeren dan de blokmethode.

Vervolgens worden de laagwater frequentie curves op basis van de gemeten afvoeren vergeleken met de laagwater frequentie curves op basis van de GRADE Referentie data. GRADE is een model dat 50 000 jaar aan dagelijkse afvoeren bij Lobith kan simuleren, wat interessant is voor extreme waarde statistiek. De geschatte fit op basis van de GRADE Referentie data geeft constant lagere afvoeren in vergelijking tot de gemeten waardes. Het grootste verschil tussen de twee fits zit hem in de hogere afvoeren, die vaker voorkomen.

Het GRADE model wordt ook gebruikt om afvoeren op basis van de KNMI'14 scenario's te bepalen. Alle 8 klimaatscenario's geven hogere afvoeren in vergelijking tot het GRADE Referentie scenario, wat onverwacht is. De *WH* scenario's hebben de laagste afvoeren van de klimaatscenario's en de *GL* scenario's hebben de hoogste afvoeren.

Het laagwater van 2018 is gekwantificeerd en een prognose is gemaakt voor vergelijkbare gebeurtenissen in de toekomst. Een 1-daagse afvoer van $732 \text{ m}^3/\text{s}$, wat het minimum van 2018 was, komt gemiddeld eens per 17.6 jaar voor. Door klimaatverandering zal dit eens per 6.5 tot 22.6 jaar voorkomen in 2085, gebaseerd op de KNMI'14 scenario's en het GRADE model. In 2085 zal een 1-daagse gebeurtenis met een herhalingstijd van 17.6 jaar een afvoer hebben tussen de 655 en $753 \text{ m}^3/\text{s}$. Dit laat zien dat een gebeurtenis vergelijkbaar met 2018 vaker of minder vaak zal voorkomen, afhankelijk van welk klimaatscenario realistischer blijkt te zijn.

Een 30-daagse afvoer van $789 \text{ m}^3/\text{s}$, het jaarminimum van 2018, komt gemiddeld eens per 21.8 jaar voor. Dit zal een keer in de 8.7 tot 34.8 jaar voorkomen in 2085 door klimaatverandering, gebaseerd op de KNMI'14 scenario's en het GRADE model. In 2085 zal een 30-daagse gebeurtenis met een herhalingstijd van 21.8 jaar een afvoer hebben tussen de 708 en $832 \text{ m}^3/\text{s}$. Dit laat zien dat een gebeurtenis vergelijkbaar met 2018 vaker of minder vaak zal voorkomen, afhankelijk van welk klimaatscenario realistischer blijkt te zijn.

De 180-daagse afvoer van 2018 was $1017 \text{ m}^3/\text{s}$ en heeft een nog hogere herhalingstijd, namelijk 29.5 jaar. Dit laat zien dat de droogte van 2018 heftig was door de lange duur van de gebeurtenis.

Summary

The year 2018 is in the top 5 of driest years since the beginning of regulated recordings in the Netherlands [Sprokkereef, 2019, KNMI, 2021b]. The precipitation deficit of August 2018 even passed record year 1976 for a few days according to the Droogtemonitor [KNMI, 2021a]. Furthermore, the water level measured in the Rhine at Lobith has never been as low as in 2018 [Sprokkereef, 2019]. However, how extreme this event was is currently unknown. Low flow return periods are important for shipping applications, risk assessments concerning water availability or preventing salinisation. Low flow return periods depend on three important aspects: discharge, duration and interdependency between low flows. However, no suitable method was found to accurately take these aspects into account. The goal of this study was to quantify the return period for the 2018 low flows and determine the effect of climate change on low flow return periods in the Rhine at Lobith.

The first step in this study was to find a suitable method to determine low flow return periods. The block method and peak-under threshold method were used to determine low flow frequency curves, based on discharges, measured at Lobith from 1901 to 2020 [Rijkswaterstaat, 2021]. The methods differ in how they determine events and they fit a different distribution. The block method takes less events into account than the peak-under threshold method, which makes the peak-under threshold method more favourable.

However, the block method resulted in a better fit compared to the peak-under threshold method. Therefore, the block method was used in the remainder of this study. The biggest differences between the two methods are found for the smaller return periods and higher discharges, where the peak-under threshold method gives lower discharges than the block method.

Next, the low flow frequency curves based on the measured data were compared to low flow frequency curves based on the GRADE Reference data. GRADE is a model that can simulate 50,000 years of daily discharges at Lobith, which is interesting for extreme value statistics. The estimated fit shows constantly lower discharges compared to the measured data. The largest difference between the two estimated fits is found in the higher discharges, which occur more often.

The GRADE model is also used to determine discharges for the KNMI'14 scenarios. All 8 climate scenarios show higher discharges compared to the GRADE Reference scenario, which is unexpected. The *WH* scenarios have the lowest discharges of the climate scenarios and the *GL* scenarios have the highest discharges.

Finally, the low flows of 2018 were quantified and a projection was made of similar events in the future. A 1 day discharge of $732 \text{ m}^3/\text{s}$, which was the minimum of 2018, is likely to occur once every 17.6 years. Due to climate change this can occur once every 6.5 to 22.6 years in 2085 based on the KNMI'14 scenarios and the GRADE model. In 2085, a 1 day event that will occur once every 17.6 years will have a discharge between 655 and $753 \text{ m}^3/\text{s}$. This shows that, depending on which climate scenario evolves to be more realistic, an event like 2018 is likely to become more or less common.

A 30 day discharge of $789 \text{ m}^3/\text{s}$, which was the minimum of 2018, is likely to occur once every 21.8 years. Due to climate change this can occur once every 8.7 to 34.8 years in 2085 based on the KNMI'14 scenarios and the GRADE model. In 2085, a 30 days event that will occur once every 21.8 years will have a discharge between 708 and $832 \text{ m}^3/\text{s}$. This again shows that, depending on which climate scenario evolves to be more realistic, an event like 2018 is likely to become more or less common.

The 180 day discharge of 2018, which was $1017 \text{ m}^3/\text{s}$, has an even larger return period of 29.5 years. This shows that the drought of 2018 was severe due to the length of the event.

Contents

Preface	i
Samenvatting	iii
Summary	v
List of Abbreviations	ix
List of Figures	xii
List of Tables	xiii
1 Introduction	1
1.1 Theoretical background	2
1.1.1 Low and high flows	2
1.1.2 Statistics	3
1.1.3 Climate change	5
1.1.4 Recent studies	6
1.2 Knowledge gap	7
1.3 Research goal and research questions	7
1.4 Thesis outline	7
2 Methodology	9
2.1 Data	9
2.1.1 Waterinfo	9
2.1.2 GRADE	10
2.2 Influence of event selection methods (RQ 1)	11
2.2.1 Block method (RQ 1.1)	11
2.2.2 Peak-under-threshold (RQ 1.2)	13
2.2.3 Comparison	15
2.3 Influence of GRADE (RQ 2)	16
2.3.1 LFFC for the GRADE reference scenario (RQ 2.1)	16
2.3.2 Comparison	16
2.4 Influence of climate change (RQ 3)	17
2.4.1 LFFC for the GRADE climate scenarios	17
2.4.2 Comparison	17
3 Results	19
3.1 Influence of event selection method (RQ 1)	19
3.1.1 Block method (RQ1.1)	19
3.1.2 Peak-under-threshold (RQ1.2)	25
3.1.3 Comparison	31
3.2 Influence of GRADE (RQ 2)	33
3.2.1 LFFC for the GRADE Reference scenario (RQ 2.1)	33
3.2.2 Comparison	35
3.3 Influence of climate change (RQ 3)	38
3.3.1 LFFC for the GRADE climate scenarios	38
3.3.2 Comparison	43
4 Discussion	49
4.1 Influence of event selection method (RQ 1)	49
4.2 Influence of GRADE (RQ 2)	51
4.3 Influence of climate change (RQ 3)	52

5 Conclusion & Recommendations	53
5.1 Influence of event selection method (RQ 1)	54
5.2 Influence of GRADE (RQ 2)	54
5.3 Influence of climate change (RQ 3)	54
5.4 Recommendations	55
Bibliography	56
Appendices	59
A National Water Model	61
B Extremes are becoming more extreme	62
C Waterinfo BM - annual minima	63
D Waterinfo BM - histograms	65
E Waterinfo BM - parameter values	67
F Waterinfo BM - extrapolated fit	68
G Waterinfo PUT - annual minima	70
H Waterinfo PUT - parameter values	72
I Waterinfo PUT - observations and fit for all durations	75
J Fitted parameter values for all scenarios	76
K Top 5's of the lowest flows for all scenarios	77

List of abbreviations

BM	Block method
GEV	Generalised Extreme Value
GP	Generalised Pareto
GRADE	Generator of Rainfall and Discharge Extremes
KNMI'14	Climate scenarios made by the 'Koninklijk Nederlands Meteorologisch Instituut' in 2014
KWA	'Climate resilient water supply' (in Dutch: Klimaatbestendige Wateraanvoer)
LFFC	Low flow frequency curve
LHM	'National Hydrological Model' (in Dutch: Landelijk Hydrologisch Model)
LSM Light	'National SOBEK Model Light' (in Dutch: Landelijk SOBEK Model Light)
LTM	'National Temperature Model' (in Dutch: Landelijk Temperatuur Model)
NHI	'Netherlands Hydrological modelling Instrument' (in Dutch: Nederlands Hydrologisch Instrumentarium)
NM7Q	Long term mean annual lowest seven day flow
NS	Nash Sutcliffe
NWM	'National Water Model' (in Dutch: Nationaal Water Model)
OLA	'Agreed low river discharge (in Dutch: overeengekomen lage rivierafvoer)
PUT	Peak-under-threshold
RQ	Research question
Q-Q plot	Quantile-quantile plot
SOBEK NDB	'SOBEK-model Northern Delta Basin' (in Dutch: SOBEK-model Noordelijk Delta Bekken)
QDF curve	Discharge duration-frequency curves

List of Figures

2.1	Daily discharge data at Lobith for 1901-2020 based on Rijkswaterstaat [2021] and fitted trend.	10
2.2	Flowchart with connections between different research questions.	17
3.1	Timing of selected annual 1-day minima for a calendar, hydrological and shifted hydrological year.	20
3.2	Annual minimum average discharge for different durations using block method.	21
3.3	Observed annual minimum discharges for different durations and their estimated fit using the block method.	23
3.4	Extrapolation of minimum annual discharges for different durations with 95% confidence intervals using the block method. Separated figures for the durations are shown in Appendix F.	23
3.5	Return period based on discharge and duration, interpolated from the LFFCs in Figure 3.3 and 3.4.	24
3.6	Annual minimum average discharge for different durations using PUT method for $u = 1500 \text{ m}^3/\text{s}$ and $r = 0$	25
3.7	Number of independent events for different thresholds for each duration using no lag ($r = 0$).	26
3.8	Histogram and fitted probability density function of minimum annual discharges for different durations.	27
3.9	Observed minimum discharges below a threshold for a 1 and 7 day duration and their estimated fit using the PUT method.	29
3.10	Extrapolation of minimum discharges below a threshold for a 1 and 7 day duration using the PUT method and the 1-day confidence interval.	29
3.11	Fitted distributions using the block method (BM) and PUT method for all durations.	30
3.12	Q-Q plots for selected quantiles, shown in Table 2.4, comparing low flows based on the block method (BM) and PUT method for the 1 and 7 day duration.	31
3.13	Boxplots of selected minima for the GRADE Reference data for different durations.	33
3.14	Selected annual minimum discharges for different durations and their estimated fit using GRADE Reference data.	34
3.15	Fitted distributions using the Waterinfo data and GRADE Reference data for all durations.	35
3.16	QQ plot of GRADE Reference fit compared to the Waterinfo fit.	37
3.17	Boxplots of selected annual minima for the different GRADE climate scenarios for different durations.	39
3.18	Extrapolation of minimum annual discharges for different climate scenarios for 2050 per duration.	41
3.19	Extrapolation of minimum annual discharges for different climate scenarios for 2085 per duration.	42
3.20	Extrapolation of minimum annual discharges for different durations and climate scenarios 2050 GL and 2050 WH.	45
3.21	Extrapolation of minimum annual discharges for different durations and climate scenarios 2085 GL and 2085 WH.	45
3.22	Extrapolation of minimum annual discharges for different most varying climate scenarios WH and GL for 2050 and 2085 per duration.	46
3.23	QQ plot of 2050 GL and 2085 GL fit compared to GRADE Reference fit.	47
3.24	QQ plot of 2050 WH and 2085 WH fit compared to GRADE Reference fit.	48

LIST OF FIGURES

4.1	Autocorrelation of selected annual minima for a duration of 1 and 180 days.	50
4.2	Expected average monthly discharges (m^3/s) at Lobith based on GRADE [Klijn et al., 2015]. (In Dutch 'referentie' means reference and 'afvoer' means discharge)	51
5.1	Return periods of 2018-like events for different durations and climate scenarios.	53
B.1	Extreme discharges are becoming more extreme.	62
C.1	Annual minimum average discharge for different durations using block method.	64
D.1	Histogram and fitted probability density function of minimum annual discharges for different durations.	66
E.1	Estimations of GEV parameters for all 5 durations and their corresponding 95% confidence interval.	67
F.1	Extrapolation of minimum annual discharges for different durations with corresponding observations and 95% confidence intervals.	69
G.1	Annual minimum average discharge for different durations using PUT method for $u = 1500 m^3/s$ for different r . The black circles are mentioned in the text and function as examples.	71
H.1	Estimated value of GP parameters for a duration of 1 day.	72
H.2	Estimated value of GP parameters for a duration of 7 days.	73
H.3	Estimated value of GP parameters for a duration of 30 days.	73
H.4	Estimated value of GP parameters for a duration of 90 days.	74
H.5	Estimated value of GP parameters for a duration of 180 days.	74
I.1	Observed minimum discharges below a threshold for different durations and their estimated fit using the PUT method.	75

List of Tables

2.1	Mean, minimum, maximum and interval of the original datasets excluding climate change.	9
2.2	Mean, minimum and maximum of the original 50,000 yrs GRADE data set including climate change.	11
2.3	Conditions for the three types of the GEV distribution [Coles, 2001].	12
2.4	Quantiles considered in the Q-Q plot.	16
3.1	Top 5 lowest discharges (m^3/s) using the block method.	22
3.2	Considerations concerning threshold value. The values show the range of threshold values (m^3/s) which perform well on one of the 4 criteria.	28
3.3	Values of return periods (in years) for a discharge of 1000 and 1200 m^3/s for the block method and PUT method.	32
3.4	Top 5 lowest discharges (m^3/s) using the GRADE Reference data. Note that the numbers 1^* until 6^* represent different years, as the years from the simulation are not important. The top 5's from other scenarios can be found in Appendix K.	34
3.5	Values of return periods (in years) for a discharge of 1000 and 1200 m^3/s for the Waterinfo and GRADE Reference data sets.	36
3.6	Top 5 lowest discharges (m^3/s) using the GRADE 2050GL, 2050WH, 2085GL and 2085WH data. Note that the numbers 7^* until 17^* represent different years, as the years from the simulation are not relevant. All years are different from the Reference top 5 in Table 3.4. The top 5's from other scenarios can be found in Appendix K.	40
3.7	Values of return periods (in years) for a discharge of 1000 and 1200 m^3/s for the GRADE Reference and most diverse GRADE climate scenarios data sets.	40
A.1	Mean, minimum and maximum of the original 100 yrs NWM dataset including climate change.	61
J.1	Values of fitted parameters for the Waterinfo data, both block method and PUT method, and the GRADE data, only block method, consisting of the reference data and the climate scenarios for 2050 and 2085.	76
K.1	Top 5 lowest discharges (m^3/s) using the GRADE 2050GL, 2050WH, 2085GL and 2085WH data. Note that the numbers 1^* until 17^* represent different years, as the years from the simulation are not relevant.	78

1

Introduction

The year 2018 is in the top 5 of driest years since the beginning of regulated recordings (1901) [Sprokkereef, 2019, KNMI, 2021b]. The precipitation deficit of August 2018 even passed record year 1976 for a few days according to the Droogtemonitor [KNMI, 2021a]. Furthermore, the water level measured in the Rhine at Lobith has never been as low as in 2018 [Sprokkereef, 2019].

This happened due to a long dry period in 2018 in the Netherlands and most of western Europe. A lack of precipitation and high temperatures resulted in a large precipitation deficit, low groundwater levels and low water levels in lakes and rivers [Kramer et al., 2019]. In 2018 the Rhine catchment had above average temperatures and below average rainfall [Sprokkereef, 2019]. From their observations it becomes clear that temperatures were very extreme as 2018 was the hottest year in the Netherlands, Germany and Austria, and in the top 5 of hottest years for Switzerland, since the beginning of recorded measurements. Precipitation measurements showed a particularly dry year as well. About 80% of the long year average precipitation in all four countries had fallen.

Furthermore, glacier melt, water levels and groundwater levels are mentioned in their evaluation of the year 2018 for the Rhine catchment [Sprokkereef, 2019]. The glacier melt in the summer of 2018 was exceptionally high. Snow started melting rapidly in April. The fact that an enormous amount of snow had fallen in the winter before (2017/2018), prevented a record loss of glacier ice. The high water levels in January 2018 even resulted in a code yellow warning in the Netherlands. Groundwater levels in Austria were above average at the beginning of 2018, but almost continuously fell until November, resulting in new minimum groundwater levels at more than 25% of the measuring stations. Similar observations were done in Switzerland, although the minimum records were observed occasionally. Details on groundwater levels in Germany and the Netherlands were not stated in the document. Even though there was an excess of water at the start of 2018, the summer of 2018 was exceptionally dry.

The economic impact of the drought in the Netherlands in 2018 has been assessed by van de Velde et al. [2019]. Total economic effects are estimated at 900 to 1650 million euros. Agriculture is the sector with the biggest losses: 820 to 1400 million euro. This was due to lack of precipitation and increase of evaporation and a shortage of sufficient ground- and surface water with good quality. After agriculture, shipping is the sector with the biggest economical effects: 65 to 220 million euro. The low water levels have a large influence on shipping, because then ships cannot be loaded to full capacity. This results in the capacity of the transport chain being under pressure.

Knowledge of the magnitude and frequency of low flows for streams is important for water-supply planning and design, waste-load allocation, reservoir storage design, and maintenance of quantity and quality of water for irrigation, recreation, and wildlife conservation [Smakhtin, 2001]. Effects on agriculture, shipping, nature and drinking water in 2018 in the Netherlands are mentioned [Beleidstafel Droogte, 2019]. Other problems that occur due to low flows or drought in the Netherlands are salt intrusion [Kramer et al., 2019, Zethof, 2011] and failure of peat dikes [van Beek, 2018].

A deep understanding of the magnitude and driving forces of trends in droughts, due to for example climate change, is important [de Niel, 2018]. The main goal of the Beleidstafel Droogte [2019] is to evaluate the issues due to the 2018 drought on a high governmental level, draw conclusions and give

recommendations, to prepare the Netherlands better for coming drought periods.

Climate change is an important factor when looking into droughts, as extremes will become more extreme [de Niel, 2018]. Following the KNMI'14 scenarios, the most recent climate scenarios for the Netherlands, it is expected that the Netherlands will experience more droughts [KNMI, 2015]. However, the scenarios are not unanimous on the increase in droughts. In two of the four scenarios the droughts will increase in number and severity. In the other two, droughts will remain similar to the current situation.

1.1 Theoretical background

Theoretical background to assist this study is given on the topics of high and low flows, statistics for determining return periods of river flows and climate change concerning the Rhine catchment. Finally, recent studies on the topic of return periods for low flows will be addressed.

1.1.1 Low and high flows

Water management in the Netherlands has focused on flood protection for a long time. Currently, a different point of view is becoming more and more relevant. Water management is not only about high flows anymore, but low flows are becoming a problem as well. Recently, this became most visible in 2018.

Droughts and low flows are not the same phenomenon [Smakhtin, 2001]. Low flows are a seasonal phenomenon and occur in the flow regime of any river. However, a drought is a natural event that results from less than normal precipitation for an extended period of time. There is no absolute river discharge that determines a drought or low flow and it depends on the application [Smakhtin, 2001]. Several options are $1020 \text{ m}^3/\text{s}$ [Beleidstafel Droogte, 2019], $1000 \text{ m}^3/\text{s}$, which is when problems occur with chlorine concentrations at drinkwater intake locations and navigation for shipping [Sperna Weiland et al., 2015] and $1200 \text{ m}^3/\text{s}$, below which problematic salt intrusion can occur [Janse and Burgdorffer, 2005]. Salt intrusion threatens the water quality of the water that is used as drinking water or for agriculture [Zethof, 2011]. In comparison, the mean discharge of the Rhine at Lobith is about $2200 \text{ m}^3/\text{s}$ [Helpdesk Water, 2007] and a high discharge is $5260 \text{ m}^3/\text{s}$, which is a code yellow and corresponds with a water level of $13.00 \text{ m} + \text{NAP}$ [Helpdesk Water, 2021a]. A code yellow is exceeded a few times per year. A code yellow means at some locations an increased water level is expected and standard measures are taken by water authorities.

Low flows at Lobith most often occur in autumn. de Wit [2004], who analysed the drought of 2003, saw lowest discharges in November. Similar results are shown for 2018, with lowest discharges in October and November [Kramer et al., 2019]. High discharges occur in the winter, mainly January and February [Disse and Engel, 2001, Kramer et al., 2019].

The durations of low flows is longer than the duration of high flows. Low flows have durations from several days up to several months. de Wit [2004] concluded that the discharge of the Rhine was below $1000 \text{ m}^3/\text{s}$ for about 60 days in 2003. The largest amount of days where the discharge was below this threshold occurred in 1921, where this was the case for more than 200 days. In contrast, high flows have durations from several hours up to several days [Disse and Engel, 2001, Trul, 2016].

Groundwater plays a large role in low flows. The drought of 2003 was not that extreme, mainly due to the fact that 2002 was a wet year, which meant groundwater reservoirs were relatively full and could provide a steady outflow [de Wit, 2004]. In more extreme years (1921 and 1976), the low discharges followed relatively dry winters, resulting in lower discharges compared to 2003. This shows the importance of groundwater for low flows.

In addition, Smakhtin [2001] states that in many cases, the majority of natural gains to streamflow during low flow periods come from releases from groundwater storage. This occurs when the stream

channel intersects the phreatic surface in a draining aquifer. Other locations where water can come from are soil and alluvial storages, which are not as deep as groundwater, but they are locations where water is concentrated after precipitation events. In short, low flow generating mechanisms are significantly affected by catchment geology.

In addition, [Arnoux et al. \[2021\]](#) studied low flows in the Alps in Switzerland. They concluded that catchments with high groundwater contribution to streamflow relative to precipitation will have a slower decrease in future summer discharge.

Another factor in the low flows in the Rhine catchment are the Alps, as [de Wit \[2004\]](#) concluded that 60% of the low discharge at Lobith in 2003 was generated in the Alps. In addition, lakes can maintain low flows, when there is a direct hydraulic connection between the two. In the case of the Rhine, an example of such a lake is the Lake Constance (Bodensee) in Switzerland. Another gain to low flows is melting snow and ice. The principal influence of glaciers in the context of low flows is similar to that of lakes and includes a decrease in runoff variation and, consequently, more sustained low flow, also referred to as a dampening effect [[Smakhtin, 2001](#)].

Summarising, high and low flows differ in the value of discharge, the timing of occurrence, duration and interdependency of flows due to groundwater.

1.1.2 Statistics

Maxima have been attracting more attention than minima in extreme value theory and a similar trend is seen in hydrology, where the analyses of floods have been performed more often than analyses of low flows [[Gottschalk et al., 2013](#)]. Low flow statistics are less common, but are becoming more relevant due to the changing climate. There are two important differences between high and low flow statistics. For high flow events it is easier to assume their independence, than for low flows. In addition, for low flow statistics not only the minimum discharge is important, but also the duration of the low flow is important.

High flow return periods

[Booij \[2015\]](#) describes how to estimate normative high discharges in three steps. Step 1 determines the return period of a high discharge. Step 2 focuses on making a fit of the peak discharges based on extreme value statistics (e.g. Gumbel, Fréchet, Weibull) and step 3 uses this fit to extrapolate to very small exceedance probabilities or very high return periods.

Step 1 is to make a selection of the annual peak discharges or peaks above a certain threshold (peak-over-threshold) with corresponding exceedance frequencies. When selecting peak discharges, it is important that the selected peaks are independent of each other. This is why a hydrological year is used (1 October - 30 September) for the selection of annual maxima [[Booij, 2015](#)]. It is assumed that peaks selected in different hydrological years are independent. Another important aspect is the homogeneity of the observations. This can be affected by differences in measuring methods, changes in the geometry of the main river or tributaries, changes in the response of subbasins (e.g. urbanisation) and changes in precipitation patterns due to climate change.

To determine the corresponding exceedance probability the selected discharges are sorted from high to low and then ranked. The highest discharge gets ranked 1st, the second highest 2nd, etc... Next, an equation is used to determine the exceedance probability, often Weibull (Equation 1.1) or Gringorten (Equation 1.2). Weibull is recommended for hydrologic applications and Gringorten is used for Gumbel distributions [[Hobson, 2015](#)].

$$P(X \geq x) = \frac{r}{N + 1} \tag{1.1}$$

$$P(X \geq x) = \frac{r - 0.44}{N + 0.12} \quad (1.2)$$

In which $P(X \geq x)$ is the exceedance probability, r is the rank number and N is the total amount of selected observations.

The exceedance probability and return period are not exactly the same. The exceedance probability ($P(X \geq x)$) is the probability the discharge (X) exceeds a threshold discharge (x), so $1/n$ times per year. The return period is interpreted as the mean time between two independent exceedances of a certain discharge, i.e. once every n years. And 'n' is in both cases the same number for the same situation. This means the return period can be determined using the exceedance probability following Equation 1.3 [Shaw et al., 2011]. In which T is the return period.

$$T = 1/P(X \geq x) \quad (1.3)$$

Step 2 is to fit the peak discharges to an extreme value distribution of probability. The Gumbel distribution will be taken as example. The non-exceedance probability ($F(x \leq X)$) is given in Equation 1.4 [Booij, 2015, Shaw et al., 2011, Maidment, 1996], in which x is the peak discharge, α and β are parameters from the Gumbel distribution, μ is the mean, γ is 0.5772 and σ is the standard deviation.

$$F(X \leq x) = 1 - P(X \geq x) = \exp\left(-\exp\left(-\frac{x - \alpha}{\beta}\right)\right) \quad (1.4)$$

$$\text{with } \alpha = \mu - \gamma\beta \quad \text{and} \quad \beta = \frac{\sigma\sqrt{6}}{\pi}$$

Step 3 allows for the extrapolation of discharges from larger return periods based on the fitted non-exceedance function. This is of importance for risk analyses and policies.

Low flow return periods

Section 1.1.1 concludes that high and low flows differ in value of discharge, timing of occurrence, duration and interdependency of low flows due to groundwater.

A Low Flow Frequency Curve (LFFC) shows the proportion of years when a flow is exceeded (either return period or recurrence interval) that a river falls below a given discharge [Smakhtin, 2001]. Normally the LFFC is based on annual minima, which is known as the block method. This can be a minimum of 1, 3, 7 or more days up to several months. In the USA the 7-day 10-year low flow and 7-day 2-year low flow are widely used indices, which are the lowest average flows that occur for a consecutive 7-day period at the recurrence intervals of 10 and 2 years, respectively [Smakhtin, 2001]. The observed flow records are often not long enough for reliable frequency quantification of extremely low flow events. Therefore, the data are used to fit a theoretical distribution to be able to extrapolate beyond observed probabilities. This step is similar to step 2 and 3 for high flows, described previously. Most used distributions for fitting low flows are different forms of Weibull, Gumbel, Pearson Type III and log-normal distributions [Smakhtin, 2001].

However, a LFFC does not provide information about the length of continuous periods below a certain threshold of interest [Smakhtin, 2001]. Not every year has to have extremely low flows. Instead of the block method the peak-over-threshold method can be used, or in the case of low flows peak-under-threshold (PUT). The choice of the threshold value depends on the objective of the study and/or the type of flow regime. A run, in low flow context, is the number of days, months or years, when the discharge remains below a certain threshold flow. The three main low flow characteristics normally considered in the theory of runs are the run duration, the severity, which is the cumulative

water deficit or the negative run sums, and the magnitude, which is the intensity and is defined by severity divided by duration [Smakhtin, 2001].

Mirghani et al. [2005] and Mondejar and Willems [2016] expand this method based on Willems [2004] to low flow duration-frequency curves (QDF curves). QDF curves represent a probabilistic picture of the low flow regime of a river in both flow and time dimensions; they describe the relationships between the flow (Q), the time scale (D) and the return period or probabilistic frequency (F). Probability distributions are fitted to minima for different aggregation periods in the range from 1 day to 2 years.

Constructing QDF curves takes three steps [Mirghani et al., 2005]. Step 1 is to select (nearly) independent low flow extremes from the full flow series. To determine independent flows, the time series is transformed taking the inverse and then the peak-over-threshold method was applied. The assumption is made that two successive exceedances are independent, when one high flow was in between the two low flows. The threshold is stated as recession constant for baseflow. This is described by Willems [2004]. Step 2 is to analyse the low flow distribution's tail with quantile plots (Q-Q plots). These two steps are repeated for several durations, which are the aggregation periods. Step 3 is to analyse the relationship between the extreme value distribution's parameters and the aggregation period. The QDF curves can then be plotted using a number of percentiles chosen, corresponding to different return periods. However, the QDF curves method is currently not fully openly accessible.

Coles [2001] describes a general method to deal with extremes of dependent sequences. In general, they state that extreme events are close to independent at times that are far enough apart. Many stationary series satisfy this property. More importantly, it is a property that is often plausible for physical processes. They specify their method for threshold models of stationary series. The most widely adopted method is declustering, which corresponds to filtering of dependent observations to obtain a set of threshold excesses that are approximately independent. This method will be explained in more detail in Section 2.2.2.

1.1.3 Climate change

In 2015 the KNMI presented four new scenarios for future climate change: the KNMI'14 climate scenarios. In 2023 new scenarios are expected. These four scenarios have a projection for the year 2050 and 2085, resulting in eight different scenarios. The KNMI'14 scenarios are based on fifth climate report by the IPCC. The scenarios are based on combinations between two processes: worldwide temperature rise ('Moderate' and 'Warm') and changes in air current patterns ('Low values' and 'High values'). The four scenarios are abbreviated as *GH* (Moderate - High), *GL* (Moderate - Low), *WH* (Warm - High) and *WL* (Warm - Low) [KNMI, 2015].

In the *G*-scenarios the worldwide temperature rise is 1°C in 2050 and 1.5°C in 2085, compared to 1981-2010. For the *W*-scenarios the worldwide temperature rise is 2°C in 2050 and 3.5°C in 2085.

In the *L*-scenarios the influence of change in air current patterns is small and for the *H*-scenarios the influence is large. In the *H*-scenarios wind in the winter comes more often from the west. This means a milder and wetter weather type. In summer the high pressure fronts will result in more wind coming from the east. This results in warmer and drier weather in the Netherlands.

In all four scenarios the mean precipitation shortage increases. This is highest for the *H*-scenarios, with the maximum occurring in the *WH* scenario in 2085 (+50%). It was not stated whether this is because droughts are more extreme or because droughts will occur for a longer period of time. It can also be the combination.

Concluding, more dry summers are expected in the *GH* and *WH* scenarios than in the current situation. For the *GL* and *WL* scenarios little change is seen.

The impact of these four climate scenarios on the river discharges of the Rhine and Meuse has been studied [Klijn et al., 2015]. A fifth climate scenario was added, WH_{dry} , which is based on the WH scenario, but adds extensive drought in the summer. They used the GRADE model for their study. They conclude that summers will be less dry than was first expected. Furthermore, they conclude that the discharge regime becomes more extreme: winter discharges increase, whilst summer discharges decrease. However, this effect is smaller for the Rhine than for the Meuse. This is due to the fact that the Rhine catchment is bigger than the Meuse catchment and includes lakes like Lake Constance, which have a damping function. Only the driest scenario, WH_{dry} , shows strong decreases in the low flows. This scenario results in a decrease in the discharge of the Rhine of 20 to 30% at the end of the summer, for 2050 and 2085 respectively. On the other hand, the GL scenario shows a small increase of the low flows of 10% in 2050 and 0% in 2085. The lowest discharges are expected to occur in September.

1.1.4 Recent studies

A recent study into the drought of 2018 in the Netherlands was done by Kramer et al. [2019]. They investigated how extreme the drought of 2018 was with respect to shipping, salinisation and the IJssellake buffer using the 'National Water Model', which is elaborated on in Appendix A. The shipping indicator they used was the number of days the discharge was below a value of $1100 \text{ m}^3/\text{s}$. This was the case for 132 days in 2018. This happened only once before since 1901: in 1949 this happened for about 150 days. This results in a return period of 60 years. The salinisation indicator is how often the climate-resilient water supply (in Dutch: Klimaatbestendige Wateraanvoer, KWA) is used and for what period. In 2018 the KWA was active for 63 days, which resulted in a return period of 60 years. The indicator for the IJssellake buffer is the water level in the IJssellake. This decreased by 8 cm in 2018. Only in 1976 the use of the IJssellake buffer was higher and in 1921 the use would have been higher, but the IJssellake did not exist yet at that time. This results in a return period of 35 years. Considering the KNMI'14 2050WH scenario the return periods would all decrease, thus occurring more often. The shipping problem will occur once every 20 years instead of 60 years, the salinisation problem will occur once every 15 years instead of 60 years and the IJssellake buffer will be used every 8 years instead of every 35 years. This study misses a broader framework to determine return periods for different durations and discharges or to extrapolate to return periods outside of the ± 100 years of data. Additionally, the method used to determine the return periods is unclear. It is expected that the return period is based on the number of occurrences in the available dataset and that no fit is made through the data.

Sprokkereef [2019] produced an annual report on the hydrology of the Rhine in 2018. Meteorological aspects as precipitation and temperature are elaborated on. Furthermore, they mention that water levels were never before measured as low at Lobith as in 2018. Shortcomings of this study are that it does not elaborate much on water levels and discharges or return periods. However, the report does give a good idea of the meteorological and hydrological state of the system in 2018.

Sperna Weiland et al. [2015] looked into the implications of the KNMI'14 climate scenarios for the discharge of the Rhine and Meuse. In this study they used the GRADE model. Among others, they give values for the long term mean annual seven day flow (NM7Q) for the current climate and for the KNMI'14 scenarios. For the current climate this is $1010 \text{ m}^3/\text{s}$ and for the climate scenarios the NM7Q value ranges from 735 to $1095 \text{ m}^3/\text{s}$. This study looks into monthly averages and the NM7Q value, however, it does not provide return periods for different discharges or durations. It does elaborately explain the influence the KNMI'14 scenarios have on the streamflow of the Rhine.

1.2 Knowledge gap

High flow return periods are widely known, however, low flow return periods are less familiar. These low flow return periods are, for example, needed for shipping applications.

In addition, three important factors for determining return periods of low flows are discharge (minima), duration and interdependency of low flows. A method to determine the return period of low flows that takes all three important factors of low flows into account was not found in literature.

Furthermore, return periods for low flows in general were not found for the Rhine near Lobith, only specific return periods for the 2018 situation are given by [Kramer et al. \[2019\]](#).

1.3 Research goal and research questions

The main goal of this research is to quantify the return period for the 2018 low flows and determine the effect of climate change on low flow return periods on the Rhine at Lobith. Intermediate goals are to determine the return period of low flows for the current climate and for the future including climate change. Another intermediate goal, which is needed to achieve the main goal, is to find a method to determine the return period, which takes into account three important factors for low flows: discharge (minima), duration and interdependency of low flows. The research goal results in the following research questions:

1. What is the influence of different low flow event selections on the return period for the low flows and their corresponding duration on the Rhine at Lobith in the current situation?
 - 1.1. What is the return period for the low flows and their corresponding duration on the Rhine at Lobith in the current situation assuming independent low flows?
 - 1.2. What is the return period for the low flows and their corresponding duration on the Rhine at Lobith in the current situation using an empirical rule to define clusters?
2. How do the results based on measured data and GRADE data compare?
 - 2.1. What is the return period for the low flows and their corresponding duration on the Rhine at Lobith in the current situation based on GRADE data?
3. What is the return period for the low flows and their corresponding duration on the Rhine at Lobith in the future situation including climate change?

1.4 Thesis outline

Chapter 2 will describe the methodology of this study. Results are given in Chapter 3. Chapter 4 consists of a discussion on this study. And finally, Chapter 5 gives the conclusions on the research questions and gives recommendations for future studies.

All Chapters will follow the order of the research questions. This means section 1 will concern research question 1, section 2 will concern research question 2 and section 3 will concern research question 3. The exception to this structure is Chapter 2, where the first section will elaborate on the used data.

Methodology

This chapter first mentions the data used in the study after which the methods for each of the three research questions will be elaborated on.

2.1 Data

Different data sets containing measured and modelled discharge data are used in this study, which will be elaborated on in the following sections.

2.1.1 Waterinfo

Observed discharges and water levels of the Rhine at Lobith are openly accessible on Waterinfo.nl [Rijkswaterstaat, 2021]. This study will focus on discharge data. The mean, minimum, maximum, period and interval of the discharge data are given in Table 2.1. The advantage of looking into discharge data, is the fact that subsidence has no influence on the discharge values, whereas it does influence the water levels. The subsidence near Lobith is estimated at about 1.5 cm/year and thus has a large influence when comparing the water level data from 1901 to 2020 [Ylla Arbós et al., 2021, van der Veen, 2010].

The disadvantage of the discharge data, is that uncertainty is introduced in the discharge data as the discharge is not measured directly. The water levels are measured and translated to a discharge by means of a Q-h-relation. This is a curve describing the relation between discharge (Q) and water depth (h). The latest update to the Q-h-relationship has been carried out in 2009 [Wijbenga et al., 2009].

Data	Mean (m^3/s)	Min (m^3/s)	Max (m^3/s)	Period	Interval
Waterinfo ¹	2211.5	575.0	12,280.0	1901-2020	Varying
GRADE Ref	2016.3	253.7	24,835.9	50,000 years	Daily

Table 2.1: Mean, minimum, maximum and interval of the original datasets excluding climate change.

The discharge data from Waterinfo have varying intervals. From 1901 to 1996 the discharge values are daily, from 1996 to 2013 the values are hourly and data from 2013 to 2020 have a 10-minute interval. All these data were used to determine daily averages. After this transformation 21 days remained without a value of which the biggest gap was 5 days. These gaps were filled using linear interpolation.

To represent the current situation (2020) the data was checked for a linear trend and then scaled to the year 2020. For the detrending Equation 2.1 was used, which was used by Kuijper et al. [2019]. In which: $Q_{DT}(j)$ is the detrended value for year j , $Q(j)$ is the not detrended discharge for year j , $Q_T(j)$ is the value according to the fit and $Q_T(2020)$ is the average for the year 2020 according to the fit.

¹Values based on data already altered to daily data; outliers ($1 * 10^{38}$) already removed; datagaps present

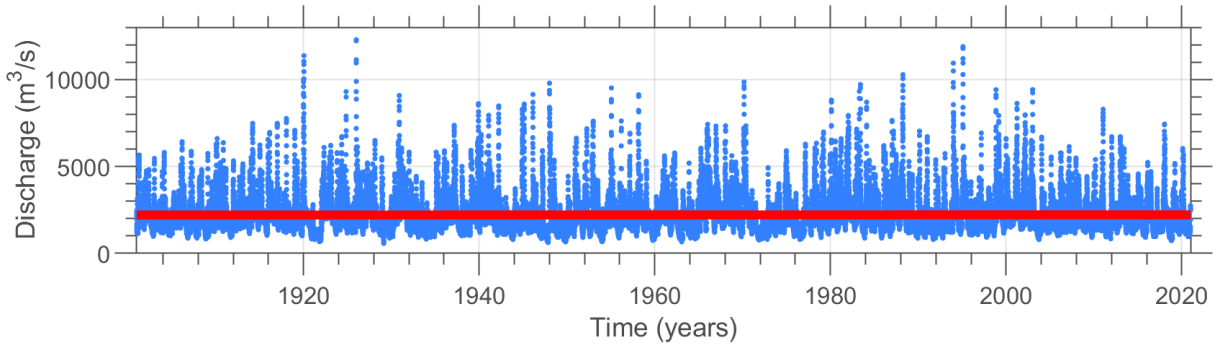


Figure 2.1: Daily discharge data at Lobith for 1901-2020 based on [Rijkswaterstaat \[2021\]](#) and fitted trend.

$$Q_{DT}(j) = Q(j) - (Q_T(j) - Q_T(2020)) \quad (2.1)$$

A small linear trend was fitted to the data using the least squares method, shown in Figure 2.1. On the left, in 1901, the value of the trend is $2205 \text{ m}^3/\text{s}$ and on the right, in 2020, the value of the trend is $2217 \text{ m}^3/\text{s}$. This is an increase of $12 \text{ m}^3/\text{s}$, which is very small. Because of the small trend, the trend is not removed from the Waterinfo data. Appendix B elaborates on trends in the annual maximum and minimum discharge values, which were also not removed from the data.

2.1.2 GRADE

The Generator of Rainfall and Discharge Extremes, or in short GRADE model, is created by Deltares, the KNMI and Rijkswaterstaat. The GRADE model is developed to provide an alternative, more physically based method for the estimation of the (extreme) design discharge [[Hegnauer et al., 2014](#)]. The advantage of this model is that long simulations can be run, a length of 50,000 years, to be able to derive frequency discharge curves. With these long time series no extrapolation is needed for the frequency discharge curves.

The GRADE model consists of three components: a stochastic weather generator to produce daily rainfall and temperature data, a HBV model, which calculates the runoff, and hydrologic and hydrodynamic routing, for which the main stretch from Maxau to Lobith is taken into account for the Rhine. The input parameters precipitation and temperature, generated by the weather generator, are based on historical observations of a period of 56 years. The output consists of estimated discharges at different locations along the Rhine or Meuse. The GRADE model can also simulate (extreme) discharges for different climate scenarios. These climate scenarios used in the GRADE model are the KNMI'14 climate scenarios. The mean, minimum and maximum values for the GRADE data set for different climate scenarios are given in Table 2.2. Note that for the maxima not all the water will reach Lobith when overland flow after dike breaches are included. For discharges higher than $16,000 \text{ m}^3/\text{s}$ at Andernach, upstream of Lobith, dike breaches are more likely to occur at the Lower Rhine, upstream of Lobith [[Bomers et al., 2019](#)]. The water will rejoin the rivers in the Netherlands downstream of Lobith.

Rijkswaterstaat and Deltares believe the National Water Model output, elaborated on in Appendix A, performs better at low flows than the GRADE model. However, the GRADE model can provide a very long discharge series, which has the advantage of not having to extrapolate the extreme discharges to get to large return periods.

GRADE	Mean (m^3/s)	Min (m^3/s)	Max (m^3/s)
Ref	2016.3	253.7	24,835.9
2050 GH	2307.0	333.7	24,835.9
2050 GL	2387.1	346.1	26,096.6
2050 WH	2326.5	340.6	24,202.7
2050 WL	2331.6	323.0	24,960.6
2085 GH	2276.9	331.6	23,923.7
2085 GL	2407.4	352.2	25,723.8
2085 WH	2464.4	353.6	27,698.4
2085 WL	2517.5	346.2	26,590.8

Table 2.2: Mean, minimum and maximum of the original 50,000 yrs GRADE data set including climate change.

2.2 Influence of event selection methods (RQ 1)

The goal of the first research question is to look into the influence of two different event selection methods. To do this, two sub questions are formulated. For both sub questions low flow frequency curves (LFFCs) are created based on the Waterinfo data. A comparison between the LFFCs based on shape and values shows the difference between the two event selection methods. The first method, the block method, assumes annually independent low flows. The second method, the peak-under-threshold method, identifies independent low flow events based on a threshold value.

Additionally, different choices are investigated concerning the methods to construct each LFFC. The choices concern what annual period to use for the block method and what threshold to use for the peak-under-threshold method.

2.2.1 Block method (RQ 1.1)

The block method assumes annually independent low flows. Elaboration is given on where the boundaries of the year are laid, on the multi-day minimum and on the fit of the distribution.

Annual period

Three logical options exist as boundaries for the year in this study: a calendar year, a hydrological year and a shifted hydrological year. The calendar year runs from January to December. The hydrological year runs from October to September. This is often used in high flow statistics, as this allows for the assumption of independent flows [Booij, 2015]. As the focus is on low flows in this study, it makes sense to shift the hydrological year by half a year to April-March. This way, the boundary of the year is away from the low flow period of the Rhine, which is October and November [de Wit, 2004, Kramer et al., 2019].

All three options are tested for the 1 day minimum discharges using the block method. The influence of the options on the results is looked into, after which a choice for one of the three options is made to continue in this study. The three different periods are tested for the fewest amount of selected 1 day minima close to each other. It is expected that the shifted hydrological year shows the best result, as this sets boundaries of the year away from the period in which the low flows occur. This way, it is harder to include one low flow period in two years and thus supports the assumption of independent low flow events.

Multi-day minimum

The duration of low flows is important for the impact it has on different river functions. This is why several durations are taken into account when determining the return periods. In several studies a range from 1 day to 1 or 2 years is used for the duration [Mondejar and Willems, 2016, Mirghani et al., 2005]. As the Rhine is a mixed river, consisting of meltwater and rainfall, the winter discharges are higher than summer discharges and are not really interesting when looking into low flows [Kramer et al., 2019, Lokin, 2020]. Therefore, in this study a range from 1 day to 180 days is used. This range includes 1 day, 1 week (7 days), 1 month (30 days), 3 months (90 days) and 6 months (180 days) minima.

To describe the multi-day minimum one value is needed. The average discharge for a duration is determined after which the minimum average is selected for each year. The average is found in literature to be used for this application [Mirghani et al., 2005]. Furthermore, the average can say something about the potential water deficit.

Fitting a distribution

Once the low flow events are selected, the plotting position can be determined. The plotting position is an estimation of the non-exceedance probability. Several plotting positions are mentioned in Maidment [1996] and Shaw et al. [2011], like the Weibull or Gringorten plotting positions. The Weibull plotting position, given in Equation 2.2, is chosen, as this gives unbiased exceedance probabilities for all distributions Maidment [1996]. In which: $P(X \leq x)$ is the non-exceedance probability, i is the i -th smallest observation, which is the opposite ranking compared to high flow statistics, and n is the sample size.

$$P(X \leq x) = \frac{i}{n + 1} \tag{2.2}$$

After the plotting positions are determined, a distribution can be fitted to the data. The Generalized Extreme Value distribution (GEV) is used to fit the data conform to the maximum likelihood method. The equation for the GEV fitting for maxima is shown in Equation 2.3, based on Coles [2001] and Beersma et al. [2019] (note that both use different symbols). In which: $G(z) \approx Pr(X \leq x)$ is the non-exceedance frequency, z is the discharge value, ξ is the shape parameter, μ is the location parameter and σ is the scale parameter.

$$G(z) = \exp\left(-\left(1 + \xi\left(\frac{z - \mu}{\sigma}\right)\right)^{\frac{-1}{\xi}}\right) \tag{2.3}$$

The GEV has three different types of distributions. Type I is the Gumbel distribution, Type II is the Fréchet distribution and type III is the Weibull distribution. Conditions for these three types of GEV distributions are given in Table 2.3. The Weibull distribution is described as a good fit and is used to fit low flows [Maidment, 1996, Smakhtin, 2001]. Gottschalk et al. [2013] even states that out of these three GEV distributions, only the Weibull is applicable for representing minimum streamflows as they are bounded towards the extreme minimum value.

Distribution	Shape parameter	Location parameter	Scale parameter	Variable z
Type I: Gumbel	$\xi = 0$	$\mu > 0$	$\sigma > 0$	$-\infty < z < \infty$
Type II: Fréchet	$\xi > 0$	$\mu > 0$	$\sigma > 0$	$z > \mu$
Type III: Weibull	$\xi < 0$	$\mu > 0$	$\sigma > 0$	$z < \mu$

Table 2.3: Conditions for the three types of the GEV distribution [Coles, 2001].

2.2.2 Peak-under-threshold (RQ 1.2)

The peak-under-threshold (PUT) method assumes independent low flow events below a threshold separated by a period above this threshold. The PUT is the counterpart of the better known peak-over-threshold. Peak-over-threshold is said to be the better option, compared to the block method, as this method gives the opportunity to select more extreme events, even when they occur in the same year [Coles, 2001]. Elaboration is given on the multi-day minimum, the threshold selection, the number of consecutive observations below the threshold and on the fit of the distribution.

Multi-day minimum

The multi-day minimum is determined in the same way as described for the block method, with a slight difference. The average discharge for a duration is determined within each independent event and then the minimum value is selected, in contrast to the block method, where the average is determined within a whole year. In general Coles [2001] states that extreme events are close to independent at times that are far enough apart. Many stationary series satisfy this property. More importantly, it is a property that is often plausible for physical processes. They specify their method for threshold models of stationary series. The most widely adopted method is declustering, which corresponds to filtering of the dependent observations to obtain a set of threshold excesses that are approximately independent. Declustering is a general method to deal with extremes of dependent sequences. Declustering for peak-over-threshold works by:

1. using an empirical rule to define clusters of exceedances
2. identifying the maximum excess within each cluster
3. assuming cluster maxima to be independent, with conditional excess distribution given by the generalised Pareto distribution
4. fitting the generalised Pareto distribution to the cluster maxima

The empirical rule described by Coles [2001] to define clusters of exceedances is based on two values, u (threshold) and r (the number of consecutive observations below the threshold). Once an observation falls below u the cluster is deemed terminated. This means a cluster is a consecutive group of observations above the threshold u . The next exceedance of u denotes a new cluster. However, this allows separate clusters to be separated by a single observation, in which case the argument for independence across the cluster maxima is debatable. Furthermore, the separation of extreme events into clusters is likely to be sensitive to a particular choice threshold. To overcome these deficiencies it is more common to consider a cluster to be active until r consecutive values fall below the threshold for some pre-specified value of r . The choice of r requires care too, just as the selection of u : too small a value will lead to the problem of independence being unrealistic for nearby clusters, too large a value will lead to a succession of clusters that could reasonably have been considered as independent, and therefore to a loss of valuable data. There are no general guidelines for these situations. In the absence of anything more formal, it is usual to rely on common-sense judgement, but also to check the sensitivity of results to the choice of r .

When a wanted duration is longer than the duration of the event, this event cannot contribute a value for the larger durations. For example, when an independent event is 15 days long, a minimum value for a duration of 1 day and 7 days can be determined, but no value is determined for a duration of 30 or more days.

Lastly, the method for peak-over-threshold is slightly adjusted to work as the peak-under-threshold method. Parallels to the peak-over-threshold and peak-under-threshold can be seen. Instead of the maxima above the threshold, the minima beneath a threshold are selected. The r value is thus the exceedances of the threshold, instead of the non-exceedance.

Threshold and number of consecutive observations below the threshold

Two choices are made in the method of declustering: the threshold value (u) and the number of consecutive observations above the threshold (r) or further called lag. A choice for threshold and lag value go hand in hand and cannot be seen completely independent of each other and is also not completely independent from the previous step 'Multi-day minimum' and the next step 'Fitting a distribution'. There are no general guidelines for the choice of the threshold or lag value, therefore a number of considerations are made:

1. A mean residual plot, as explained by Coles [2001] is made. A good choice of threshold is where some form of linearity can be seen or assumed.
2. The GP distribution is fit for all threshold values, ranging from $500 m^3/s$ to $8000 m^3/s$. The same holds as for the residual life plot, a good choice of threshold is where some form of linearity can be seen or assumed in the parameter values [Coles, 2001].
3. The percentage of data that is included in the independent events. This is set at about 25% as was done by Hurkmans et al. [2010]. This will include more data than the block method, but still keeps its extreme character.
4. Lastly, a sensitivity analysis is done for the number of independent events, for varying threshold and lag values. Threshold values ranged from $500 m^3/s$ to $8000 m^3/s$ and the lag ranged between no lag and 7 days of lag. Excesses over the threshold, which might be due to a short precipitation event, will then no longer split two or more events.

Based on the influence of the lag on the number of events in combination with the threshold values and the threshold values coming from the first three considerations a choice for both the lag and the threshold is made. This is done for all 5 durations (1, 7, 30, 90 and 180 days).

Fitting a distribution

The same plotting position is used as with the block method, which is the Weibull plotting position from Equation 2.2 [Coles, 2001]. The only difference is that this equation is multiplied by the average amount of events per year, to account for the multiple events per year. The distribution which is known to often describe data above a threshold is the Generalised Pareto distribution (GP) [Coles, 2001, Hurkmans et al., 2010], which is given in Equation 2.4. In which: $Pr(X > x|X > u)$ is the exceedance frequency, x is the discharge value, u is the threshold value, ξ is the shape parameter and σ is the scale parameter.

$$Pr(X > x|X > u) = \left(1 + \xi \left(\frac{x - u}{\sigma}\right)\right)^{-\frac{1}{\xi}} \quad (2.4)$$

The return levels are given in Equation 2.5 [Coles, 2001], by rewriting Equation 2.4. In which: x_m is the m -th largest discharge, m is the m -th ranked observation and ζ_u is the probability that the threshold u is exceeded. Assumptions in rewriting are $Pr(X > x) \approx \frac{1}{m}$ and $Pr(X > u) = \zeta_u$.

$$x_m = u + \frac{\sigma}{\xi} \left((m\zeta_u)^\xi - 1 \right) \quad (2.5)$$

ζ_u can be approximated by Equation 2.6. In which k is the number of data points that exceeded the threshold and n is the total amount of data points.

$$\hat{\zeta}_u = \frac{k}{n} \quad (2.6)$$

Equation 2.5 shows that the excess ($x_m - u$) can be written as $\frac{\sigma}{\xi} ((m\zeta_u)^\xi - 1)$. Assuming this function can also describe deficits ($u - x_m$), gives Equation 2.7.

$$x_m = u - \frac{\sigma}{\xi} \left((m\zeta_u)^\xi - 1 \right) \quad (2.7)$$

Rewriting Equation 2.7 back into a similar form to Equation 2.4 gives Equation 2.8. In which: $Pr(X < x|X < u)$ is the non-exceedance frequency, x is the discharge value, u is the threshold value, ξ is the shape parameter and σ is the scale parameter. This rewriting used similar assumptions: $Pr(X < x) \approx \frac{1}{m}$, which means ranking from low to high instead of high to low values, and $Pr(X < u) = \zeta_u \approx \frac{k}{n}$, in which k is now the the number of data points that stayed below the threshold u . In addition, the non-exceedance probability is multiplied by the average number of events per year, similar to the Weibull plotting position used for the PUT method.

$$Pr(X < x|X < u) = \left(1 + \xi \left(\frac{u - x}{\sigma} \right) \right)^{-\frac{1}{\xi}} \quad (2.8)$$

Equation 2.8 resembles the equation given by [Gottschalk et al. \[2013\]](#) to describe the GP distribution for deficits. This equation is shown in Equation 2.9. In which: H_Y is the non-exceedance frequency, $y = x - u$ is the deficit, k is the form parameter and α is the scale parameter.

$$H_Y(y) = \begin{cases} \left(1 + \frac{ky}{\alpha} \right)^{\frac{1}{k}}; & k \neq 0; \quad y < 0 \\ \exp\left(\frac{y}{\alpha}\right); & k = 0; \quad y < 0 \end{cases} \quad (2.9)$$

The fact that Equation 2.8 shows resemblances to Equation 2.9, gives confidence in the assumption that $\frac{\sigma}{\xi} ((m\zeta_u)^\xi - 1)$ can describe deficits, which was used to get to Equation 2.7.

Equation 2.8 is used to fit the data, as these parameters can be found fitting the GP distribution.

2.2.3 Comparison

The LFFCs, which are the fitted parameter values and corresponding distribution, resulting from the block method and PUT method are compared to see their differences. This is done by comparing the return periods of several discharges, based on current problems and by Q-Q plots (quantile-quantile plots). Eventually, a choice is made on which method is used in the continuation of this study for research questions 2 and 3.

The return periods of certain discharges are compared to each other. These discharges are 1000 m^3/s and 1200 m^3/s . 1000 m^3/s is the agreed low river discharge (in Dutch: overeengekomen lage rivierafvoer, OLA) which corresponds to a water depth at Lobith of 2.5 m [[Bosschieter, 2005](#), [Sperna Weiland et al., 2015](#)]. Below this water depth navigation can be affected. Additionally, at this discharge, chloride concentrations can increase above the concentration of 250 mg/l , which is critical for water intake for drinking water [[Sperna Weiland et al., 2015](#)]. Salinisation is not a problem with a discharge of 1200 m^3/s and proper management of the Haringvliet sluices [[Janse and Burgdorffer, 2005](#)]. Discharges below 1200 m^3/s might lead to short salinisation of several tides. For both discharges holds that the longer this discharge continues, the bigger the problems will be.

A Q-Q plot compares two values from different data sets or fits at the same quantile. For this study that means the discharge at the certain probability of non-exceedance based on the block method is compared to the discharge at the same probability of non-exceedance based on the PUT method. The quantiles that are considered are given in Table 2.4.

Probability of non-exceedance	Return period (years)
$2 * 10^{-5}$	50 000
$5 * 10^{-5}$	20 000
$1 * 10^{-4}$	10 000
$5 * 10^{-4}$	2 000
$1 * 10^{-3}$	1 000
$5 * 10^{-3}$	200
$1 * 10^{-2}$	100
$5 * 10^{-2}$	20
0.10	10
0.25	4
0.5	2
0.75	1.33
0.90	1.11
0.99	1.01
0.999	1.00

Table 2.4: Quantiles considered in the Q-Q plot.

2.3 Influence of GRADE (RQ 2)

The goal of this second research question is to compare the LFFC based on the Waterinfo data and the LFFC based on the GRADE data from the current climate. To do this, a sub question is formulated, which asks for a LFFC based on the GRADE data from the current climate. After this LFFC is created, a comparison between the Waterinfo data and GRADE reference data can be made, which shows the influence of the GRADE model.

2.3.1 LFFC for the GRADE reference scenario (RQ 2.1)

The LFFC based on the GRADE data for the current climate, shown in Table 2.2 as 'Ref', is made following the same steps as the LFFC based on the Waterinfo data. As mentioned in Section 3.1.3 the block method is used to construct this LFFC.

Firstly, the borders of the annual period are April to March, which is the shifted hydrological year, which was used in RQ 1. Next, the multi-day minima are determined identical to RQ 1, see Section 2.2.1: Block method (RQ 1.1). Lastly, the same distribution is fit, the GEV shown in Equation 2.3 with the same plotting position shown in Equation 2.2. The only difference is that the GRADE Reference data set has a longer period of discharges compared to the Waterinfo data.

2.3.2 Comparison

The comparison between the LFFC based on the Waterinfo data and the GRADE Reference data is done similarly as described in Section 2.2.3. Since both LFFCs are constructed using the same method, the block method, the parameter values ξ , σ and μ can be compared as well.

2.4 Influence of climate change (RQ 3)

The goal of this third research question is to see the influence of climate change on the return periods of low flows by comparing the LFFCs from the GRADE Reference data to the LFFCs from the GRADE climate scenarios. In order to do this, first the LFFCs for the different KNMI'14 climate scenarios need to be made after which they can be compared to the reference.

2.4.1 LFFC for the GRADE climate scenarios

The LFFCs based on the GRADE climate scenarios, shown in Table 2.2 as '2050 GH' until '2085 WL', are made following the same steps as the LFFCs based on the GRADE Reference data. The method is described in Section 2.3.1.

2.4.2 Comparison

The comparison between the LFFCs based on the GRADE Reference data and the GRADE climate change data is done similarly as described in Section 2.3.2.

Figure 2.2 shows how the different research questions are connected to each other and help to answer the research goal. The goal of RQ1 is to find a good method and quantify the low flows of 2018. The goal of RQ2 is to compare the LFFCs based on the Waterinfo and GRADE Reference data, to see how the GRADE model performs for low flows. The goal of RQ3 is to quantify the return periods of low flows taking climate change into account. Comparing the results of RQ2 and RQ3 will show how the return periods of low flows will change in the future.

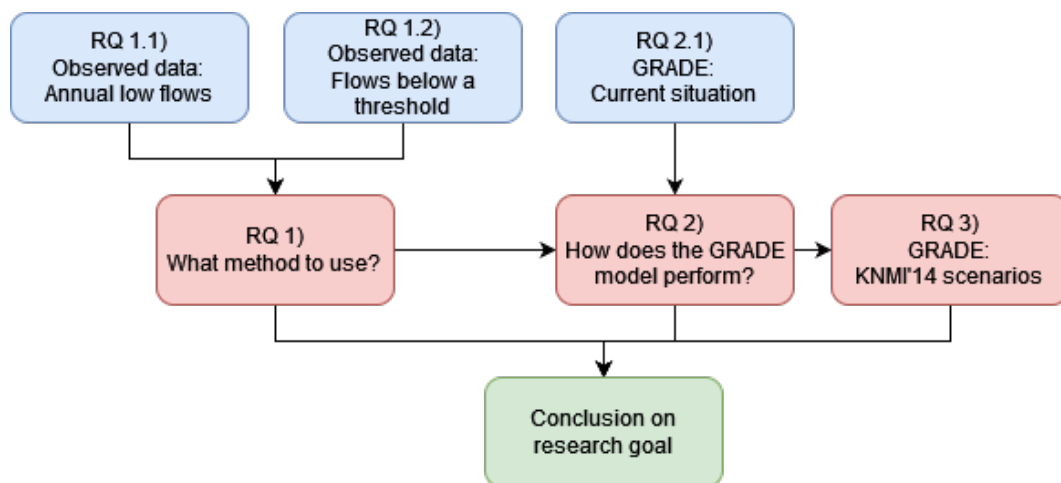


Figure 2.2: Flowchart with connections between different research questions.

3

Results

The following sections show the results for each of the research questions: starting with the influence of the selection method, followed by the influence of the GRADE model and lastly the influence of climate change on the return period of low flows at Lobith.

3.1 Influence of event selection method (RQ 1)

First, the results using the block method are shown (RQ1.1), followed by the results of the PUT method (RQ1.2), after which these results will be compared to answer RQ1.

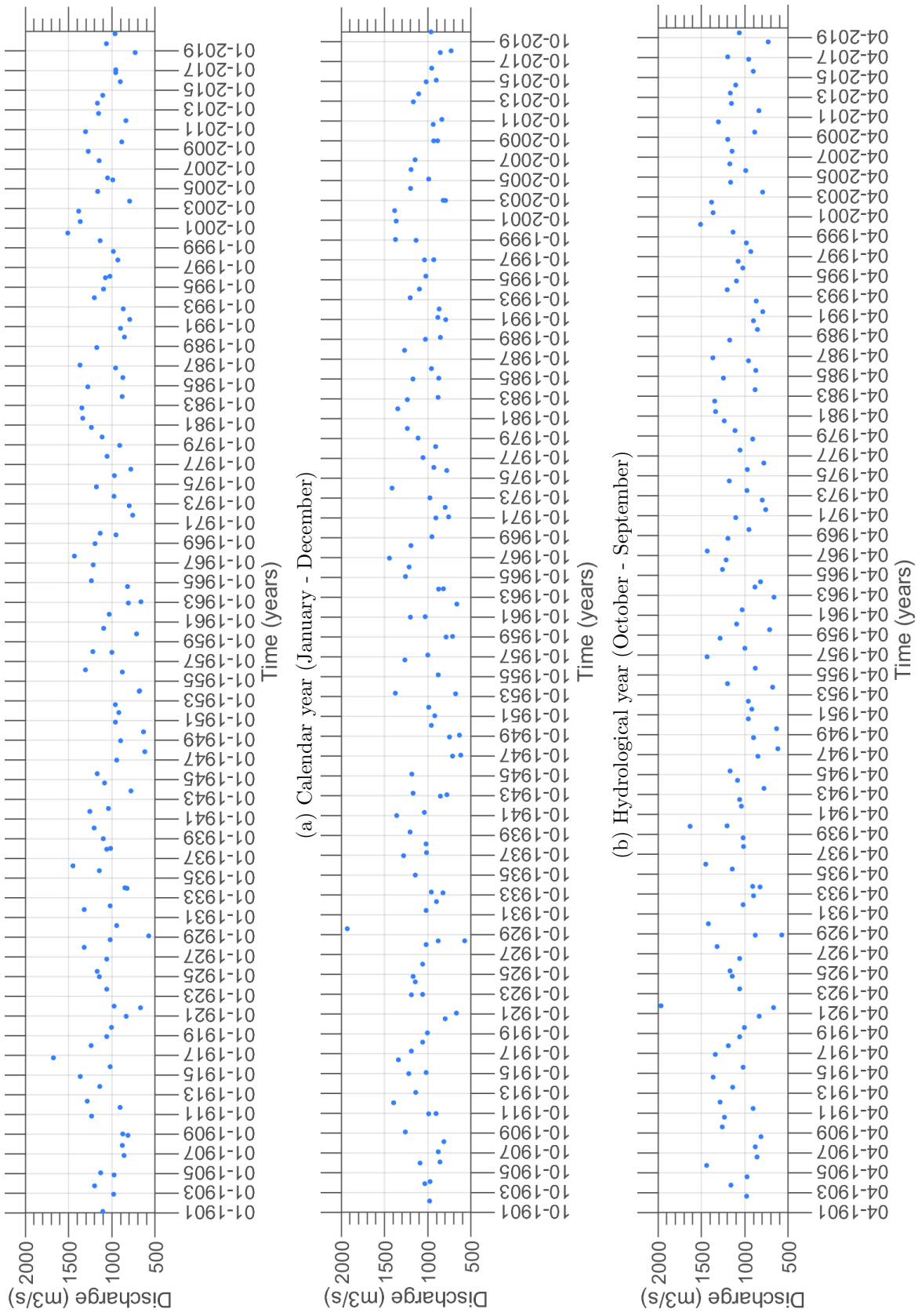
3.1.1 Block method (RQ1.1)

Elaboration is given on where the boundaries of the year are laid, on the multi-day minimum and on the fit of the distribution. Finally the low flow frequency curves are given for the observed Waterinfo data using the block method.

Annual period

Figure 3.1 shows the selected annual 1-day minima for the three different types of years: the calendar year, the hydrological year and the shifted hydrological year. When the dots are located close to each other, it means that the selected minima have a short time interval between them. This does not support the assumption of annually independent flows. This is why the year-type with the least amount of dots close to each other is chosen as the standard type of year in the continuation of this study.

The hydrological year does not score well on the criterion of fewest events close to each other. 17 times events have less than 50 days between them. For the calendar year this is 5 times and for the shifted hydrological year this is even less, with only 3 times that events have less than 5 days in between. This is why the shifted hydrological year is chosen as the standard when the block method is used.



(a) Calendar year (January - December)
 (b) Hydrological year (October - September)
 (c) Shifted hydrological year (April - March)

Figure 3.1: Timing of selected annual 1-day minima for a calendar, hydrological and shifted hydrological year.

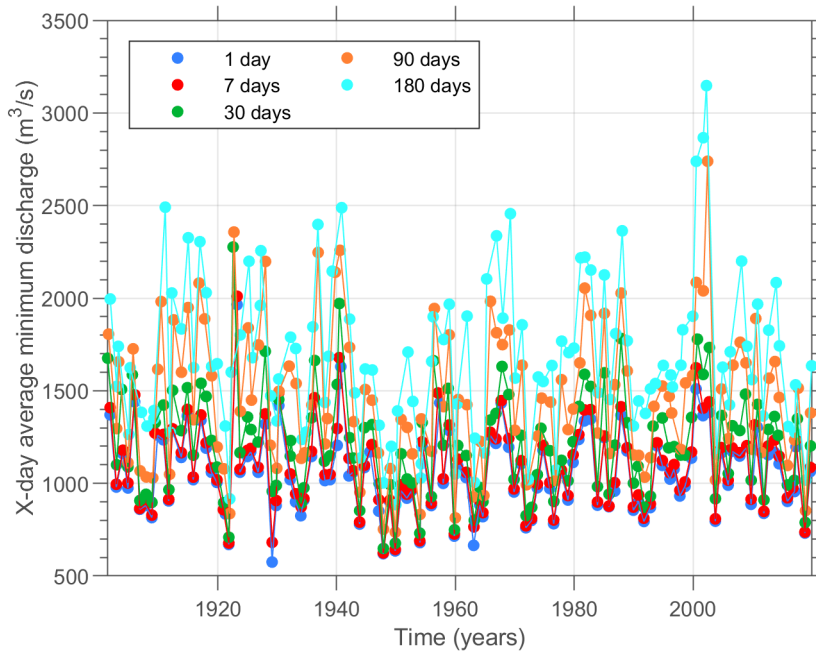


Figure 3.2: Annual minimum average discharge for different durations using block method.

Multi-day minimum

The minimum average annual discharge values, when using the block method and the shifted hydrological year, are shown in Figure 3.2. Little difference is seen between the discharge values with a duration of 1 and 7 days. The durations of 90 and 180 days clearly show higher discharge values than the duration of 30 days. A remarkable observation is that the 180 days discharge of 1922 is lower than that of the other durations. In this year this is due to the fact that the long duration allows to include the low discharges of November 1921.

The lowest 1 day discharge of $575 \text{ m}^3/\text{s}$ occurred in February 1929. Three of the five 1 day minima occurred in November, but the other two occurred during the winter in February 1929 and January 1963. Low flows are expected to occur in November, but the two other low flows in winter show another cause for low flows: ice. [de Wit \[2004\]](#) found the same low discharge values for 1929 and 1963 and stated that ice was present on the Rhine, resulting in lower discharges.

Table 3.1 shows the top 5 lowest discharges for all 5 durations from 1901 to 2020 at Lobith. This shows a year with very low discharges, like 1929, which only occurs in the 1 and 7 day lowest discharges. On the other hand, the year 2018 only occurs in the top 5 lowest discharges for the longest duration of 180 days. This shows the drought in 2018 was severe due to the length of the event. To zoom in on the recent dry year 2018 specifically: for the 1 day lowest discharge 2018 was placed in 8th position with a discharge of $732 \text{ m}^3/\text{s}$, for the 7 days on position 7 with a discharge of $737 \text{ m}^3/\text{s}$ and for the 30 and 90 days on position 6, with a discharge of 789 and $852 \text{ m}^3/\text{s}$ respectively.

Fitting a distribution

The GEV distribution is used to fit the selected discharge data with different durations, seen in Figure 3.2. Appendix C shows the different durations from Figure 3.2 in separate figures. Appendix D shows the histograms and fitted probability density function. This probability density function fit is made on intervals of $10 \text{ m}^3/\text{s}$. The values of the parameters of these fits are given in Appendix E.

ξ is the shape parameter. The shape parameter does not change much for the different durations and is about -0.1 . For all durations the 95% confidence interval is completely or mostly below a ξ

	#1	#2	#3	#4	#5
1 day	575 (Feb 1929)	620 (Nov 1947)	635 (Nov 1949)	665 (Jan 1963)	670 (Nov 1921)
7 days	624 (Nov 1947)	644 (Nov 1949)	678 (Nov 1921)	681 (Feb 1929)	690 (Dec 1953)
30 days	648 (Nov 1947)	677 (Nov 1949)	709 (Nov 1921)	731 (Dec 1953)	749 (Nov 1959)
90 days	736 (Nov 1949)	752 (Nov 1947)	814 (Dec 1959)	832 (Jan 1954)	837 (Dec 1921)
180 days	885 (Dec 1949)	916 (Jan 1922)	1003 (Nov 1947)	1005 (Mar 1963)	1017 (Dec 2018)

Table 3.1: Top 5 lowest discharges (m^3/s) using the block method.

value of 0. This means it is highly likely all the data fit the Weibull distribution the best.

σ is the scale parameter and resembles the standard deviation of the data. The value of σ increases with increasing duration. This is not strange, since the discharge values for higher durations also increase, seen in Figure 3.2 and Figure E.1c.

μ is the location parameter and resembles the mean of the dataset. The value of μ increases with increasing duration. However, the value of $\frac{\sigma}{\mu}$ remains fairly constant with a range of 0.21 to 0.26.

Figure 3.3 shows the observed discharges plotted using the Weibull plotting position from Equation 2.2 and the fitted GEV distribution for the different durations. All fits seem reasonably well. Only the most extreme cases are not represented well by the fit. However, this can be explained by the fact that this is an extreme value analysis. The most extreme event has the most uncertain return period, as there are few cases to determine the occurrence. The most extreme event in the 100 year period does not have to be an event with a return period of 100 years, but could also be an event with a larger return period. Taking this into account, the fit looks good.

Furthermore, Figure 3.3 shows that discharges with a similar return period become higher for higher durations. The 1, 7 and 30 day durations lie close to each other, whilst the 90 and 180 days are clearly visible and have higher discharge values than the lower durations.

Figure 3.4 shows the extrapolation of the fit seen in Figure 3.3 and the corresponding 95% confidence intervals. Figure 3.4 shows that the 1 and 7 day discharges lie close to each other for the smaller return periods, showing little difference in the discharge value with similar return periods. They deviate more for larger return periods, however, the confidence intervals still overlap. Furthermore, this figure shows that the confidence interval of the 180 day discharges lies completely outside of the other confidence intervals. The most remarkable observation is the fact that the fitted distributions of the 7, 30 and 90 day are intersecting each other at a return period of about 7000 years. This underlines the uncertainty in extreme value analysis. Extrapolation beyond a return period of 1000 years, which extrapolates the observations with a factor of about 10, is therefore not recommended.

Appendix F shows the extrapolation of the different durations in separate figures, Figure F.1b to F.1f. The discharge value corresponding to a 1000 year return period are 510, 530, 540, 560 and 710 m^3/s for 1, 7, 30, 90 and 180 days respectively.

The results can also be plotted differently compared to the LFFCs. This is shown in Figure 3.5. This form makes it more applicable for potential users. A combination between the discharge and duration can be made to see what the corresponding return period of this event is. For example, Figure 3.5 shows that a problematic discharge for shipping of 1000 m^3/s occurs almost every year. However, this is for a short period of time. This average discharge has a probability of occurring once every 5 years for a period of 30 days and once every 10 years for a period of 60 days.

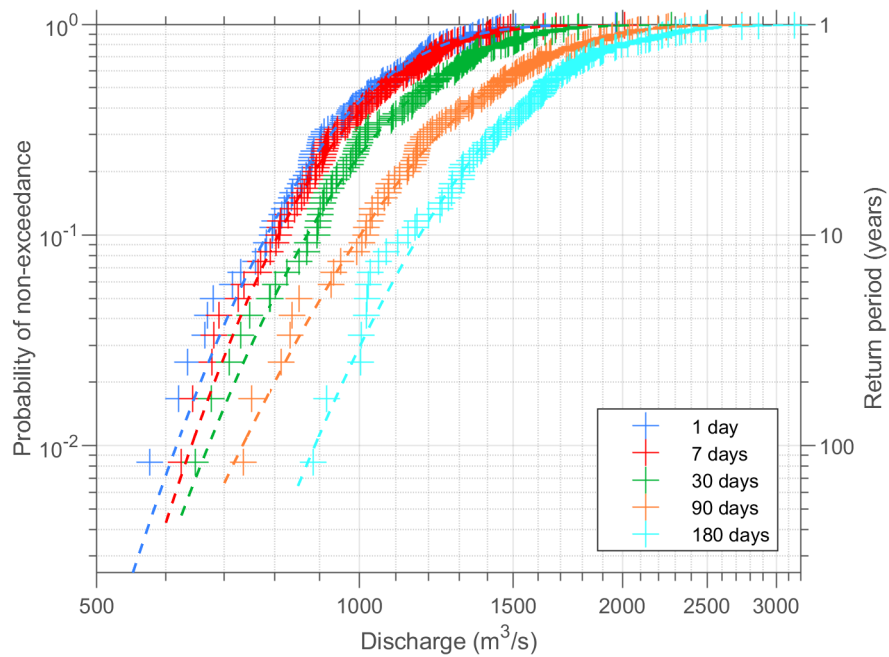


Figure 3.3: Observed annual minimum discharges for different durations and their estimated fit using the block method.

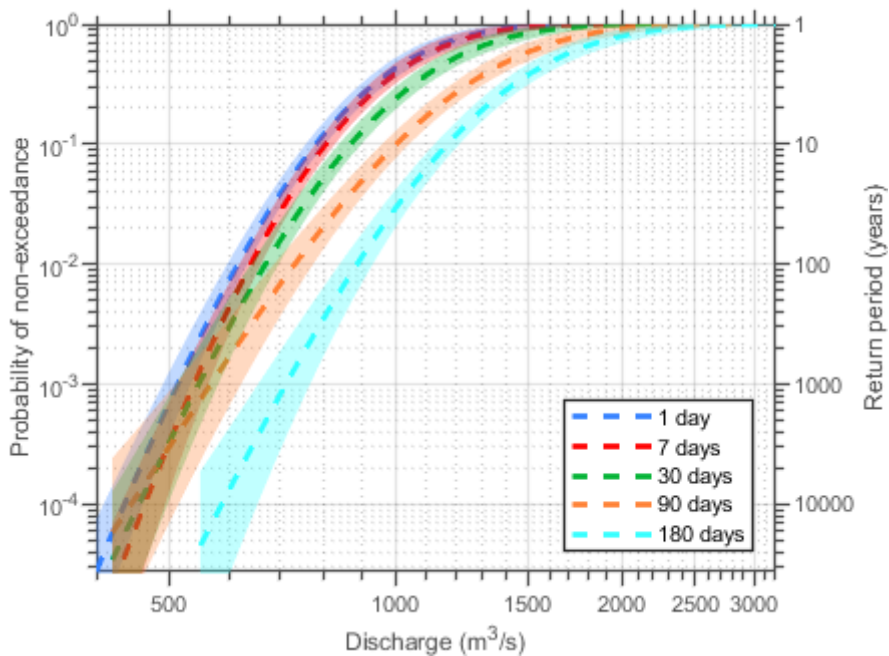


Figure 3.4: Extrapolation of minimum annual discharges for different durations with 95% confidence intervals using the block method. Separated figures for the durations are shown in Appendix F.

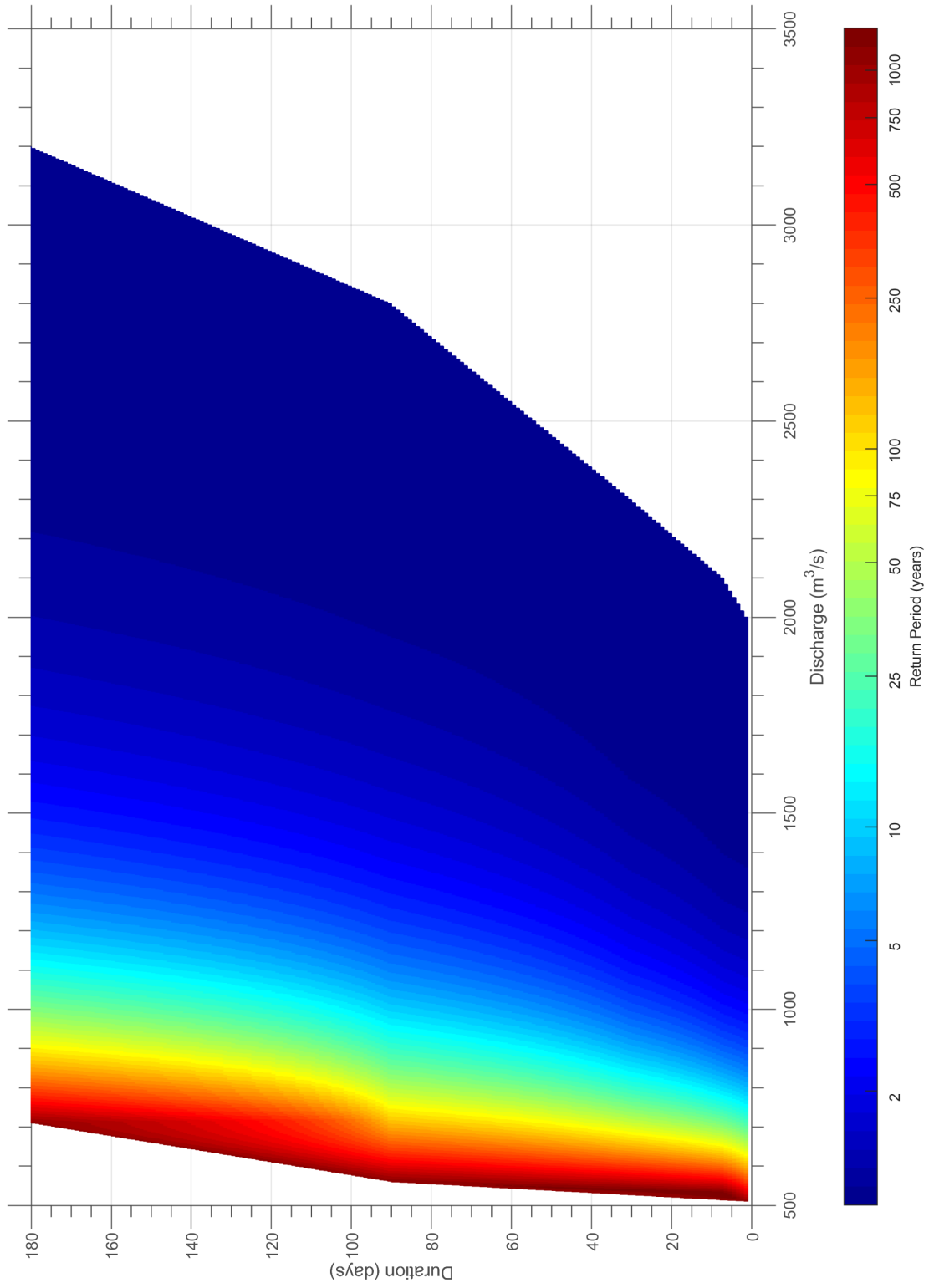


Figure 3.5: Return period based on discharge and duration, interpolated from the LFFCs in Figure 3.3 and 3.4.

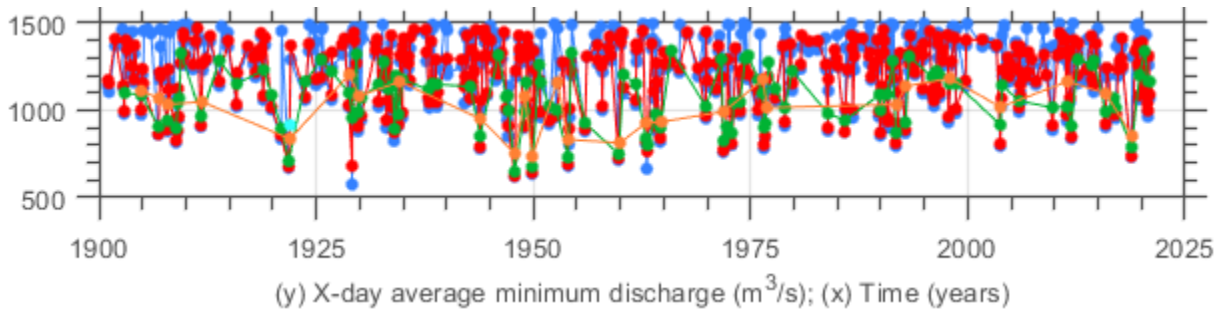


Figure 3.6: Annual minimum average discharge for different durations using PUT method for $u = 1500 \text{ m}^3/\text{s}$ and $r = 0$.

3.1.2 Peak-under-threshold (RQ1.2)

Elaboration is given the multi-day minimum, the choice of the threshold value (u) and lag value (r) and the fit of the distribution. Finally, the low flow frequency curves are given for the observed Waterinfo data using the peak-under-threshold method.

Multi-day minimum

The minimum discharges below a threshold of $1500 \text{ m}^3/\text{s}$ using the PUT method are shown in Figure 3.6. Considering no lag, so $r = 0$, the top 5 lowest discharges for each duration are given in Table 3.1, as the PUT method gives the same results as the block method. The choice for the value of u , which varies per duration, and r are explained in the next section.

The top 5's are identical to the top 5's of the block method, so Table 3.1 shows the top 5 lowest discharges at Lobith between 1901 and 2020 for different durations for both the block and PUT method. 2018 only occurs in the top 5 of the longest duration, 180 days. The specific rankings for 2018 on the other durations are position 8 for a duration of 1 day, position 7 for a duration of 7 days, position 6 for a duration of 30 days and position 6 for a duration of 90 days. This is also equal to the result from the block method. The fact that the top 5's for the block method and PUT method are identical, means that there are no 2 extremely low flow events in one year, as these would come up in the PUT method.

The events in Figure 3.6 are less structured than in the block method, which only gives one value for each duration for each year. When using the PUT method the events can occur several times per year or not once in a year. This is shown in Figure 3.7 as the number of independent events per threshold.

The independent events in Figure 3.7 do not include any lag (r). This shows that the most independent events occur around a threshold of $2200 \text{ m}^3/\text{s}$ for the 1 and 7 day duration and is slightly higher for the higher durations. Left of the peak in the number of events, a lower threshold means less events. This is a result of fewer days where this threshold is met. Right of the peak in the number of events, a higher threshold means less events. This is a result of events being added into one longer event, as more days meet the threshold.

Figure 3.7 also shows that the lowest durations have the highest amount of events. The 90 and 180 day durations (almost) do not even have one event per year on average. This makes it questionable if the PUT method is well applicable here, as the strong point of the PUT method over the block method, is the fact that more data can be used than 1 event per year.

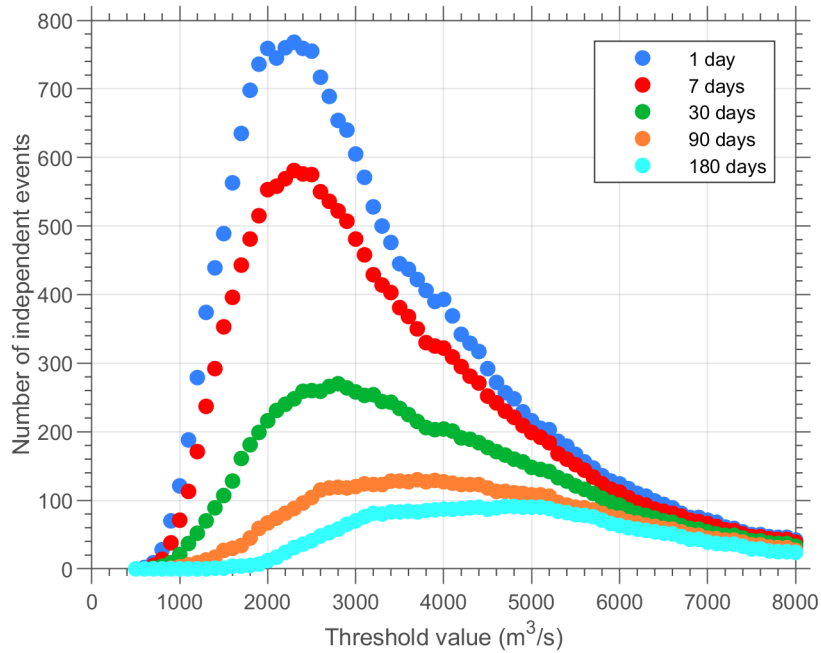


Figure 3.7: Number of independent events for different thresholds for each duration using no lag ($r = 0$).

Threshold and number of consecutive observations below the threshold

A general overview of the changing number of events for different values of u and r is given in Figure 3.8. This shows no lag or 1 day of lag do not differ much in the total amount of independent events. In addition, the difference in the number of events does not differ much depending on the value of r below a threshold value of $1800 \text{ m}^3/\text{s}$ for all durations. This value of u is even higher for the 180 day events. Furthermore, it can be seen that in general the number of events will decrease with an increasing number of consecutive observations below the threshold. This means that on average more events disappear than appear due to the joining of two or more events. Elaboration on how events 'appear' and 'disappear' is given in Appendix G.

It is not possible to draw conclusions on the independence of events and lag based on the results in Figure 3.8. The choice on the value of r is therefore only based on the influence on the total amount of events. r does not have a big influence when the threshold value is low, which is the lower spectrum of discharges we are interested in. This is why the choice is made to not include a lag value and set r at a value of 0 days. In addition, for the higher durations, including a lag will decrease the already small amount of events, which is also not wanted. This choice is revisited after the choice on the value of u , because these two values of u and r influence each other, and the reasoning still holds.

Based on the 4 criteria mentioned in the Methodology in Section 2.2.2, a choice is made on the threshold value. A summary of the range for a value of u for the 4 criteria is given in Table 3.2. The 4 criteria consist of a mean residual plot, parameter values based on the threshold value, the use of 25% of the data and the number of events.

The mean residual plot did not provide a reason to select or to not select a certain threshold, as a smooth line is visible when the mean deficit was plotted against the threshold value.

The parameter values refer to the figures in Appendix H. The figures show the estimated value of ξ and σ for each value of u . Linearity is visible for a range of threshold values with a duration of 1 or 7 days. This becomes less clear for the 30 day duration and is hardly visible for the 90 and 180

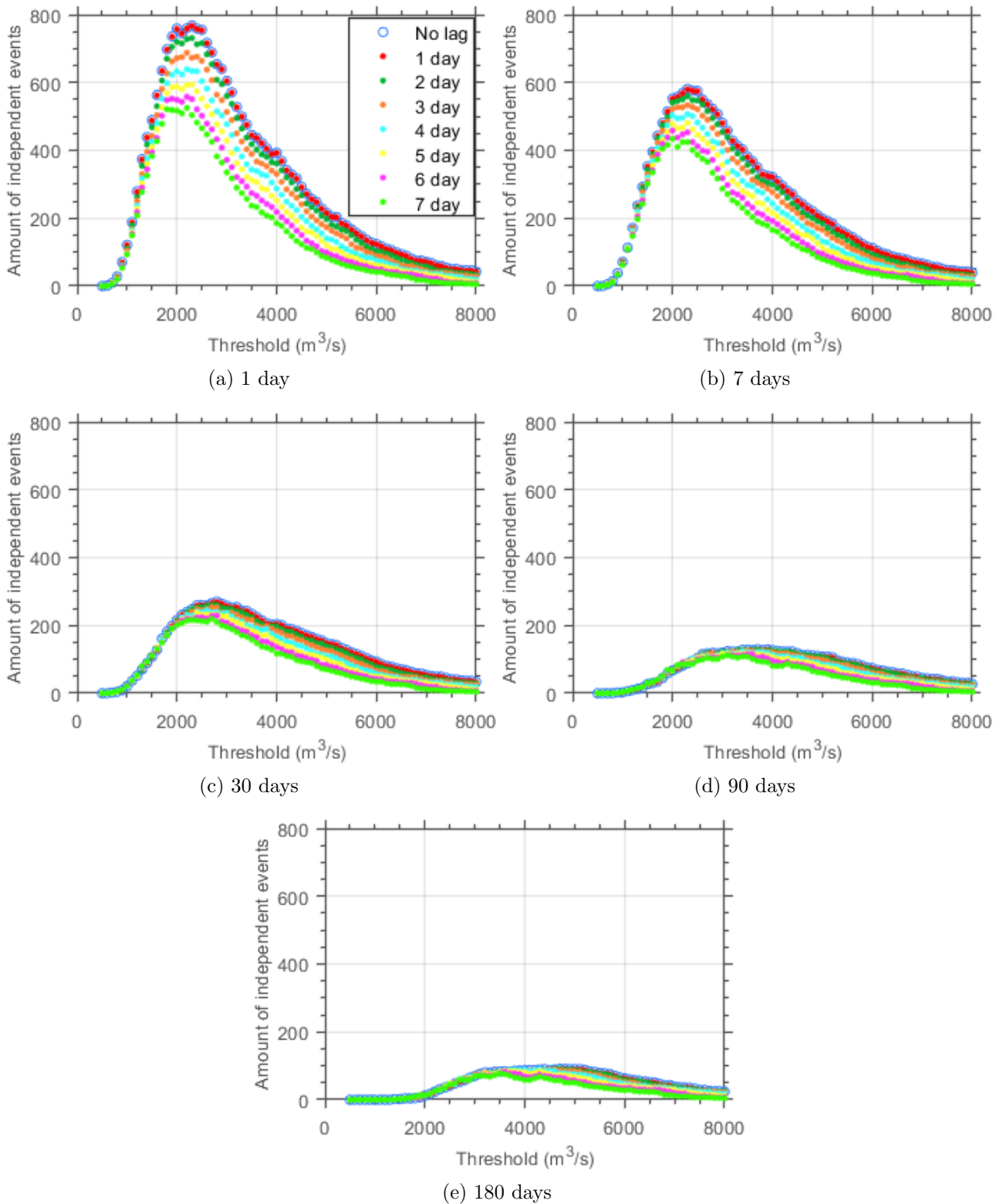


Figure 3.8: Histogram and fitted probability density function of minimum annual discharges for different durations.

day duration. Besides the low amount of events mentioned in the last section, this is another sign the PUT method might not be suitable for the higher duration data.

The 25% criterion, where a quarter of the data is involved in an event, is met at a threshold of $1500 \text{ m}^3/\text{s}$. However, this does not mean 25% of the data is included in the selected minima, as events might be shorter than the duration, which results in not taking the event into account in that situation. Since this is less likely to happen at the lower durations, this criterion is more important for the 1 and 7 day durations than the higher durations.

The number of events is selected in such a range that the threshold results in 1 to 4 events each year. This method is thought to allow for more data to be taken into account compared to the block method, whilst still keeping in mind the longer duration of low flow events compared to high flow events. This results in a small range of threshold values for the 1 and 7 day durations, as they often have more than 4 independent events per year on average, shown in Figure 3.7. For the higher durations, this resulted in a larger range of threshold values. For the 180 day duration it was not possible to find a threshold with 1 or more events per year, so a range where more than 2/3 of the years had an event is selected.

All these considerations on the 4 criteria give a range of possible threshold values, shown in Table 3.2. This resulted in the choice of the threshold for the 1 and 7 day duration of $1500 \text{ m}^3/\text{s}$, for the 30 day duration of $2500 \text{ m}^3/\text{s}$, for the 90 day duration of $3500 \text{ m}^3/\text{s}$ and for the 180 day duration of $5000 \text{ m}^3/\text{s}$. As mentioned in this section, after the choice was made on the value of u , the influence of r was checked and the choice for a lag of 0 days was confirmed.

	Mean residual plot	Parameter values	25%	Number of events	Choice of u
1 day	–	1300 – 5100	1500	1000 – 1300	1500
7 days	–	1000 – 3800	1500	1100 – 1600	1500
30 days	–	1800 – 2600	1500	1500 – 5500	2500
90 days	–	–	1500	2300 – 5500	3500
180 days	–	–	1500	3800 – 5200	5000

Table 3.2: Considerations concerning threshold value. The values show the range of threshold values (m^3/s) which perform well on one of the 4 criteria.

Fitting a distribution

The 30, 90 and 180 day durations do not give good results when the PUT method is applied. The focus is thus put on the 1 and 7 day duration. Several reasons can be named for this decision, as they were mentioned before. The parameter values for different threshold values do not show linearity. For the 180 day duration it was not possible to select 1 event per year on average. Furthermore, the selected thresholds for these three durations are higher than the mean river flow at Lobith of $2200 \text{ m}^3/\text{s}$, which is illogical when looking into low flows. Additionally, the fit gives an asymptote for all durations. This asymptote is reached for low return periods for the larger durations. This makes extrapolation to larger return periods not possible. Appendix I shows the fit for all 5 durations and from this figure it is also visible that the fit for the higher durations is not good. The 30, 90 and 180 day durations will not be included anymore in the remainder of this study when the PUT method is applied.

After the choice on the value of u and r , the final fit of the GP distribution on the data is estimated. The observations and estimated fit are shown in Figure 3.9 and the parameter values for ξ , σ and u are given in Appendix J. This table shows that the value of σ and u increase with increasing duration and that the value of ξ decreases with increasing duration.

What stands out from these parameter values is the high value of σ , which is representative of the standard deviation as the scale parameter. This is expected to be higher for higher durations,

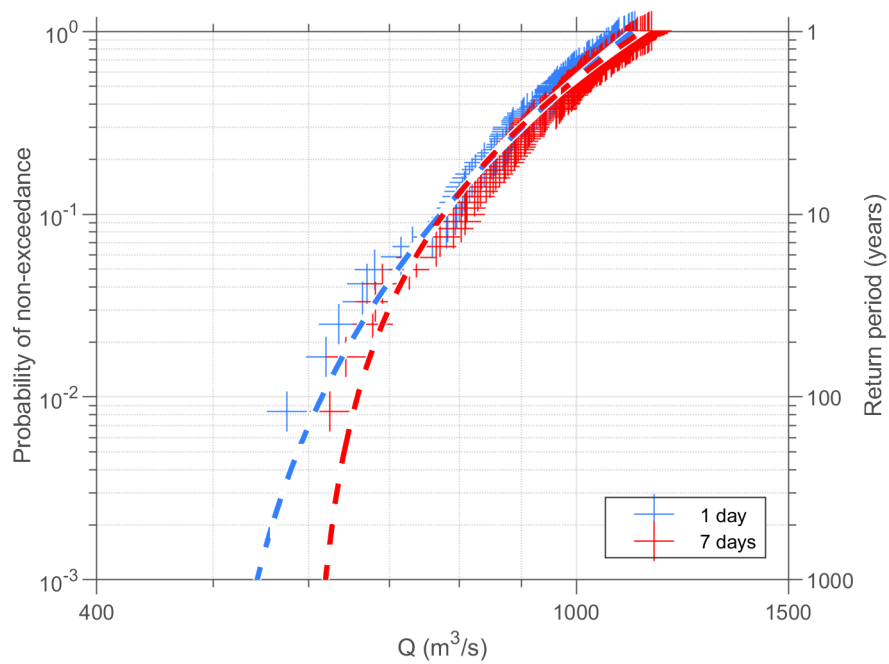


Figure 3.9: Observed minimum discharges below a threshold for a 1 and 7 day duration and their estimated fit using the PUT method.

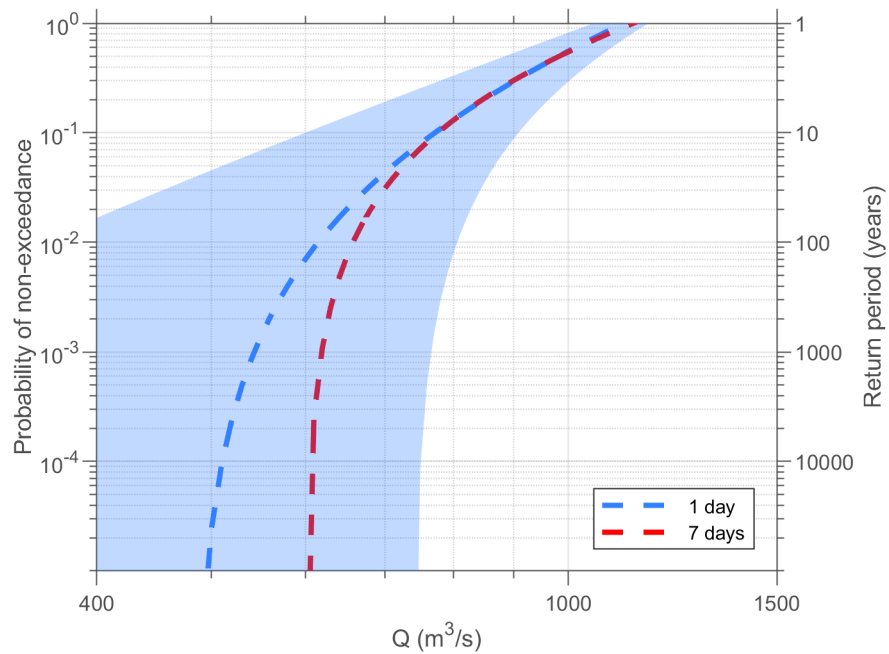


Figure 3.10: Extrapolation of minimum discharges below a threshold for a 1 and 7 day duration using the PUT method and the 1-day confidence interval.

similar to the block method, however, the differences are big. It is expected that the selected threshold is slightly high, which results in more events with higher discharges influencing the standard deviation.

The estimated fit is shown in Figure 3.9. Visually, the fit looks good. The same observation can be made as for the block method in Figure 3.3, which is that the fit is better for the higher discharges and the most extreme low discharges are not represented well by the fit. This is not strange as the uncertainty in the return period of the most extreme events is highest. Furthermore, the figure shows that until a discharge of $800 \text{ m}^3/\text{s}$, there is little to no difference between the 1 and 7 day fit, but for smaller discharges, the 1 day fit gives lower results.

Figure 3.10 shows the extrapolation of the fit shown in Figure 3.9 and the corresponding 95% confidence interval for the 1 day duration. As explained in Appendix H not all durations have a (complete) 95% confidence interval, because they have a ξ value below -0.5 and this does not result in a consistent confidence interval or none at all. The confidence interval for the 1 day duration is very large and includes the fit for the 7 days duration.

The discharge values corresponding to a 1000 year return period are 550 and $620 \text{ m}^3/\text{s}$ for 1 and 7 days respectively.

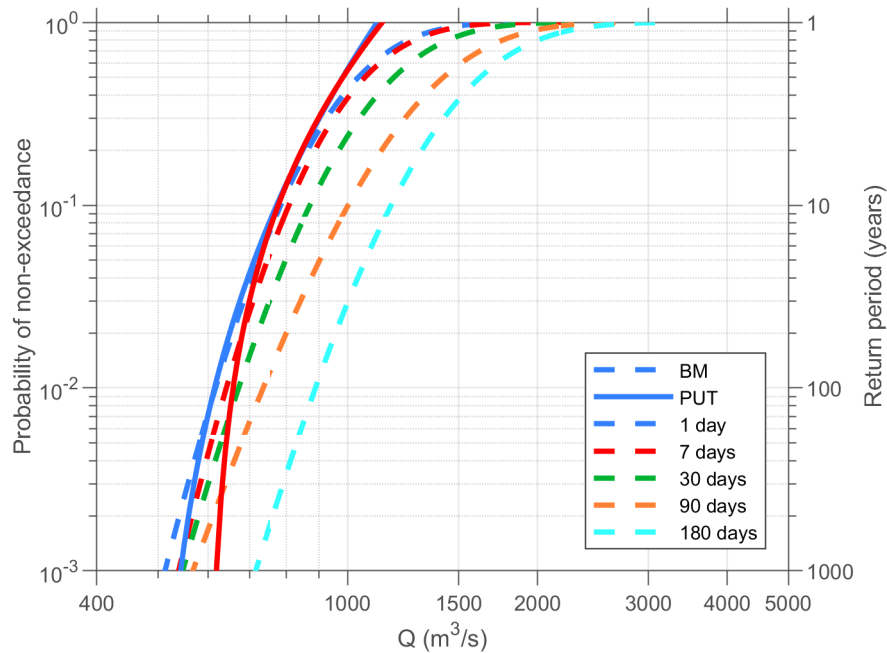


Figure 3.11: Fitted distributions using the block method (BM) and PUT method for all durations.

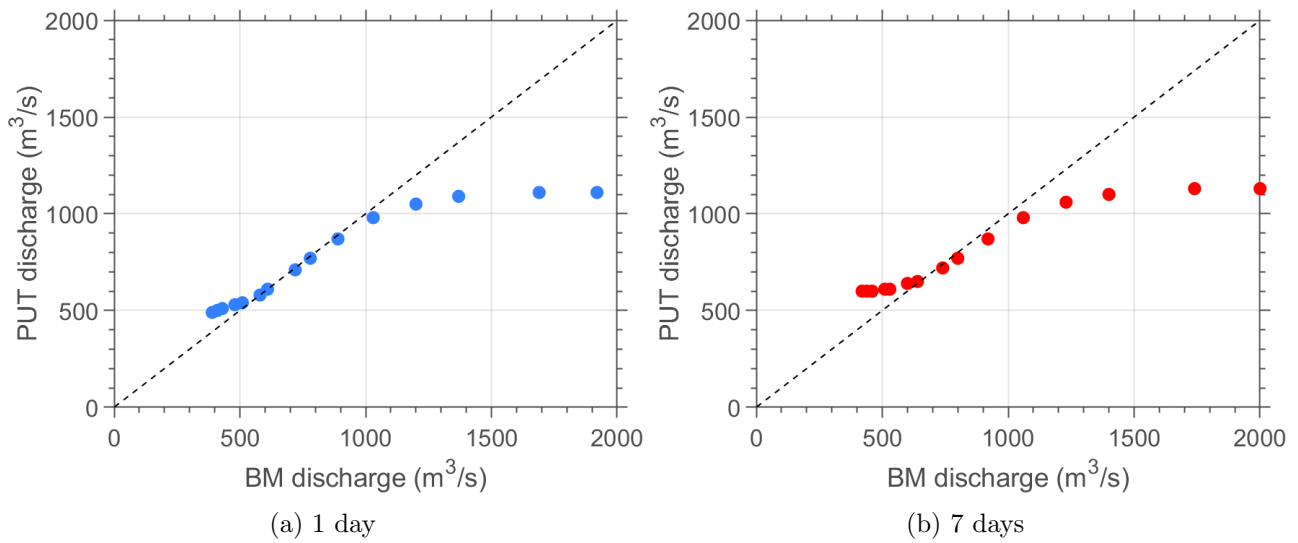


Figure 3.12: Q-Q plots for selected quantiles, shown in Table 2.4, comparing low flows based on the block method (BM) and PUT method for the 1 and 7 day duration.

3.1.3 Comparison

An overview of the estimated parameters for both the GEV distribution in combination with the block method and the GP distribution in combination with the PUT method is given in Appendix J. Since different distributions are used, the parameters cannot be compared directly. However, for both methods σ represents the standard deviation in the data set and it can be seen that the values for σ are much higher for the PUT method.

Figure 3.11 shows the estimated fit for all durations for both the block method and the PUT method in one figure. This shows that the shape of the fit differs between the two methods. Furthermore, the extreme discharges, from a 100 year return period onwards, are estimated higher with the PUT method. This is in accordance with the 1000 year return period discharges mentioned before, where the discharges for the PUT method were higher than the discharges for the block method. For more frequent events, the PUT method estimates slightly lower discharges compared to the block method.

The Q-Q plots in Figure 3.12 show similar results as seen from Figure 3.11. For the 1 and 7 day durations the PUT method results in higher discharges for the lower range of discharges. For the higher range of discharges, which occur more often, the block method gives higher discharges than the PUT method. The biggest differences between the two methods are found for the smaller return periods and higher range of discharges. This implies that the PUT method finds more events with a discharge above $1000 \text{ m}^3/\text{s}$ than the block method, as the block method then often finds one value that is lower in that year.

The return periods corresponding to a discharge of $1000 \text{ m}^3/\text{s}$, based on shipping and chlorine levels, and $1200 \text{ m}^3/\text{s}$, based on salinisation, are given in Table 3.3. The PUT method always gives smaller return periods for these discharges compared to the block method, as they fall in the lower range of discharges.

Discharge	Method	1 day	7 days	30 days	90 days	180 days
1000 m^3/s	BM	2.3	2.6	4.2	10.1	34.0
	PUT	1.8	1.8			
1200 m^3/s	BM	1.3	1.4	1.9	3.8	8.5
	PUT	<1	<1			

Table 3.3: Values of return periods (in years) for a discharge of 1000 and 1200 m^3/s for the block method and PUT method.

Based on the results, the block method is used in the remainder of this study. This has several reasons. Firstly, the fit shown in Figure 3.3 and Appendix I visually looks better for the block method. Secondly, several observations were made in the previous sections, which reflected on the PUT not being suitable for all durations. It was mentioned that not all durations had an average of 1 or more events per year and not all fits for the different durations have a 95% interval, as explained in Appendix H. Lastly, the PUT method shows an asymptote, which does not make it possible for all durations to extrapolate to large return periods.

One of the drawbacks of the block method is the fact that the 7, 30 and 90 day duration curves cross each other at a return period of 7000 years. However, this is due to the uncertainty in extrapolation. Another drawback is the fact that the block method uses less data for the lower durations. This means that only the lowest minimum is selected each year using the block method, whereas there could be multiple events below a threshold according to the PUT method. The opposite is also true, where a high annual minimum discharge is selected, which would not be selected using the PUT method as it is above the threshold.

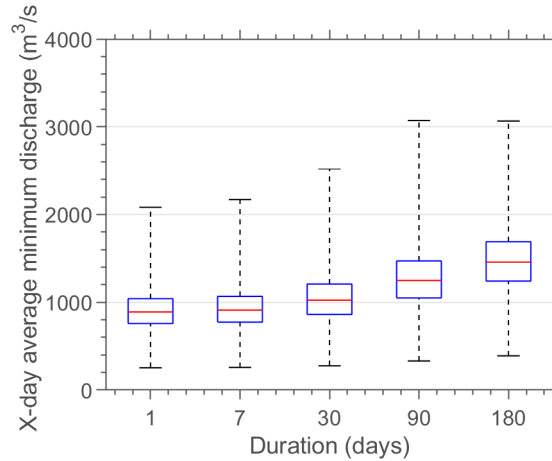


Figure 3.13: Boxplots of selected minima for the GRADE Reference data for different durations.

3.2 Influence of GRADE (RQ 2)

First the results of the LFFCs of the GRADE Reference scenario are given (RQ2.1), after which they are compared to the LFFC of the Waterinfo data.

3.2.1 LFFC for the GRADE Reference scenario (RQ 2.1)

Figure 3.13 shows an overview of the selected annual minima for each duration as a boxplot. This shows the median increases slightly with increasing duration. Furthermore, it shows that half of the discharges are very close to the median and the other half have a wider range. The values for the estimated GEV fit based on the GRADE Reference data is shown in Appendix J.

The top 5 lowest discharges for all 5 durations from the GRADE Reference data set are shown in Table 3.4. The numbers 1^* until 6^* represent different years, as the actual year in the simulation is not important. What is striking is the timing of the lowest discharges, which occur throughout the whole year, but not often in October or November, which is when the lowest flows are expected. Another observation is that the year 1^* occurs twice in the top 5 for both the 1 and 7 day duration, once in March and once in April. This can happen due to the fact that the shifted hydrological year is used to determine the borders of a year. However, it is not desirable to have the selected minima close together, as this does not support the assumption of the block method that selected annual minima are independent.

The fit and selected annual minima from Figure 3.13 are shown in Figure 3.14. Similar observations can be made as for the Waterinfo data in Figure 3.3. The fit looks very good, but deviations from the fit are seen for the extremely low discharges. These extreme events still have the most uncertain probability of non-exceedance.

In addition, Figure 3.14 shows that a higher duration will result in a higher discharge for the same return period. The fit for the 1 and 7 day duration are very close to each other. More difference is seen between the 30, 90 and 180 day durations. The 95% confidence interval is not given in a separate figure, as the interval is so small due to the large amount of data, that it is not visible in a figure. According to the 95% interval range of ξ , the fits for all durations are a Weibull distribution, as all values of ξ are below 0.

Discharge values corresponding to a 1000 year return period are 400, 400, 430, 520 and 645 m^3/s for a duration of 1, 7, 30, 90 and 180 days respectively. The fact that the 1 and 7 day duration have a similar discharge can be due to the baseflow in the HBV model from GRADE. However, if this is true is unclear.

	#1	#2	#3	#4	#5
1 day	254 (Apr 1*)	263 (Jul 3*)	273 (Mar 1*)	278 (May 4*)	288 (Mar 5*)
7 days	258 (Apr 1*)	268 (Jul 3*)	280 (May 4*)	283 (Mar 1*)	292 (Mar 5*)
30 days	276 (Apr 1*)	282 (Jul 3*)	311 (May 4*)	316 (Jan 2*)	316 (Dec 6*)
90 days	331 (Aug 3*)	353 (Feb 2*)	361 (May 1*)	364 (Apr 5*)	369 (Dec 6*)
180 days	390 (Jun 5*)	394 (Oct 3*)	436 (May 1*)	457 (Jan 6*)	462 (Jun 4*)

Table 3.4: Top 5 lowest discharges (m^3/s) using the GRADE Reference data. Note that the numbers 1^* until 6^* represent different years, as the years from the simulation are not important. The top 5's from other scenarios can be found in Appendix K.

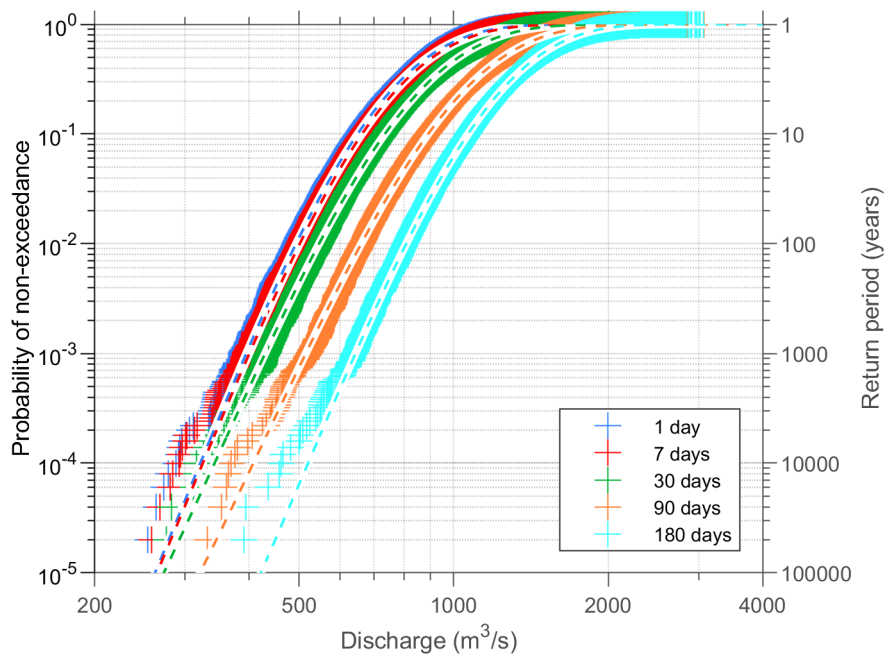


Figure 3.14: Selected annual minimum discharges for different durations and their estimated fit using GRADE Reference data.

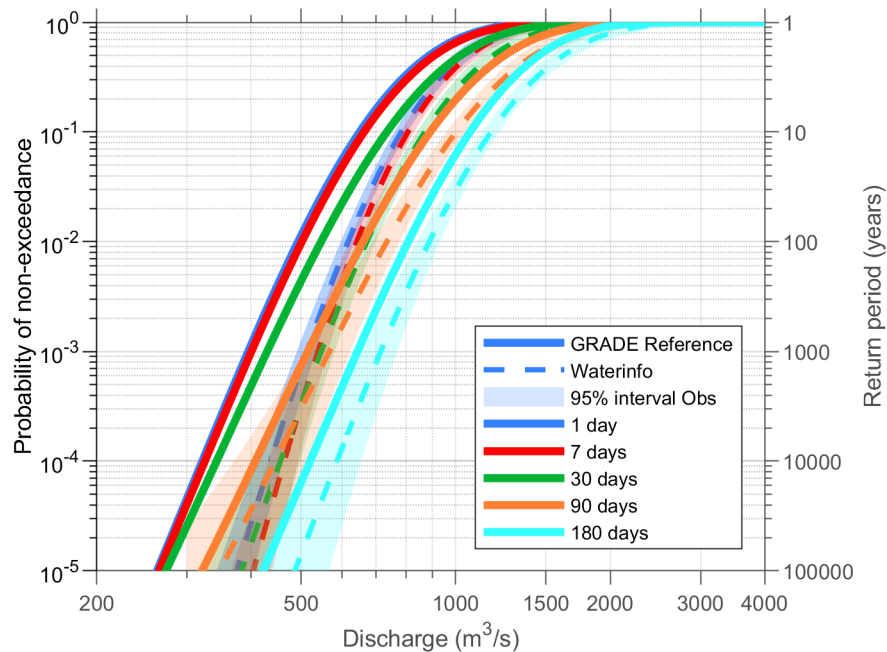


Figure 3.15: Fitted distributions using the Waterinfo data and GRADE Reference data for all durations.

3.2.2 Comparison

The top 5 lowest discharges for the GRADE Reference data, shown in Table 3.4 are much lower compared to the top 5 based on the Waterinfo data using the block method, shown in Table 3.1. This can be explained by the fact that the GRADE Reference data is much longer and these discharges are thus more extreme. Furthermore, the timing of these extremely low discharges differs between the two data sets. For the Waterinfo data the minima occur in autumn or winter, whereas for the GRADE Reference data the minima occur throughout the whole year, but most often during spring.

Appendix J shows the estimated parameters for the GEV distribution for both the Waterinfo data and the GRADE Reference data. The value of ξ is fairly similar for all durations in both data sets. The value of σ increases with increasing duration for both data sets, however, the value is generally lower for the GRADE Reference. The same observations hold for μ . The value of $\frac{\sigma}{\mu}$ remains constant for the Reference data at a value of about 0.24. This is similar to the value of $\frac{\sigma}{\mu}$ for the Waterinfo data, which ranged from 0.21 to 0.26.

The fits for the Waterinfo and GRADE Reference scenario, based on the estimated parameters from Appendix J, are shown in Figure 3.15. This figure shows that for similar return periods the LFFC based on the GRADE Reference data consistently estimates lower discharges. Both data sets show that the 1 and 7-day duration fits are very close to each other, whilst the 90 and 180 day durations are clearly separable.

The Q-Q plots shown in Figure 3.16 show the same results. In addition, they show that the difference between estimated discharges becomes higher for smaller return periods paired with the higher discharges.

Table 3.5 shows the return periods corresponding to the discharges of $1000 \text{ m}^3/\text{s}$ and $1200 \text{ m}^3/\text{s}$. It shows that the GRADE Reference always has a lower return period, which is in line with the Q-Q plots.

As mentioned in Section 3.1.1 under [Multi-day minimum](#) the discharge in 2018 was 732, 737, 789, 852 and $1017 \text{ m}^3/\text{s}$ for a duration of 1, 7, 30, 90 and 180 days respectively. They correspond with a

return period of 17.6, 22.4, 21.8, 30.5 and 29.5 years based on the Waterinfo fit. The return periods are all lower based on the GRADE Reference fit: 4.7, 5.1, 6.4, 12.6 and 14.1 years. The other way around, taking the return periods of the corresponding durations in 2018, results in the following discharges based on the GRADE Reference fit: 436, 425, 457, 593 and 745 m^3/s . These are all much lower than the 2018 discharges.

Discharge	Data set	1 day	7 days	30 days	90 days	180 days
1000 m^3/s	Waterinfo	2.3	2.6	4.2	10.1	34.0
	GRADE Ref	1.4	1.5	2.1	5.1	16.0
1200 m^3/s	Waterinfo	1.3	1.4	1.9	3.8	8.5
	GRADE Ref	1.1	1.1	1.3	2.3	4.8

Table 3.5: Values of return periods (in years) for a discharge of 1000 and 1200 m^3/s for the Waterinfo and GRADE Reference data sets.

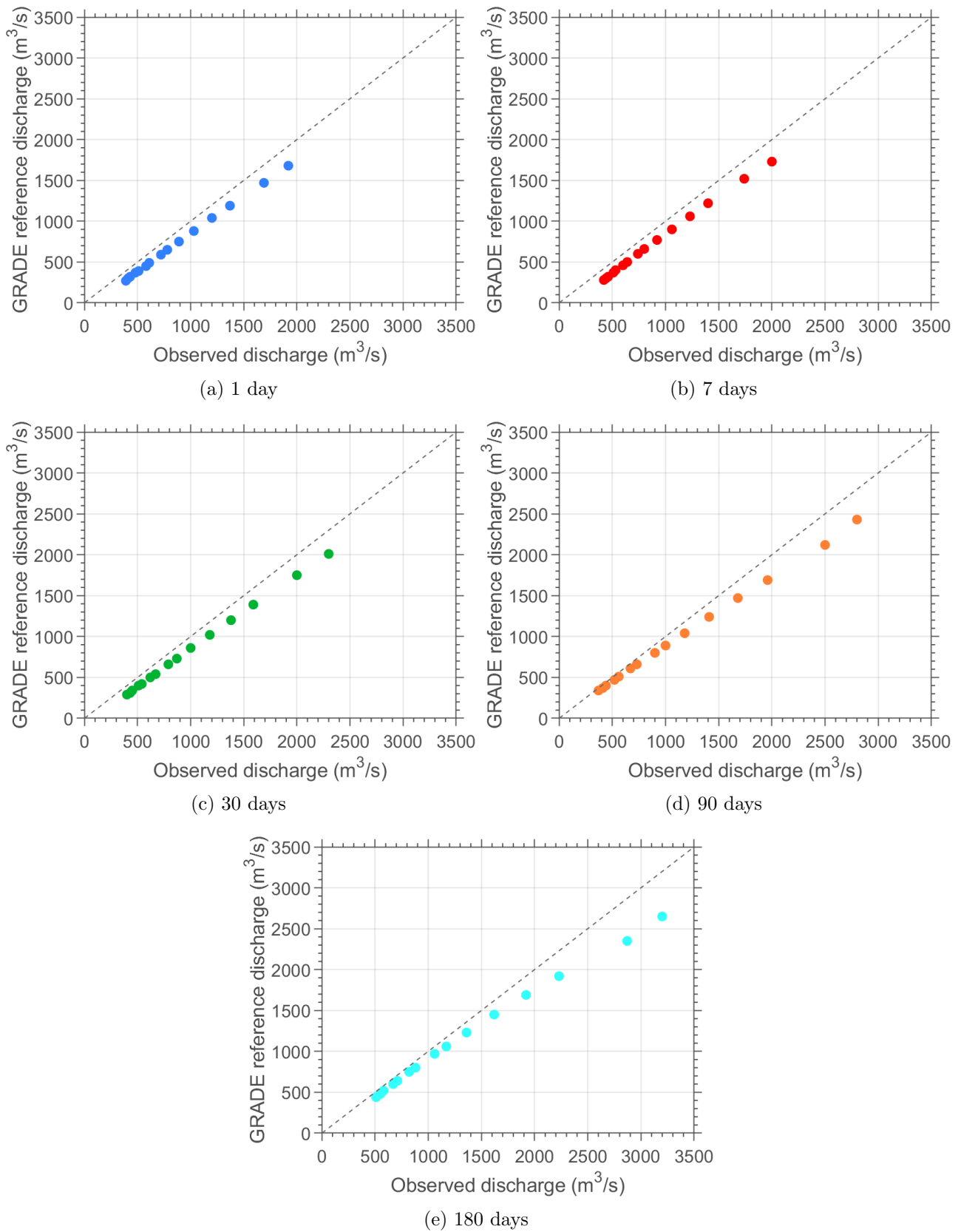


Figure 3.16: QQ plot of GRADE Reference fit compared to the Waterinfo fit.

3.3 Influence of climate change (RQ 3)

First the results of the LFFCs of the GRADE climate scenarios are given, after which they are compared to the LFFC of the GRADE Reference scenario.

3.3.1 LFFC for the GRADE climate scenarios

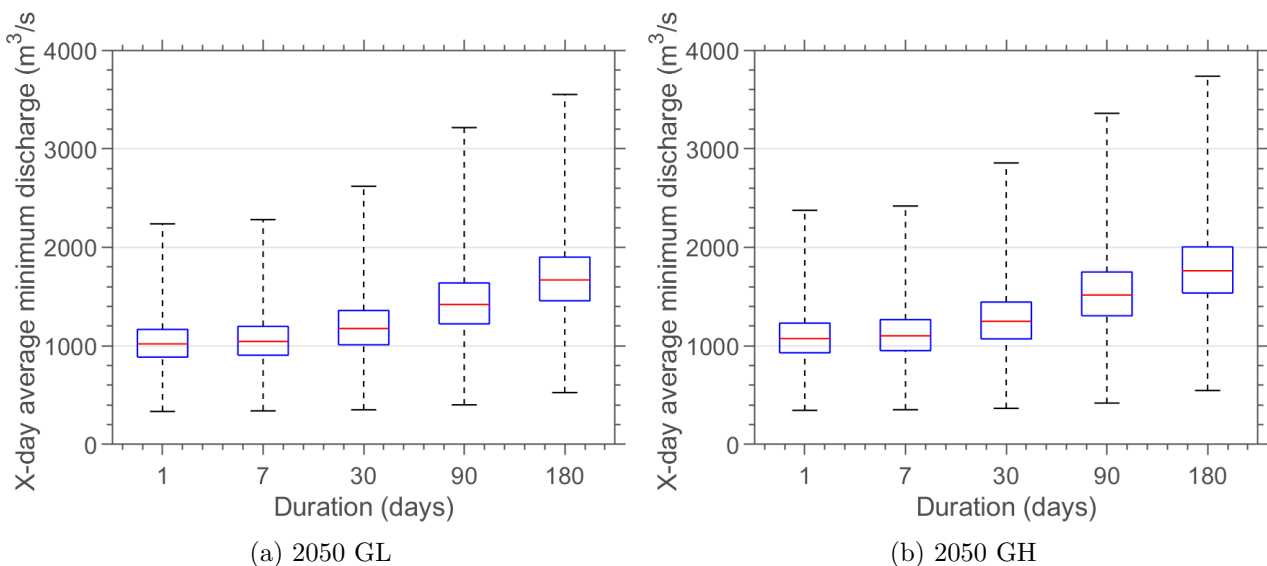
Figure 3.17 shows an overview of the selected annual minima for each KNMI'14 scenario for each duration as a boxplot. The same general observations can be made as for Figure 3.13: the median increases slightly with increasing duration and half of the discharges are very close to the median and the other half has a wider range. The estimated GEV parameters based on these annual minima are given in Appendix J.

Table 3.6 shows the top 5 lowest discharges for all 5 durations for the most extreme climate scenario's: *GL* and *WH* in both 2050 and 2085. The timing of these extremes do not correspond with the expectation of low discharges occurring in October and November, as mentioned in Section 1.1.1.

Figure 3.18 shows the estimated fit for the 2050 climate scenarios and the GRADE Reference scenario for the 5 different durations. It shows that the Reference scenario is the scenario with the lowest discharges. Between the climate scenarios, 2050WH often gives the lowest discharges and 2050GL gives the highest discharges. The 2050WL scenario gives the second highest discharges followed by the 2050GH scenario.

Figure 3.19 shows the estimated fit for the 2085 climate scenarios and the GRADE Reference scenario for the 5 different durations. Similar observations can be made as for the 2050 scenarios in Figure 3.18: the Reference scenario has the lowest discharges for all durations, the 2085WH scenario generally gives the lowest discharges of the climate scenarios and 2085GL gives the highest discharges. The 2085WL and GH scenarios are very similar for the lower durations. For the 90 and 180 day duration, the 2085GH scenario gives slightly lower discharges than the 2085WL scenario, which is contrary to the 2050 scenarios.

Table 3.7 shows return periods for different durations corresponding with a discharge of 1000 and 1200 m^3/s . The *GL* scenarios have higher return periods than the *WH* scenarios, with the biggest difference for the 180 days duration.



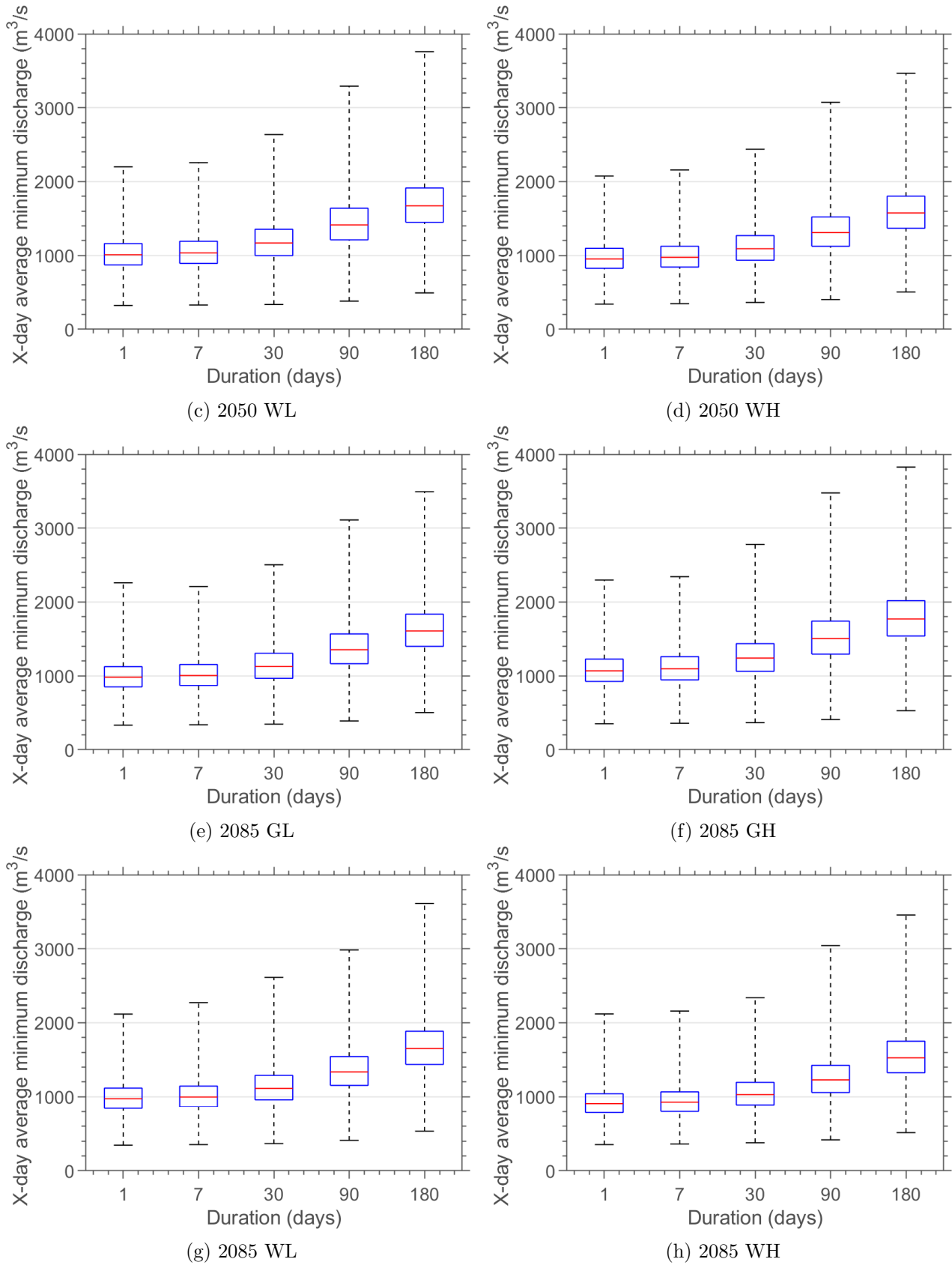


Figure 3.17: Boxplots of selected annual minima for the different GRADE climate scenarios for different durations.

		#1	#2	#3	#4	#5
2050	GL					
	1 day	346 (Mar 10*)	381 (Mar 16*)	393 (Feb 15*)	398 (Feb 7*)	408 (Jan 11*)
	7 days	352 (Mar 10*)	384 (Mar 16*)	402 (Feb 15*)	403 (Feb 7*)	418 (Mar 17*)
	30 days	366 (Mar 10*)	399 (Apr 10*)	416 (Mar 16*)	438 (Apr 16*)	439 (Feb 7*)
	90 days	419 (Mar 10*)	420 (Apr 10*)	475 (Mar 16*)	523 (Apr 16*)	534 (Mar 15*)
180 days	547 (Apr 10*)	572 (Apr 16*)	629 (Mar 10*)	631 (Mar 16*)	642 (Apr 15*)	
2050	WH					
	1 day	341 (Feb 10*)	378 (Dec 14*)	383 (Jan 11*)	386 (Dec 9*)	390 (Dec 8*)
	7 days	348 (Feb 10*)	386 (Dec 14*)	390 (Jan 11*)	394 (Dec 9*)	397 (Dec 8*)
	30 days	364 (Mar 10*)	397 (Apr 10*)	417 (Jan 11*)	417 (Dec 14*)	423 (Dec 9*)
	90 days	403 (Mar 10*)	405 (Apr 10*)	471 (Mar 16*)	474 (Apr 16*)	490 (Dec 8*)
180 days	506 (Apr 10*)	540 (Apr 16*)	552 (Mar 10*)	568 (Mar 16*)	606 (Mar 15*)	
2085	GL					
	1 day	352 (Mar 10*)	396 (Mar 16*)	400 (Feb 15*)	401 (Feb 7*)	402 (Jan 11*)
	7 days	358 (Mar 10*)	400 (Mar 16*)	406 (Feb 7*)	410 (Feb 15*)	413 (Jan 11*)
	30 days	366 (Mar 10*)	388 (Apr 10*)	427 (Mar 16*)	439 (Feb 7*)	444 (Mar 16*)
	90 days	409 (Apr 10*)	414 (Mar 10*)	484 (Mar 16*)	486 (Apr 16*)	529 (Jan 14*+1)
180 days	529 (Apr 10*)	578 (Apr 16*)	609 (Mar 10*)	628 (Mar 16*)	638 (Apr 15*)	
2085	WH					
	1 day	354 (Feb 10*)	367 (Nov 12*)	368 (Dec 14*)	378 (Dec 8*)	384 (Dec 9*)
	7 days	362 (Feb 10*)	374 (Nov 12*)	376 (Dec 14*)	384 (Dec 8*)	390 (Oct 13*)
	30 days	378 (Mar 10*)	397 (Dec 14*)	414 (Apr 10*)	415 (Nov 12*)	417 (Dec 9*)
	90 days	418 (Mar 10*)	421 (Apr 10*)	474 (Dec 8*)	484 (Dec 14*)	492 (Nov 13*)
180 days	516 (Apr 10*)	549 (Mar 10*)	585 (Apr 16*)	592 (Mar 16*)	592 (Jan 11*)	

Table 3.6: Top 5 lowest discharges (m^3/s) using the GRADE 2050GL, 2050WH, 2085GL and 2085WH data. Note that the numbers 7* until 17* represent different years, as the years from the simulation are not relevant. All years are different from the Reference top 5 in Table 3.4. The top 5's from other scenarios can be found in Appendix K.

Discharge	Data set	1 day	7 days	30 days	90 days	180 days
1000 m^3/s	2050GL	2.7	3.0	5.9	27.3	222.1
	2050WH	1.7	1.8	2.8	8.4	58.4
	2085GL	2.6	2.9	5.6	25.1	221.2
	2085WH	1.5	1.5	2.2	5.6	42.3
1200 m^3/s	2050GL	1.4	1.5	2.3	6.5	27.9
	2050WH	1.2	1.2	21.5	2.8	10.0
	2085GL	1.4	1.5	2.2	6.2	28.2
	2085WH	1.1	1.1	1.3	2.2	7.8

Table 3.7: Values of return periods (in years) for a discharge of 1000 and 1200 m^3/s for the GRADE Reference and most diverse GRADE climate scenarios data sets.

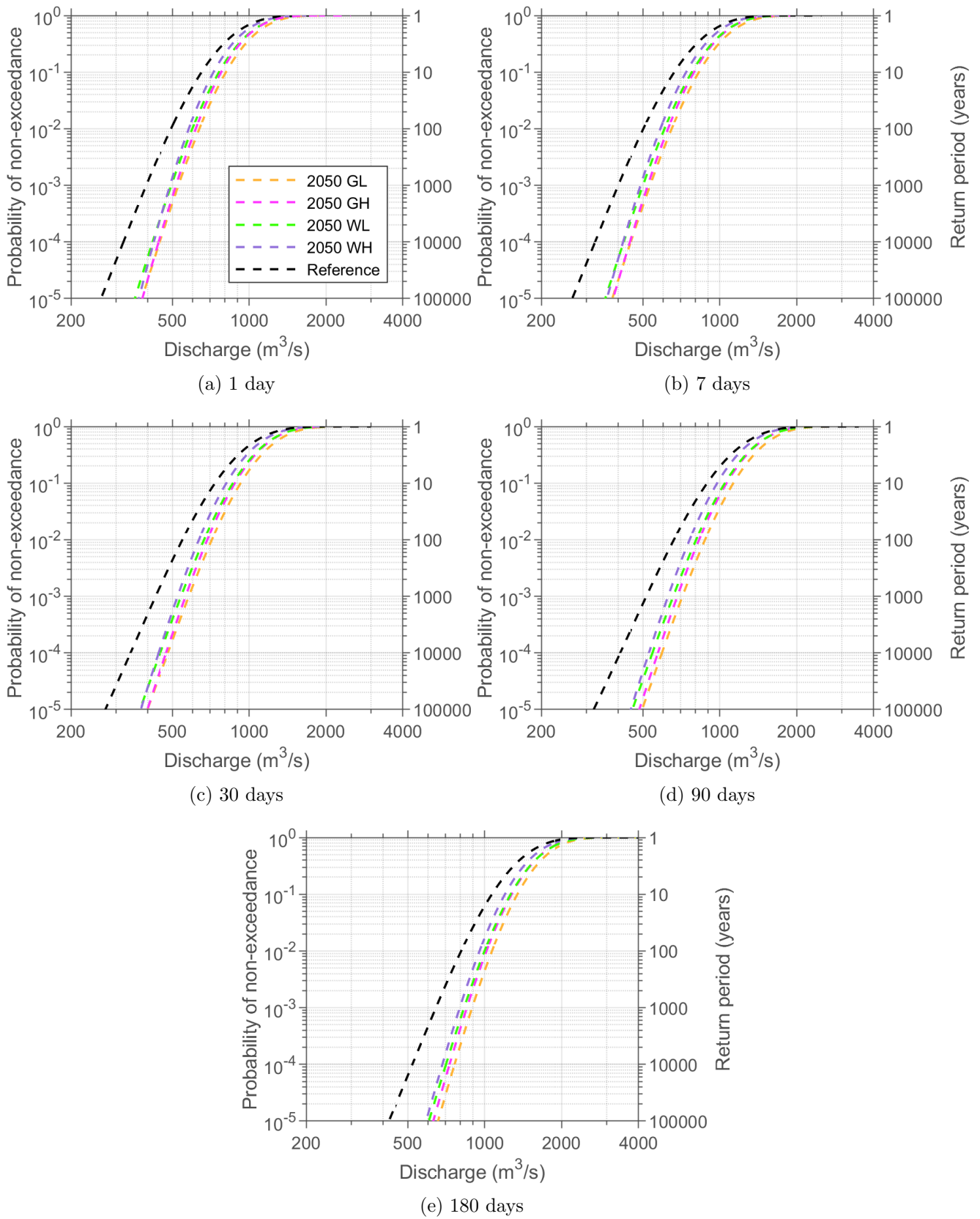


Figure 3.18: Extrapolation of minimum annual discharges for different climate scenarios for 2050 per duration.

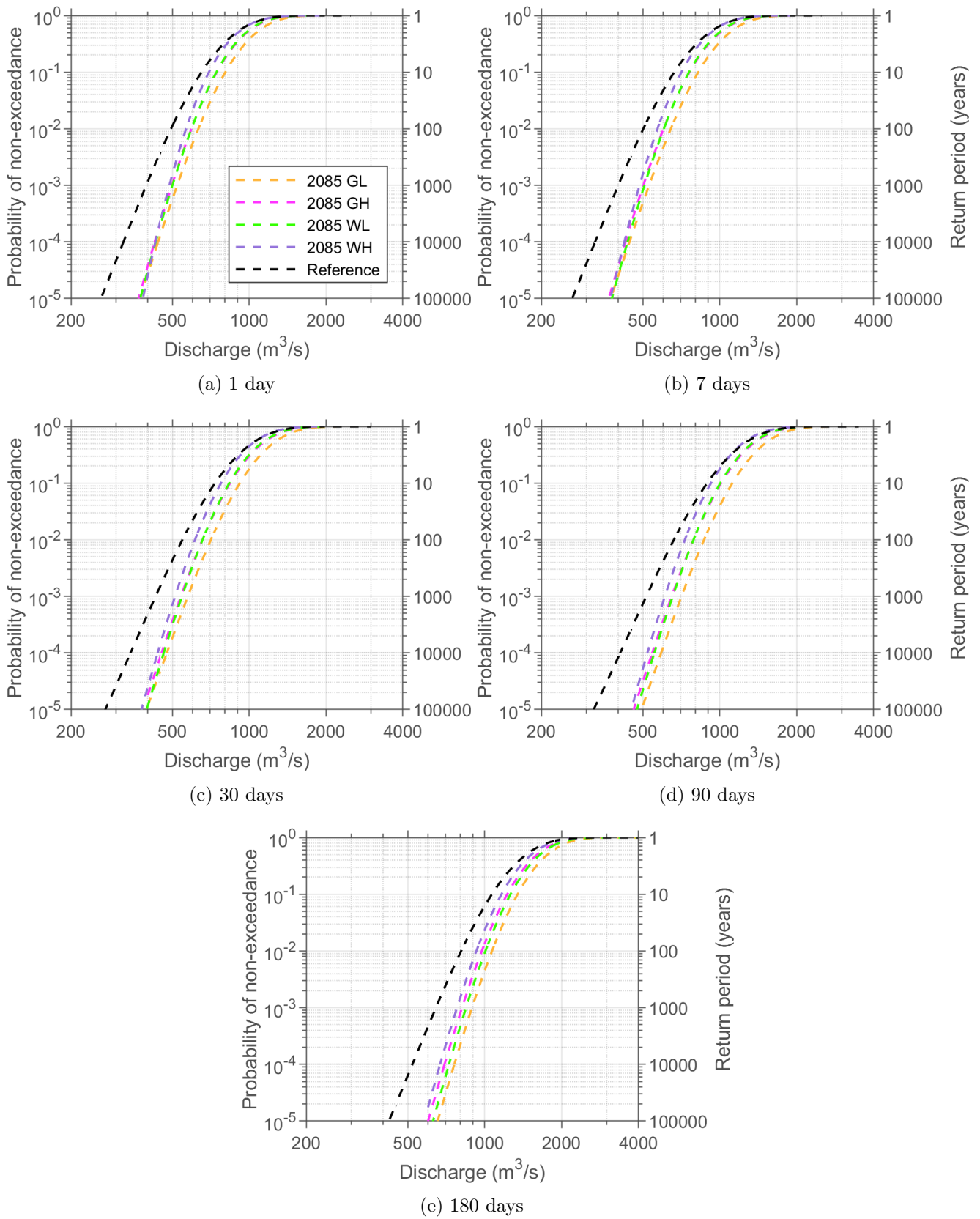


Figure 3.19: Extrapolation of minimum annual discharges for different climate scenarios for 2085 per duration.

3.3.2 Comparison

The top 5 lowest discharges for all 5 durations for the climate scenarios 2050GL, 2050WH, 2085GL and 2085WH, shown in Table 3.6 are all higher compared to the GRADE Reference scenario, shown in Table 3.4. This means that according to the GRADE model extreme low flow events will likely become less extreme in the future. The timing of these events differs for the *GL* and *WH* scenarios. For the *GL* scenario the extremely low flow events are likely to occur in March, similar to the Reference scenario, whereas for the *WH* scenario they are likely to occur in December. What stands out from Table 3.6 is that year d has the lowest discharges for all scenarios and durations. Furthermore, the years d and j often occur more than once for a duration, once before April and once in April. This has the same explanation as the Reference data in Table 3.4, as the shifted hydrological year is used to determine the borders of a year. However, this might not be the best option for the climate scenarios.

The estimated GEV parameters for the GRADE Reference data and all 8 climate scenarios are given in Appendix J. The value of ξ does not differ much between all data sets and all fits are very likely to be a Weibull distribution. For all scenarios the value of σ and μ increase with increasing duration, but $\frac{\sigma}{\mu}$ remains constant. For the climate scenario, this value ranges from 0.20 to 0.21, for the Reference scenario this value ranges from 0.23 to 0.24 and for the Waterinfo data this value ranges from 0.21 to 0.26.

Figure 3.20 and 3.21 show the LFFCs for all durations for the GRADE Reference scenario and the 2050 *GL* and *WH* and the 2085 *GL* and *WH* scenario, which are the most diverse climate scenarios. Figure 3.20 again shows the GRADE Reference scenario gives the lowest discharges for all durations, followed by the 2050WH and the 2050GL scenario. The 1, 7 and 30 day duration are close to each other for each of the three scenarios. The 1 and 7 day duration for the 2050WH scenario give higher discharges than the 30 day duration for the GRADE Reference scenario for higher return periods. The 1, 7 and 30 day duration for the 2050GL scenario even give higher discharges than the 90 day duration for the GRADE Reference scenario for higher return periods. The same observations hold for the 2085GL and 2085WH scenarios shown in Figure 3.21.

Figure 3.22 shows the LFFCs for the Waterinfo data, the GRADE Reference and the two most diverse climate scenarios: *GL* and *WH* for both 2050 and 2085. This gives an idea of the range for possible LFFCs based on the KNMI'14 scenarios for the future. The figure shows that the 2085WH scenario has slightly lower discharges than the 2050WH scenario. The figure also shows that the 2050GL and 2085GL scenario do not differ much. All 4 climate scenarios have lower discharges compared to the Reference scenario. This means that extremely low discharges will become less extreme in the future according to the GRADE predictions.

Figure 3.23 and 3.24 show the Q-Q plots for the 4 climate scenarios, 2050GL, 2085GL, 2050WH and 2085WH, compared to the GRADE Reference scenario. The Q-Q plots of the *GL* scenarios, Figure 3.23, show that the GRADE Reference fit always gives lower discharges for the corresponding quantiles than the *GL* scenarios. There also is little difference between the 2050GL and 2085GL scenarios. This is both in line with the observations from Figure 3.22. The Q-Q plots of the *WH* scenarios, Figure 3.24, show that the GRADE Reference fit always gives lower discharges for the corresponding quantiles than the 2050WH scenario. For higher return periods, the 2050WH and 2085WH scenarios seem to have similar discharges, but for higher return periods, the 2085WH scenario will give lower discharges compared to the 2050WH scenario. Furthermore, Figure 3.24 shows that for the 1, 7 and 180 day duration the GRADE Reference fit gives lower discharges for the corresponding quantiles than the 2085WH scenario. However, for the 30 and 90 day duration, the GRADE Reference fit does not always show lower discharges or the corresponding quantiles, but for high quantiles, so small return periods, the 2085WH scenario gives lower discharges than the GRADE Reference fit.

Table 3.7 shows return periods for different durations corresponding with a discharge of 1000 and 1200 m^3/s . Comparing these results to the return periods based on the GRADE Reference data, shown in Table 3.5, shows that the return periods for all scenarios and durations are similar or larger. The 2085WH scenario shows almost the same return periods as the Reference scenario except for the 180 days duration, where it has much higher return periods. The *GL* scenarios have higher return periods than the *WH* and Reference scenarios, with the biggest difference for the 180 days duration. Based on GRADE, the range of results for the *WH* and *GL* scenarios show that discharges of 1000 and 1200 m^3/s have a similar or lower probability of being exceeded in the future compared to the current climate. This means that shipping and salinisation will be less of a problem in the future according to the GRADE model.

As mentioned in Section 3.1.1, the minimum discharges in 2018 were 732, 737, 789, 852 and 1017 m^3/s for a duration of 1, 7, 30, 90 and 180 days respectively. They correspond with a return period of 17.6, 22.4, 21.8, 30.5 and 29.5 years based on the Waterinfo fit. The return periods are all lower based on the GRADE Reference fit: 4.7, 5.1, 6.4, 12.6 and 14.1 years, as stated in Section 3.2.2. The corresponding return periods for the 2018 discharges based on the 2085GL scenario are: 22.6, 25.4, 34.8, 120.5 and 179.5 years. The corresponding return periods for the 2018 discharges based on the 2085WH scenario are: 6.5, 7.2, 8.7, 19.8 and 35.3 years. Comparing the Reference scenarios to the climate scenarios results shows that an event like 2018 will be less likely to happen in the future, especially for the 2085GL scenario.

The other way around, taking the return periods of the corresponding durations in 2018, results in the following discharges based on the GRADE Reference fit: 436, 425, 457, 593 and 745 m^3/s . The corresponding discharges for the 2085GL scenario based on the 2018 drought return periods are: 753, 747, 832, 979 and 1195 m^3/s . For the 2085WH scenario these values are: 655, 649, 708, 815 and 1035 m^3/s . These values show that an event with a similar return period in the future climate will have higher discharges.

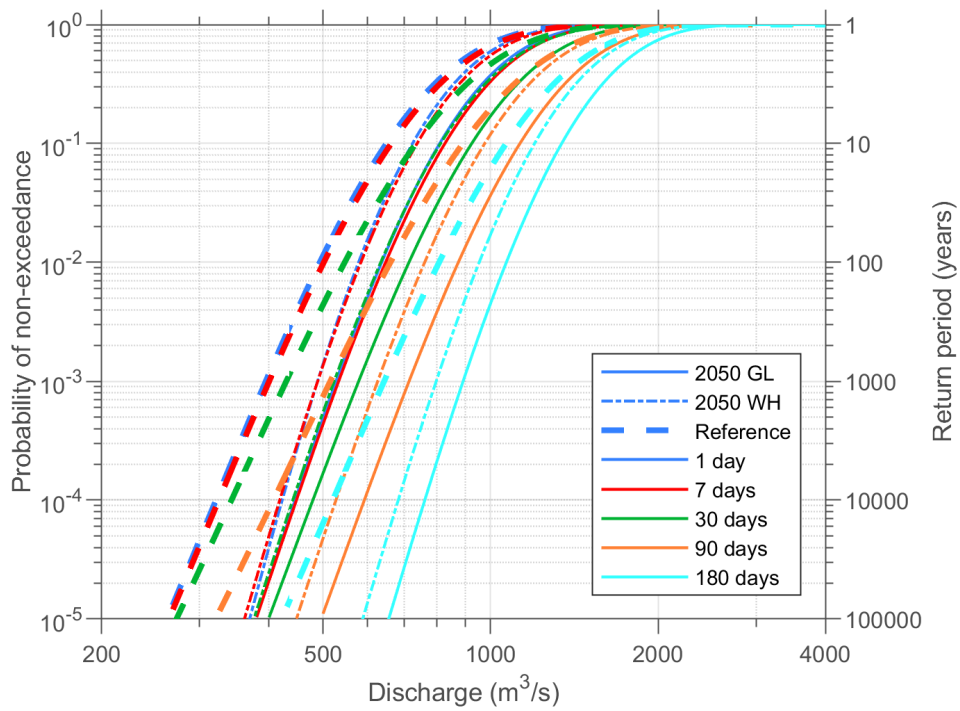


Figure 3.20: Extrapolation of minimum annual discharges for different durations and climate scenarios 2050 GL and 2050 WH.

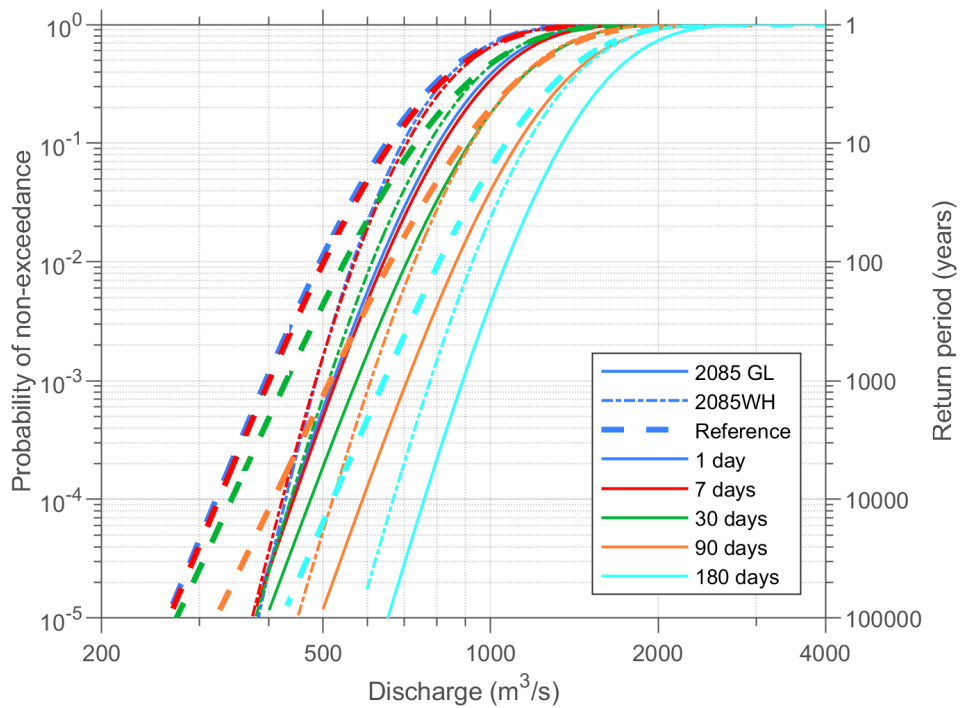


Figure 3.21: Extrapolation of minimum annual discharges for different durations and climate scenarios 2085 GL and 2085 WH.

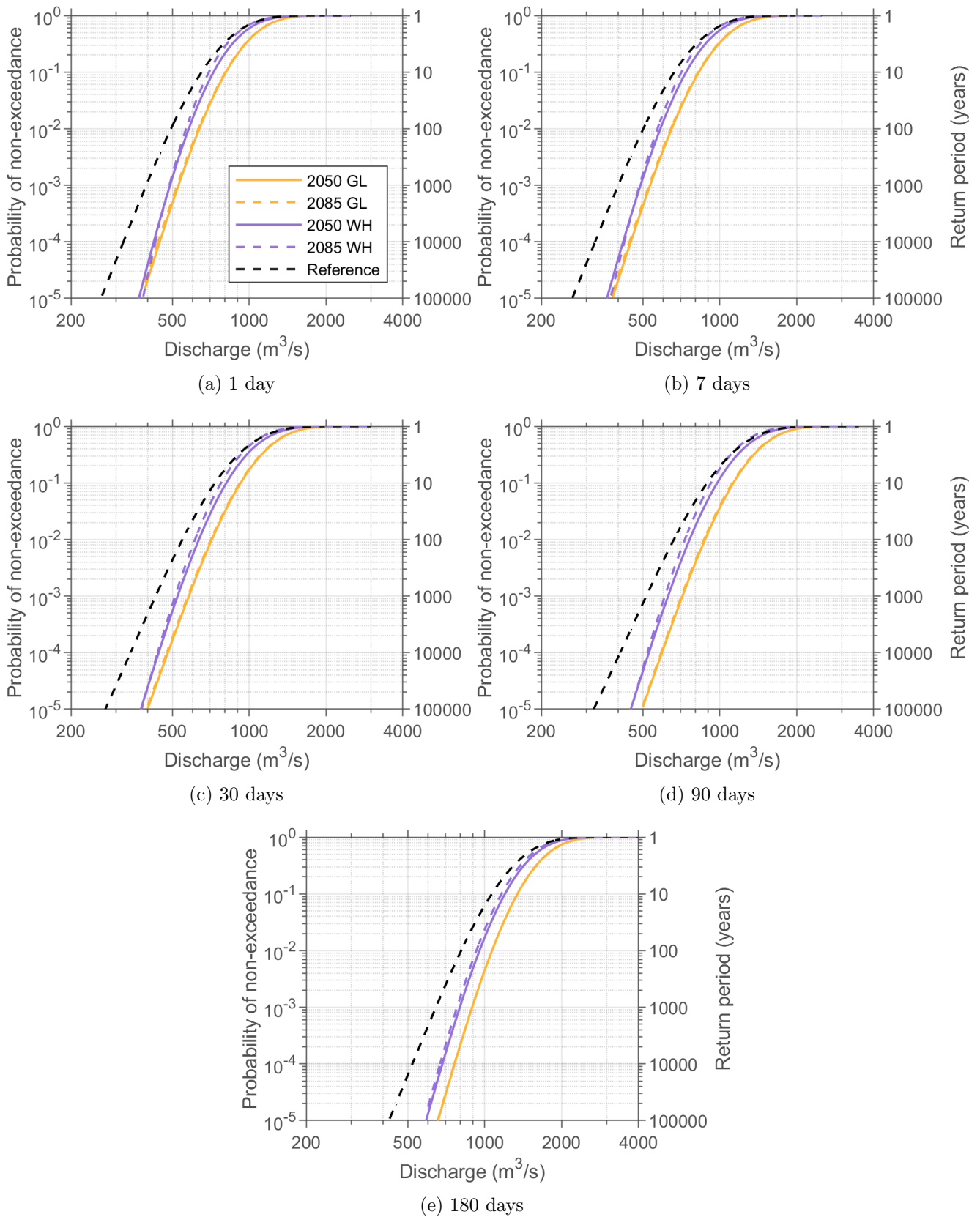


Figure 3.22: Extrapolation of minimum annual discharges for different most varying climate scenarios *WH* and *GL* for 2050 and 2085 per duration.

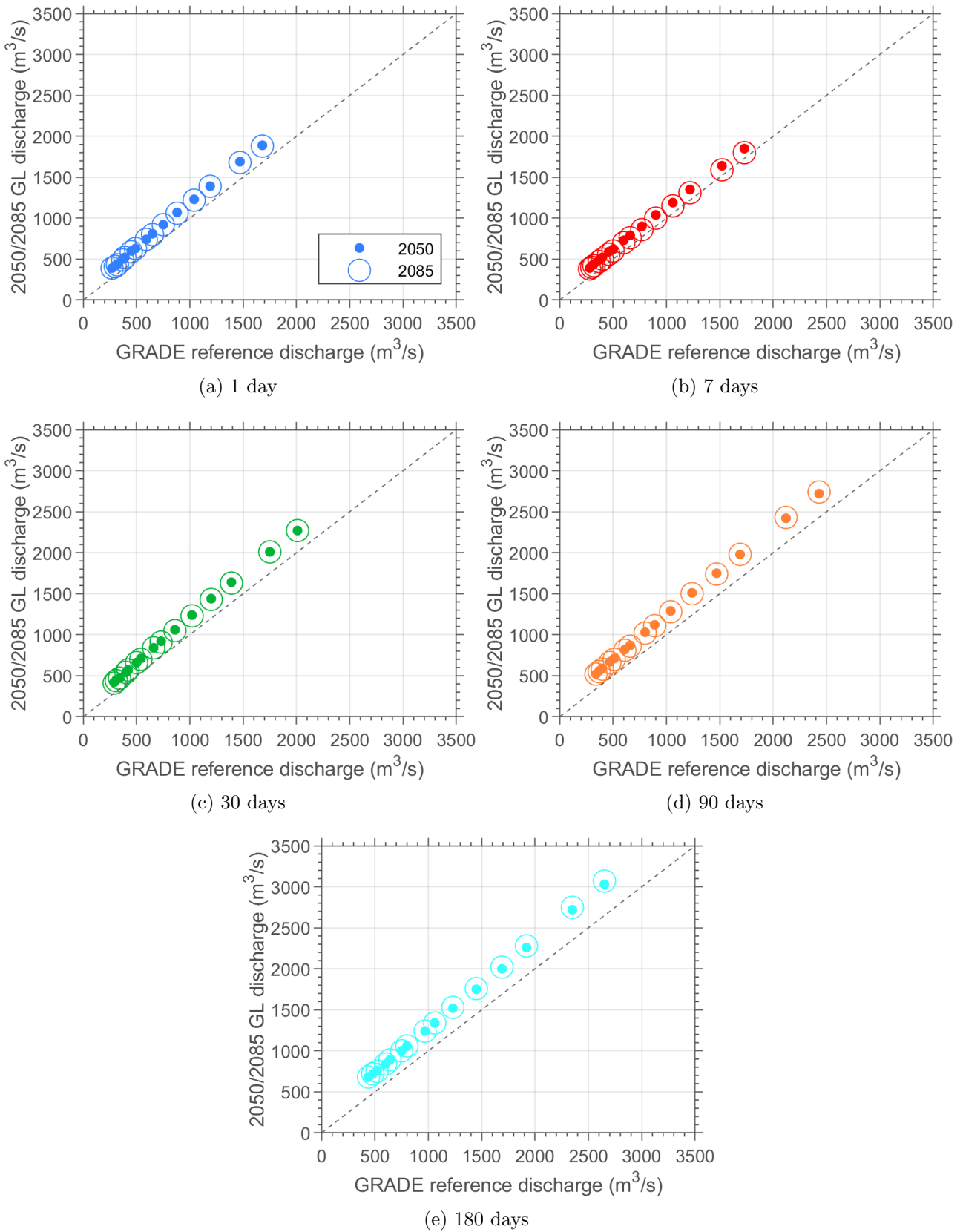


Figure 3.23: QQ plot of 2050 GL and 2085 GL fit compared to GRADE Reference fit.

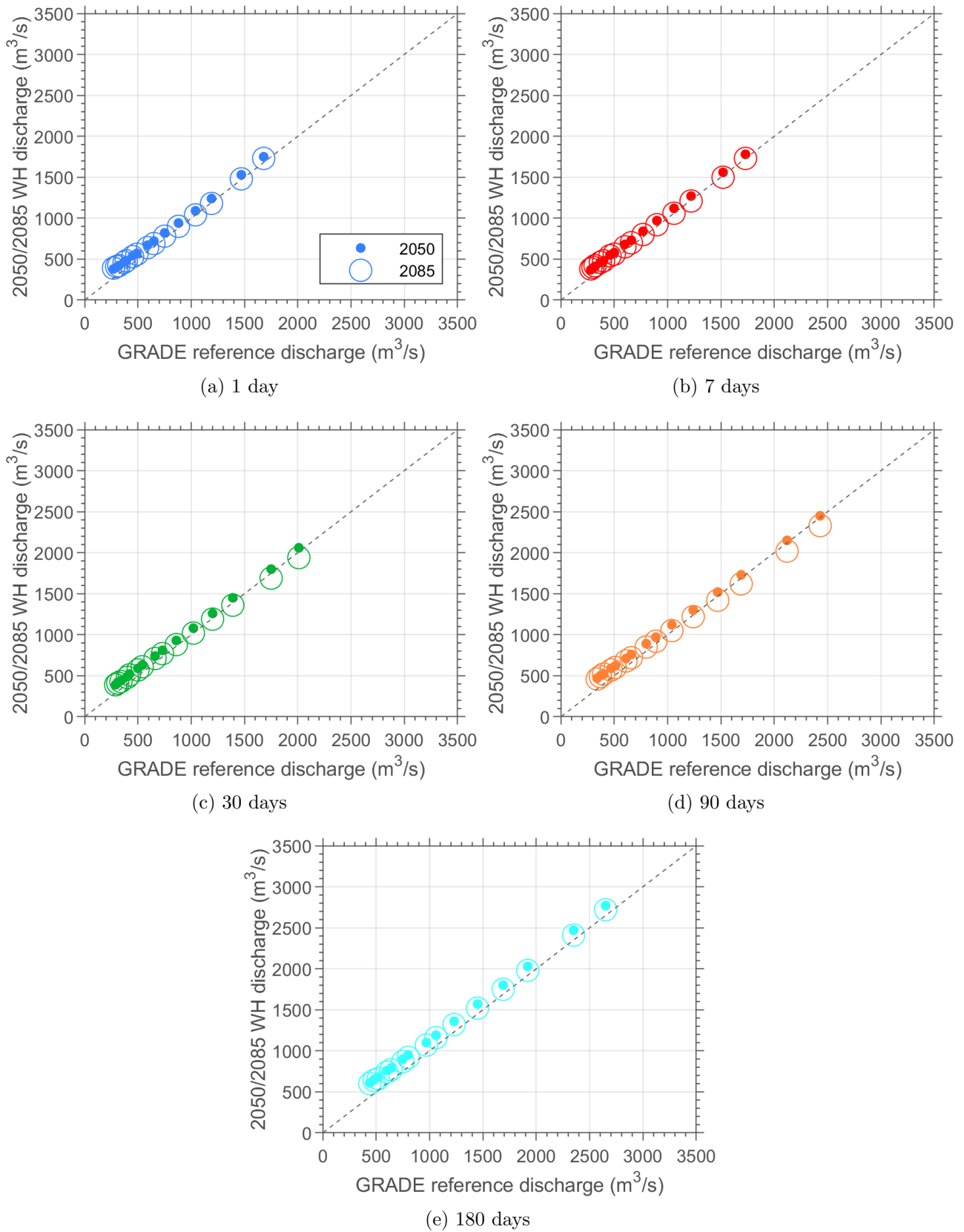


Figure 3.24: QQ plot of 2050 WH and 2085 WH fit compared to GRADE Reference fit.

Discussion

Results gained from this study are put into context by comparing them to recent similar studies, mentioned in Section 1.1.4.

Kramer et al. [2019] estimated that a 135 day period of discharges below $1100 \text{ m}^3/\text{s}$ will take place once every 60 years in the current climate. It will take place more often, once every 20 years, when considering the 2050WH climate scenario. This was done using the NWM. These results cannot be compared one on one to the results of this study, as there is a difference between a period below a threshold and an average minimum discharge. This means the return period determined by Kramer et al. [2019] should be larger than the return period found in this study for an average discharge of $1100 \text{ m}^3/\text{s}$. Figure 3.5 gives a return period of about 10 years for a 135 day event with an average discharge of $1100 \text{ m}^3/\text{s}$. Furthermore, Kramer et al. [2019] showed that return periods will decrease considering the 2050WH scenario. This does not agree with the results of this study, however, it is expected that this is due to the limitations of the GRADE model, on which Section 4.2 will elaborate.

Sperna Weiland et al. [2015] estimates that the NM7Q for the current climate is $1010 \text{ m}^3/\text{s}$ and ranges from 735 to $1095 \text{ m}^3/\text{s}$ in the future climate. The NM7Q might be comparable to the discharge of 7 day event with a return period of 1 year from this study, however, it is expected that results from this study will be higher, as the mean annual lowest discharge is not exactly the same as a 1 year return period. For the current climate Sperna Weiland et al. [2015] give a value of $1010 \text{ m}^3/\text{s}$, whereas this study gives a value of $1934 \text{ m}^3/\text{s}$. For the 2085GL scenario they give a value of $1085 \text{ m}^3/\text{s}$, whereas this study finds a value of $1735 \text{ m}^3/\text{s}$. For the 2085WH scenario they give a value of $915 \text{ m}^3/\text{s}$, whereas this study finds a value of $1506 \text{ m}^3/\text{s}$. The values by Sperna Weiland et al. [2015] are lower compared to this study, which was expected.

4.1 Influence of event selection method (RQ 1)

The first discussion point regarding research question 1 is the fact that the discharges of the Waterinfo data are not directly observed and uncertainty is introduced, which was mentioned in Section 2.1.1. Especially for extremely low flows, the Q-h-relation is not often updated, as they do not often occur. Even though it is unclear how often the Q-h-relation is updated, the Waterinfo discharges are assumed to represent the reality well.

An aspect that influences both the block method and PUT method is the independence of selected low flow events. Currently, there are no guidelines on when low flow events can be considered independent from another low flow event. It is expected that the time between two low flow events needs to be longer than for to high flow events, as groundwater plays a large role in the value of the low discharge and reacts slower than direct runoff from a precipitation event. For the PUT method it was assumed that a low flow event can occur at maximum 4 times per year on average. For the block method, the interdependence of 1 day and 180 day events were looked into using an autocorrelogram, shown in Figure 4.1. This figure shows that there is not much autocorrelation in the selected minima. Apart from the high peak of a correlation of 1 at a lag of 0 years, the highest correlations found are 0.17 for the 1 day duration and 0.34 for the 180 day duration. For the 1 day duration this maximum occurred at a lag of 13 years and for the 180 day duration this maximum occurred at a lag of 1 year. This shows interdependency between low flows is more important for longer durations.

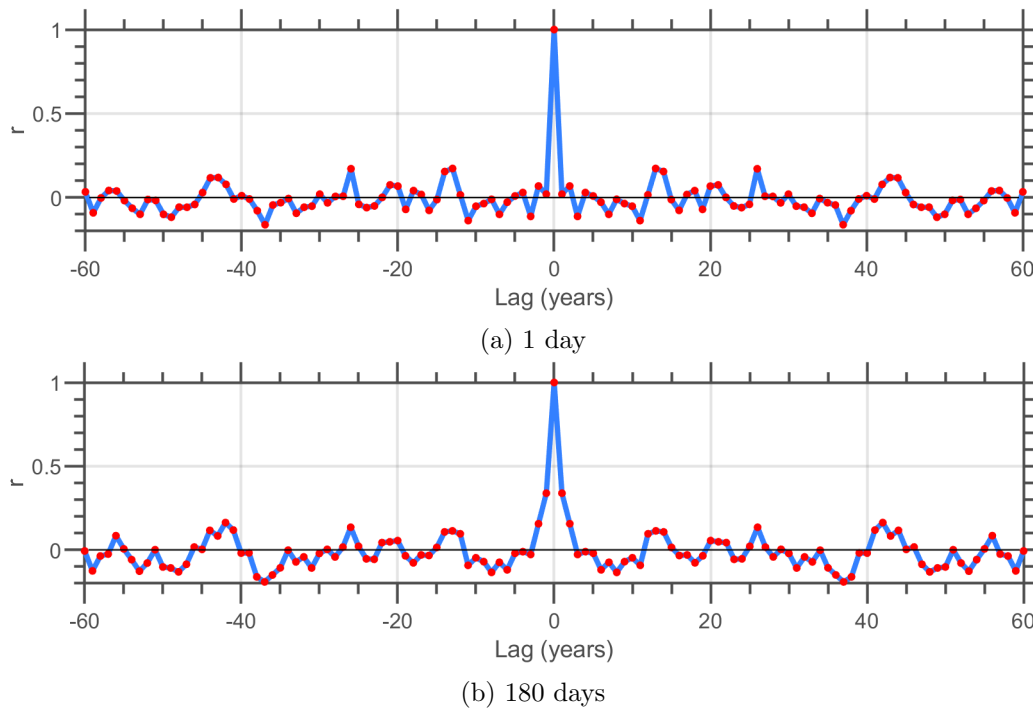


Figure 4.1: Autocorrelation of selected annual minima for a duration of 1 and 180 days.

In the top 5 lowest discharges based on the Waterinfo data using the block method, Table 3.1, several years come up: 1921/22, 1929, 1947, 1949, 1953/54, 1959, 1963 and 2018. According to KNMI [2021b] the top 5 driest years based on precipitation shortage are 1976, 1959, 1911, 1921 and 2018. What is remarkable is that the driest year, 1976, and 1911 do not show up in Table 3.1. The other dry years do show up, which is expected. This shows that precipitation shortage might not be the only factor heavily influencing low discharges. It is expected that not only regional precipitation shortage is important, but the upstream flow component and groundwater levels also play a big role in the discharge value.

The timing of the top 5 lowest discharges during the year, seen in Table 3.1, ranges from November to February. As mentioned in Section 1.1.1, the lowest discharges at Lobith are expected in October and November [Kramer et al., 2019, de Wit, 2004]. The Rhine is a mixed river, which means that the discharge is fed by rain and meltwater. Furthermore, the Rhine has a large catchment with origin in the Alps, where Lake Constance is located. Lake Constance works as a water buffer and has a damping function on the discharge in the Rhine. These three factors result in a discharge regime at Lobith of a dampened rain river: higher discharges in the winter and lower discharges in the summer that do not differ much from the average discharge [Lokin, 2020, Klijn et al., 2015]. The precipitation in the Alps during the winter falls as snow and is thus not directly discharged, but is discharged when it melts in the spring. This results in the lowest discharges occurring in October and November, when the snow is already melted and discharged, but the heavy precipitation from the winter has not yet fallen. Additionally, Lokin [2020] states that from June to August the discharge at Lobith consists of almost 70% alpine meltwater on average and in January and February the discharge consists of about 70% rainfall on average. This also shows that the autumn months lie in between the rainfall and meltwater peaks, resulting in lower discharges. The low flows in the top 5 which occurred in January and February showed another explanation for the low discharges, as ice was present in the river Rhine in 1929 and 1963 [de Wit, 2004]. It is expected that either the ice causes extra friction, which slows the water down and lowers the discharge or that the water that formed the ice is not measured as discharge.

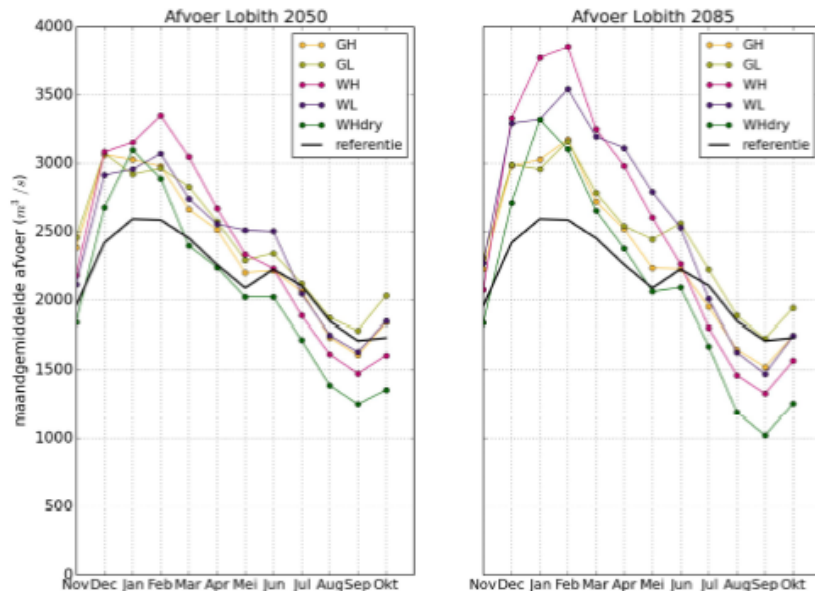


Figure 4.2: Expected average monthly discharges (m^3/s) at Lobith based on GRADE [Klijn et al., 2015]. (In Dutch 'referentie' means reference and 'afvoer' means discharge)

4.2 Influence of GRADE (RQ 2)

The fit on the GRADE Reference scenario consistently gives lower discharges than the Waterinfo data, as shown by the Q-Q plots in Figure 3.16. Table 2.1 and 2.2 show that the mean and minimum of the GRADE Reference data are lower compared to the Waterinfo data and the climate scenarios. As the GRADE model is currently primarily used to evaluate high flows, it is expected that the model is calibrated for this purpose and may perform worse for low flows and other applications.

The LFFC from the GRADE data, Figure 3.14, shows that the observations fit tightly on the fitted distribution. This is less visible for the Waterinfo data. This raises the question whether this is due to the difference in the number of selected minima or if the model lacks some physical variability in the weather generator for example. This last uncertainty in the model is mentioned by Bomers [2020], who used high discharge series of GRADE in her study into decreasing uncertainty in flood frequency relations. The weather generator introduces uncertainty, as the variability in the data set is based on only 56 years of daily observations.

Kersbergen [2016] studied the GRADE model for low flows and concluded that the model performs well for determining the return period of durations of events at Lobith. However, the model performs well for the wrong reasons as two parts of the model cancel their mistakes. The weather generator does not simulate extreme dry periods and the simulation of snow is not good at every location. This results in higher low flows, which are countered by the HBV model, which underestimates the low discharges and causes more and more severe low flows. Kersbergen [2016] recommends not using the GRADE model in its current condition for estimating probabilities of low flows.

In addition, it is known that the HBV model in the GRADE model discharges really fast. For low flow situations this means that water might be discharged too early, leaving little water resulting in extremely low flows. Furthermore, it is known that the behaviour of glaciers and snow is implemented roughly in the HBV model. This is due to the fact that this is less important for high flows than for low flows. The performance of the glaciers and snow in the model might also contribute to the extremely low flows. These two factors might also explain the dip in monthly averages in April shown in Figure 4.2. In April it is expected that rainfall is still important, but is discharged too fast, and that meltwater is starting to become more important, but is not working optimally yet in the model.

Another explanation for the performance can be the fact that groundwater and in particular deep groundwater are not modelled (well) and thus drying of the soil is not simulated well. Especially multiyear droughts are then not predicted well. Propagation of meteorological drought conditions through the hydrological cycle during multiyear drought involves several nonlinear responses and is very complex [van Dijk et al., 2013]. This makes simulations of low flows less accurate.

The top 5 lowest annual flows shown in Table 3.4 show different timing to the Waterinfo data. Most low discharges occur in April and May. This does not line up with the statement that lowest discharges at Lobith occur in October and November. However, this matches the previous explanation of the dip in monthly averages in April, seen in Figure 4.2. The low flows occurring in April and May raise the question whether a shifted hydrological year (April - March) is a good method for placing annual boundaries when the GRADE model is used. However, it could also be a model issue.

Summarising, it is expected that GRADE does not perform well for low flows as the model is calibrated for high flows. First steps into calibration for low flows are taken in Davids et al. [2015], however, the performance for high flows is lowered compared to the current GRADE model. Currently, the model does not perform well for low flow events and especially not for extremely low flow events, which occur at a different timing compared to the expected October and November. This is expected to be due to the performance of glaciers and snow, fast discharging and (deep) groundwater.

4.3 Influence of climate change (RQ 3)

The fits on the 8 GRADE climate scenarios generally give higher discharges than the fit on the GRADE Reference scenario, as shown by the Q-Q plots in Figure 3.23 and 3.24 among others. Table 2.2 shows that the mean and minimum of the GRADE Reference scenario are lower compared to the climate scenarios. Interesting is the fact that the minimum and average discharge value are lowest for the Reference scenario, but the maximum discharge is not lowest for the Reference scenario. The reason for the low Reference values compared to the climate scenarios is unknown at the moment, but it probably has to do with the fact that the model is calibrated for high flow applications.

The timing of the top 5 lowest discharges differs between the *GL* and *WH* scenarios. For the *GL* scenario the events occur in spring and for the *WH* scenario they occur during the winter. The *GL* scenario is based on a slight increase in the worldwide temperature and little change in the air current patterns, as explained in Section 1.1.3. The *WH* scenario is based on a higher increase in the worldwide temperature and more change in the air current patterns. The difference in timing can thus be due to the fact that the temperature is higher or the different air current patterns. Currently, the winter discharge at Lobith consists mostly of rainfall and spring discharges consist of a mix of rain and meltwater [Lokin, 2020]. It is expected that the change in air current patterns for the *WH* scenarios results in less precipitation in the winter compared to the *GL* and Reference scenario, even though the change in air current patterns is generally paired with the thought of a wetter climate during the winter. Another reason for the difference in timing might be the fact that the GRADE model is calibrated for use of high flows and this can introduce errors for the low flows. What the exact reason for the difference in the timing of the extreme minima is currently unknown.

Comparing the LFFCs of Figure 3.22 to the monthly averages given in Figure 4.2 leads to the observation that they do not give the same results. The lowest monthly average is found for the 2050WH and 2085WH scenario and occurs in September. The *GL* scenarios have the highest monthly discharges in September. The fact that the *WH* scenarios result in lower discharges than the *GL* scenarios is in line with this study, for example Figure 3.22. The timing of the low flow events, however, does not match with Figure 4.2 or the October or November observations [de Wit, 2004]. However, these results cannot be compared one on one, as they look into different aspects, namely the average and minimum discharge values. And as stated in the previous section, the GRADE model is expected to not perform well for extremely low flows.

Conclusion & Recommendations

Concluding from this study, the return period of the low flows in 2018 can be quantified. Furthermore, a framework is given to make LFFCs that include the key aspects for low flows: discharge, duration and interdependency between low flow events. With this method and climate scenario discharge data, the influence of climate change on the return period of low flows can be determined. However, the GRADE model that is used in part of this study is not simulating low flows well enough to reasonably determine low flow return periods.

The 180 day discharge of 2018, which was $1017 \text{ m}^3/\text{s}$, has a return period of 29.5 years. The drought of 2018 was severe due to the length of the event, as the discharges for the shorter durations had smaller return periods. Figure 3.5 on page 24 gives an overview of return periods for different durations and discharges. This contour plot interpolates the 1, 7, 30, 90 and 180 days LFFCs to be able to determine different return periods for different combinations of durations and discharges. A visual representation of the return periods of 2018 and 2018-like events in the future is given in Figure 5.1.

A 1 day discharge of $732 \text{ m}^3/\text{s}$, which was the minimum of 2018, is likely to occur once every 17.6 years. However, due to climate change this can occur once every 6.5 to 22.6 years in 2085 based on the KNMI'14 scenarios and the GRADE model. In 2085, a 1 day event that will occur once every 17.6 years will have a discharge between 655 and $753 \text{ m}^3/\text{s}$. This shows that whether a 1 day event similar to 2018 is likely to become more or less common, depends on which climate scenario evolves to be more realistic.

A 30 day discharge of $789 \text{ m}^3/\text{s}$, which was the minimum of 2018, is likely to occur once every 21.8 years. However, due to climate change this can occur once every 8.7 to 34.8 years in 2085 based on the KNMI'14 scenarios and the GRADE model. In 2085, a 30 days event that will occur once every 21.8 years will have a discharge between 708 and $832 \text{ m}^3/\text{s}$. This again shows that whether a 30 day event similar to 2018 is likely to become more or less common, depends on which climate scenario evolves to be more realistic.

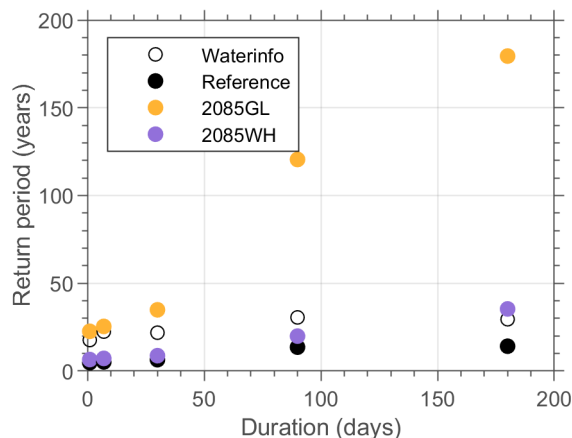


Figure 5.1: Return periods of 2018-like events for different durations and climate scenarios.

5.1 Influence of event selection method (RQ 1)

The first research question was: *"What is the influence of different low flow event selections on the return period for the low flows and their corresponding duration on the Rhine at Lobith in the current situation?"*. The two methods used to select low flow events are the block method and the peak-under-threshold method.

The methods differ in how they determine events and the distribution they fit. The block method takes less events into account than the PUT method, which makes the PUT method more favourable. However, the block method results in a better fit for the Waterinfo data, shown in Figure 3.3, compared to the PUT method, shown in Figure 3.9. Therefore, the block method is used in the remainder of this study. Q-Q plots, Figure 3.12, show that the biggest differences between the two methods are found for the lower return periods and higher range of discharges, where the block method gives higher discharges.

Figure 3.4 gives the estimated fits for the 1, 7, 30, 90 and 180 day durations using the block method on the Waterinfo data and the corresponding 95% confidence interval. The estimated values for ξ are almost all below 0, making it highly certain that a Weibull distribution is the best fit for the data. The Weibull distribution was also found in literature to be a good fit for low flow events. The fitted parameters for the GEV and GP fit on Waterinfo data are given in Appendix J.

5.2 Influence of GRADE (RQ 2)

The second research question was: *"How do the results based on measured data and GRADE data compare?"*.

The GRADE Reference data and its estimated GEV fit showed constantly lower discharges compared to the Waterinfo data, shown in Figure 3.15. This is consistent with the Q-Q plots in Figure 3.16. The biggest difference between the two estimated fits is for the higher discharges, which occur more often. It is expected that this underestimation of the discharge is due to the fact that the GRADE model is primarily calibrated for high flow applications. The HBV model discharges water very fast and glaciers and snowmelt are implemented roughly into the model. Besides the low discharge values, the timing of the top 5 lowest discharges differs from the Waterinfo data and expectations. Most extremely low flow events in GRADE occur in spring, whilst the Waterinfo and expectations are that this occurs in autumn.

The GRADE Reference data suggest that we need to be more scared of problems regarding shipping and salinisation compared to the Waterinfo data. These problems occur at a discharge of 1000 and 1200 m^3/s respectively. Currently, they occur once every 2.3 and 1.3 years for a duration of 1 day, once every 4.2 and 1.9 years for a duration of 30 days and once every 34.0 and 8.5 years for a duration of 180 days, for a discharge of 1000 and 1200 m^3/s respectively. According to the GRADE Reference data this will occur more often: once every 1.4 and 1.1 years for a duration of 1 day, once every 2.1 and 1.3 years for a duration of 30 days and once every 16.0 and 4.8 years for a duration of 180 days, for a discharge of 1000 and 1200 m^3/s respectively.

Figure 3.14 gives the selected annual minima and their estimated fit. The fitted parameters for the GEV fit on the GRADE Reference scenario are given in Appendix J.

5.3 Influence of climate change (RQ 3)

The third research question was: *"What is the return period for the low flows and their corresponding duration on the Rhine at Lobith in the future situation including climate change?"*.

All 8 climate scenarios show higher discharges compared to the GRADE Reference scenario. The WH scenarios have the lowest discharges of the climate scenarios and the GL scenarios have the

highest discharges. Together, these two scenarios give a range of estimated discharges for the years 2050 and 2085. The 2085WH scenario gives the lower discharges than the 2050WH scenario, whilst the 2050GL and 2085GL scenario LFFCs are very similar to each other. The timing of the low flow events is different based on the climate scenario. For the *GL* scenarios, the simulated extremely low flow events occur mostly in March, similar to the GRADE Reference data. For the *WH* scenarios, the simulated extremely low flow events occur mostly in December.

According to the GRADE model we can be less scared of problems regarding shipping and salinisation in the future. These problems occur at a discharge of 1000 and 1200 m^3/s respectively. Currently, they occur once every 2.3 and 1.3 years for a duration of 1 day, once every 4.2 and 1.9 years for a duration of 30 days and once every 34.0 and 8.5 years for a duration of 180 days, respectively. In 2085 a 1000 m^3/s discharge will occur once every 1.5 to 2.6 years for a duration of 1 day, once every 2.2 to 5.6 years for a duration of 30 days and once every 42.3 to 221.2 years for a duration of 180 days. In 2085 a 1200 m^3/s discharge will occur once every 1.1 to 1.4 years for a duration of 1 day, once every 1.3 to 2.2 years for a duration of 30 days and once every 7.8 to 28.2 years for a duration of 180 days. So, whether the return period of shipping and salinisation problems will increase or decrease, depends on which climate scenario is closer to future reality.

Figure 3.22 gives the LFFCs for the climate scenarios 2050GL & WH and 2085GL & WH. The corresponding fitted GEV parameters are given in Appendix J.

5.4 Recommendations

The first recommendation is to look into the interdependence of low flows in a more elaborate way than the autocorrelograms from the Discussion. It is suggested to also look into autocorrelation on daily data instead of annual minima and see how long low flow events can be. This way it can be estimated how many low flow events per year can occur and it might help to find better motivations for the choices of threshold (u) and lag value (r) for the PUT method. During this study it is interesting to keep physical cycles like El Niño in mind to see if they show up in the data as well, as the El Niño Southern Oscillation was found to play a role in the Australian Millennium Drought [van Dijk et al., 2013].

The second recommendation is to find out why the GRADE model gives such low discharges for the Reference scenario and why the timing of the extremely low discharges differs from the Waterinfo data and literature. As mentioned in the Discussion, it is expected that the underestimation of the discharges is due to the calibration for high flows, the rough implementation of glaciers and snow and the fast discharge of water in the HBV model. Furthermore, attention should be given to the modelling of (deep) groundwater. When the Reference data set gives discharges that are more in line with the Waterinfo data and the climate scenarios of GRADE, the conclusions on the return periods for low flows will likely change a lot. In addition, the influence of the climate can be studied better, as it can then be compared to the Reference data set.

The third recommendation is to use the results of this study in risk assessments concerning the shipping industry. The year 2018 resulted in millions of euros of economical damage in the shipping sector in the Netherlands and this study showed that this can happen once every few decades. This can be taken into account when estimating prices for transport. The extra needed transport can be done over water, but also over land, which is more expensive but likely to be more reliable during low flow periods. Furthermore, Rijkswaterstaat can use the results of this study to make decisions on water allocation, keeping problems like salt intrusion, drinking water, agriculture and nature in mind and how often they will occur according to this study.

Bibliography

- M. Arnoux, P. Brunner, B. Schaeffli, R. Mott, F. Cochand, and D. Hunkeler. Low-flow behavior of alpine catchments with varying quaternary cover under current and future climatic conditions. *Journal of Hydrology*, 592(October 2020):125591, 2021. ISSN 00221694. doi:[10.1016/j.jhydrol.2020.125591](https://doi.org/10.1016/j.jhydrol.2020.125591).
- J. Beersma, H. Hakvoort, R. Jilderda, A. Overeem, and R. Versteeg. Neerslagstatistiek en reeksen voor het waterbeheer 2019. Technical report, STOWA, 2019.
- Beleidsstafel Droogte. Nederland beter weerbaar tegen droogte - Eindrapportage Beleidsstafel Droogte. Technical report, Ministerie van Infrastructuur en Waterstaat, 2019.
- A. Bomers. *Hydraulic modelling approaches to decrease uncertainty in flood frequency relations*. PhD thesis, University of Twente, 2020. URL <http://purl.org/utwente/doi/10.3990/1.9789036549288>.
- A. Bomers, R. M. Schielen, and S. J. Hulscher. Consequences of dike breaches and dike overflow in a bifurcating river system. *Natural Hazards*, 97(1):309–334, 2019. ISSN 15730840. doi:[10.1007/s11069-019-03643-y](https://doi.org/10.1007/s11069-019-03643-y).
- M. Booiij. *Dictaat Waterbeheer*. Enschede, 2015.
- C. Bosschieter. Klimaatverandering en binnenvaart: Effecten op de binnenvaart van meer extreem lage (en hoge) waterstanden op de Rijn. Technical report, Port Research Centre Rotterdam-Delft, Rotterdam, Delft, 2005.
- S. Coles. *An introduction to statistical modeling of extreme values*. Springer Series in Statistics. Springer London, London, 2001. ISBN 978-1-84996-874-4. doi:[10.1007/978-1-4471-3675-0](https://doi.org/10.1007/978-1-4471-3675-0). URL <http://link.springer.com/10.1007/978-1-4471-3675-0>.
- F. Davids, C. ten Velden, D. Eilander, and W. van Verseveld. Kalibratie en aanpassingen HBV model voor de Rijn voor laagwater. Technical report, Deltares, 2015.
- J. de Niel. *Variability of river flow extremes in Flanders : impact of atmospheric and catchment drivers*. PhD thesis, KU Leuven, 2018.
- M. de Wit. Hoe laag was het laagwater van 2003? (How low were the 2003 low flows?). *H2O*, 37: 15–17, 2004.
- M. Disse and H. Engel. Flood Events in the Rhine Basin : Genesis , Influences and Mitigation. *Natural Hazard*, 23:271–290, 2001.
- L. Gottschalk, K. x. Yu, E. Leblois, and L. Xiong. Statistics of low flow: Theoretical derivation of the distribution of minimum streamflow series. *Journal of Hydrology*, 481:204–219, 2013. ISSN 00221694. doi:[10.1016/j.jhydrol.2012.12.047](https://doi.org/10.1016/j.jhydrol.2012.12.047).
- M. Hegnauer, J. Beersma, H. Van den Boogaard, T. Buishand, and R. Passchier. Generator of Rainfall And Discharge Extremes (GRADE) for the Rhine and Meuse basins 2.0. Technical report, Deltares, 2014.
- Helpdesk Water. Leidraad rivieren. Technical report, 2007.
- Helpdesk Water. Grenswaarden kleurcodering Rivieren, 2021a. URL <https://www.helpdeskwater.nl/onderwerpen/waterveiligheid/crisismanagement/landelijke-plannen/samenvatting/grenswaarden-0/>.

- Helpdesk Water. Nationaal Water Model, 2021b. URL <https://www.helpdeskwater.nl/onderwerpen/applicaties-modellen/applicaties-per/watermanagement/watermanagement/nationaal-water-model/>.
- P. Hobson. Using different formulations of plotting positions, 2015. URL https://matplotlib.org/mpl-probscale/tutorial/closer_look_at_plot_pos.html.
- R. Hurkmans, W. Terink, R. Uijlenhoet, P. Torfs, D. Jacob, and P. A. Troch. Changes in streamflow dynamics in the Rhine basin under three high-resolution regional climate scenarios. *Journal of Climate*, 23(3):679–699, 2010. ISSN 08948755. doi:10.1175/2009JCLI3066.1.
- J. Janse and M. Burgdorffer. Waterakkoord Hollandsche IJssel en Lek. Technical report, Ministerie van Verkeer en Waterstaat, 2005.
- A. Kersbergen. *Skill of a discharge generator in simulating low flow characteristics in the Rhine basin*. PhD thesis, University of Twente, 2016.
- F. Klijn, M. Hegnauer, J. Beersma, and F. Sperna Welland. Wat betekenen de nieuwe klimaatscenario's voor de rivierafvoeren van Rijn en Maas? Technical Report september, 2015. URL http://publications.deltares.nl/1220042_004.pdf.
- KNMI. KNMI '14 Klimaatscenario's voor Nederland. Technical report, 2015. URL www.klimaatscenarios.nl.
- KNMI. Droogtemonitor. (Date accessed: 2 July 2021), 2021a. URL <https://www.knmi.nl/nederland-nu/klimatologie/droogtemonitor>.
- KNMI. Uitleg over: Droogte. (Date accessed: 12 March 2021), 2021b. URL <https://www.knmi.nl/kennis-en-datacentrum/uitleg/droogte>.
- N. Kramer, M. D. Mens, J. K. Beersma, and N. R. Kielen. Hoe extreem was de droogte van 2018 ? *H2O*, pages 1–7, 2019.
- B. Kuijper, R. Hurkmans, and C. Geerse. Pilot probabilistisch rekenen droogte 2. Technical report, HKV Lijn in Water, 2019.
- L. Lokin. Literature Report: Dune dynamics under high and low flows. Technical Report December, University of Twente, 2020. URL <https://research.utwente.nl/en/publications/dune-dynamics-under-high-and-low-flows-literature-report>.
- D. Maidment. *Handbook of Hydrology*. McGraw-Hill, inc., 1996.
- M. Mirghani, P. Willems, and J. Kabubi. QDF Relationships for low flow return period prediction. pages 1–8, 2005. ISBN 5639200200. doi:10.13140/2.1.1586.5921.
- J. Mondejar and P. Willems. Low Flow Duration Frequency Relationships of Low Flow Duration Frequency Relationships of Selected Catchments in the Blue Nile Basin. *JPAIR Multidisciplinary Research*, 23(1), 2016. doi:10.7719/jpair.v23i1.350.
- Rijkswaterstaat. Waterinfo. (Date accessed: 11 May 2021), 2021. URL <https://waterinfo.rws.nl#!/nav/themakaarten/>.
- E. M. Shaw, K. J. Beven, N. A. Chappell, and R. Lamb. *Hydrology in Practice*. Spon Press, London/New York, fourth edition, 2011. ISBN 978-0-415-37041-7.

- V. U. Smakhtin. Low flow hydrology: a review. *Journal of Hydrology*, 240:147–186, 2001. ISSN 00221694. doi:[https://doi.org/10.1016/S0022-1694\(00\)00340-1](https://doi.org/10.1016/S0022-1694(00)00340-1).
- F. Sperna Weiland, M. Hegnauer, L. Bouaziz, and J. Beersma. Implications of the KNMI'14 climate scenarios for the discharge of the Rhine and Meuse. Technical report, Deltares, 2015.
- E. Sprokkereef. Commission for the Hydrology of the Rhine Basin Annual Report 2018. Technical report, International Commission for the Hydrology of the Rhine Basin, 2019.
- H. Trul. Performance of GRADE in simulating flood wave characteristics in the Rhine basin. Technical report, University of Twente, 2016.
- R. van Beek. Wat is het risico op dijkdoorbraak bij droogte? (Date accessed: 2 July 2021), 2018. URL <https://www.uu.nl/nieuws/wat-is-het-risico-op-dijkdoorbraak-bij-droogte>.
- I. van de Velde, S. van der Kooij, K. van Hussen, and R. Läkamp. Economische schade door droogte in 2018. Technical report, Ecorys, 2019.
- R. van der Veen. Memo 1004290Rb-1: Bodemparameters in Qf-relatie. Technical report, Rura-Arnhem, 2010.
- A. I. J. M. van Dijk, H. E. Beck, R. S. Crosbie, R. A. M. de Jeu, Y. Y. Liu, G. M. Podger, B. Timbal, and N. R. Viney. The Millennium Drought in southeast Australia (2001 – 2009): Natural and human causes and implications for water resources , ecosystems , economy , and society. *Water Resources Research*, 49:1040–1057, 2013. doi:10.1002/wrcr.20123.
- J. Wijnbenga, D. van Haaren, and R. Versteeg. Beheer en onderhoud afvoerreeksen Rijntakken Deelonderzoek A: Operationaliseren Qf-relatie en IJssel. Technical report, HKV Lijn in Water, 2009.
- P. Willems. ECQ: Hydrological extreme value analysis tool, 2004.
- C. Ylla Arbós, A. Blom, E. Viparelli, M. Reneerkens, R. M. Frings, and R. M. Schielen. River Response to Anthropogenic Modification: Channel Steepening and Gravel Front Fading in an Incising River. *Geophysical Research Letters*, 48(4):1–10, 2021. ISSN 19448007. doi:10.1029/2020GL091338.
- M. Zethof. Risk-based control of salt water intrusion for the Rhine-Meuse Estuary. Technical report, TU Delft, 2011. URL <http://resolver.tudelft.nl/uuid:b704a5d0-e464-4410-83ba-d369c8a0cff9>.

Appendices



National Water Model

The 'National Water Model' (in Dutch: Nationaal Water Model, NWM) is used in the study of [Kramer et al. \[2019\]](#). Furthermore, Rijkswaterstaat and Deltares believe that the NWM performs better on low flows than the GRADE model. The NWM is a selection of existing water models coupled together [[Helpdesk Water, 2021b](#)] and the successor of the Deltamodel. This model gives insight in the effects of climate change and socio-economic developments for water management in the Netherlands. Basic prognoses are available for three topics: water safety, fresh water and water quality. Basic prognoses are available for the current situation (latest update fresh water: 2017, 2018 on demand), 2050 and 2085. The future scenarios are based on the Deltascenarios, which are based on KNMI'06 scenarios combined with scenarios for the development of the welfare and living environment. The fresh water model of the NWM, which focuses on water availability, consists of four models, which are used for calculations in the following order: 'National Hydrological Model' (in Dutch: Landelijk Hydrologisch Model, LHM), 'SOBEK-model Northern Delta Basin (in Dutch: SOBEK-model Noordelijk Delta Bekken, SOBEK-NDB), 'National SOBEK Model Light' (in Dutch: Landelijk SOBEK Model Light, LSM Light) and 'National Temperature Model' (in Dutch: Landelijk Temperatuur Model, LTM).

The NWM uses precipitation, evaporation and Meuse and Rhine discharges as input. The model can deal with drought in space and time, the correlation between precipitation deficit and low discharges, the buffer function and the (current) management of the water system. Results are values for the groundwater levels (LHM), water distribution (LHM, SOBEK-NDB and LSM Light), salt content (SOBEK-NDB) and temperature (LSM Light and LTM).

The NWM can simulate (extreme) discharges for different climate scenarios. These climate scenarios used in the NWM are the KNMI'14 climate scenarios. The KNMI'14 scenarios and their effect on low flows in the Rhine end Meuse are explained in [Section 1.1.3](#). The mean, minimum and maximum values for the NWM dataset for different climate scenarios is given in [Table A.1](#).

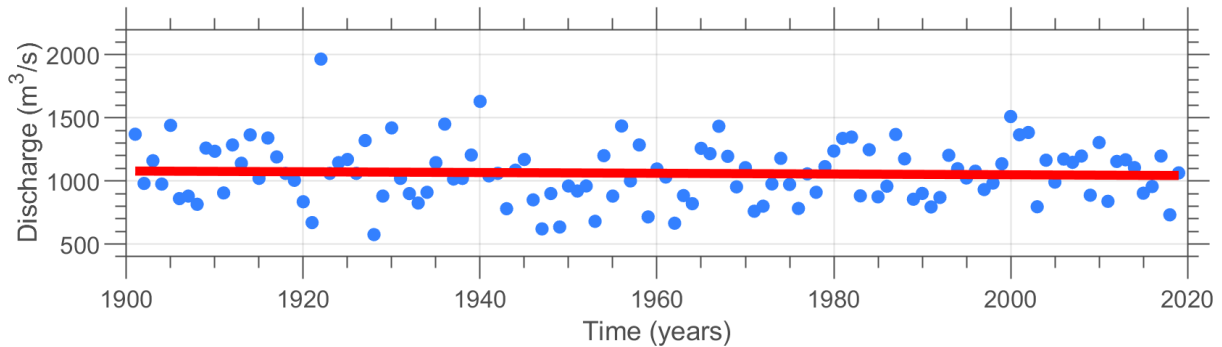
NWM	Mean (m^3/s)	Min (m^3/s)	Max (m^3/s)
Ref2015	2225.4	575.0	12,280.0
2050 GL	2506.0	643.7	15,080.2
2050 WH _{dry}	2135.3	504.0	13,937.4
2085 GL	2529.0	660.2	15,313.8
2085 WH _{dry}	2170.0	400.0	15,969.8

Table A.1: Mean, minimum and maximum of the original 100 yrs NWM dataset including climate change.

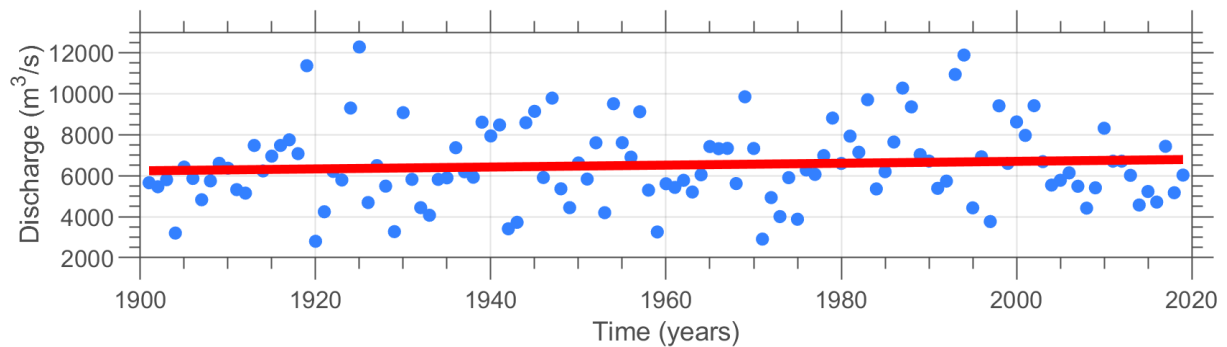
B

Extremes are becoming more extreme

Section 2.1.1 concluded a small trend is visible in the daily discharge data. However, in the maxima and minima trends are more present. This is shown in Figure B.1. For the minima the value of the trend is $1078 \text{ m}^3/\text{s}$ in 1901 and in 2020 the value of the trend is $1043 \text{ m}^3/\text{s}$. This is a decrease of $25 \text{ m}^3/\text{s}$, which is bigger than the increase in the total data set. For the maxima the value of the trend is $6242 \text{ m}^3/\text{s}$ in 1901 and in 2020 the value of the trend is $6787 \text{ m}^3/\text{s}$. This is an increase of $545 \text{ m}^3/\text{s}$, which is much larger than the increase in the total data set. In literature it is also found that extremes become more extreme [de Niel, 2018, Klijn et al., 2015]. These trends are not removed from the data, resulting in the fact that the original data transformed into daily values are used in this study to represent the current climate.



(a) Trend in annual minimum discharges.

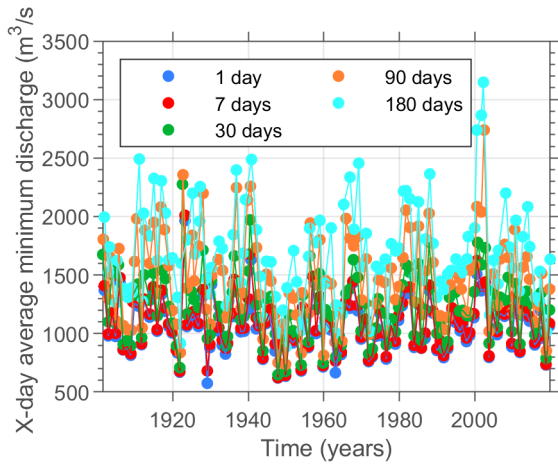


(b) Trend in annual maximum discharges.

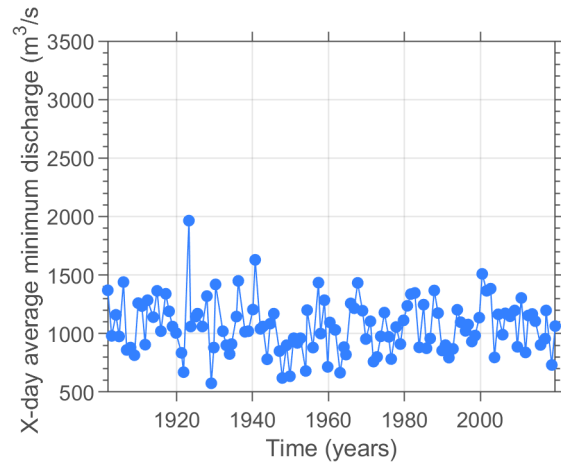
Figure B.1: Extreme discharges are becoming more extreme.



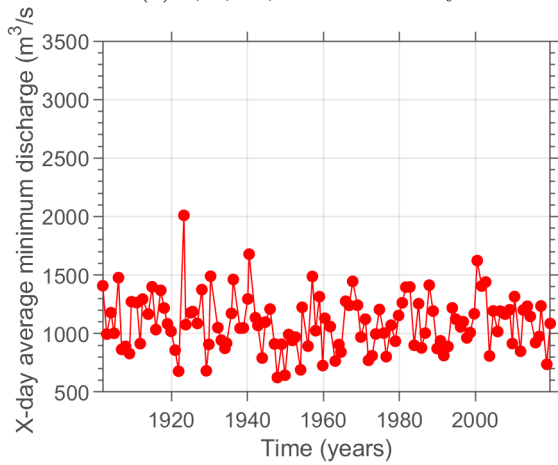
Waterinfo BM - annual minima



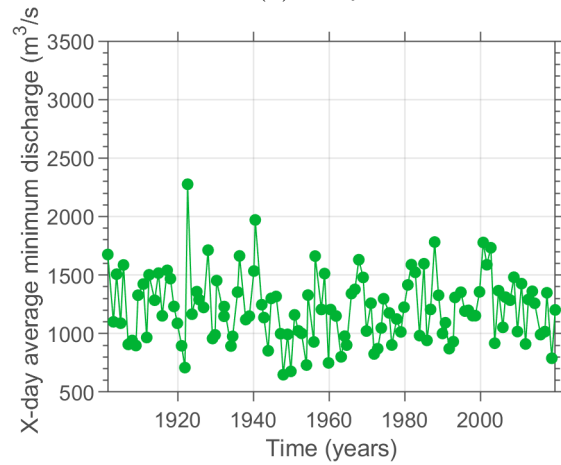
(a) 1, 7, 30, 90 and 180 days



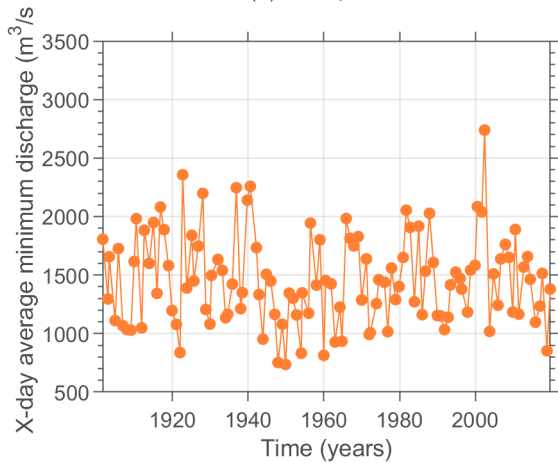
(b) 1 day



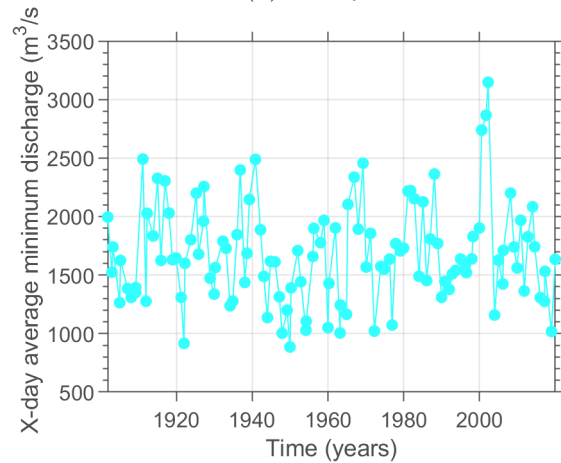
(c) 7 days



(d) 30 days



(e) 90 days



(f) 180 days

Figure C.1: Annual minimum average discharge for different durations using block method.

D

Waterinfo BM - histograms

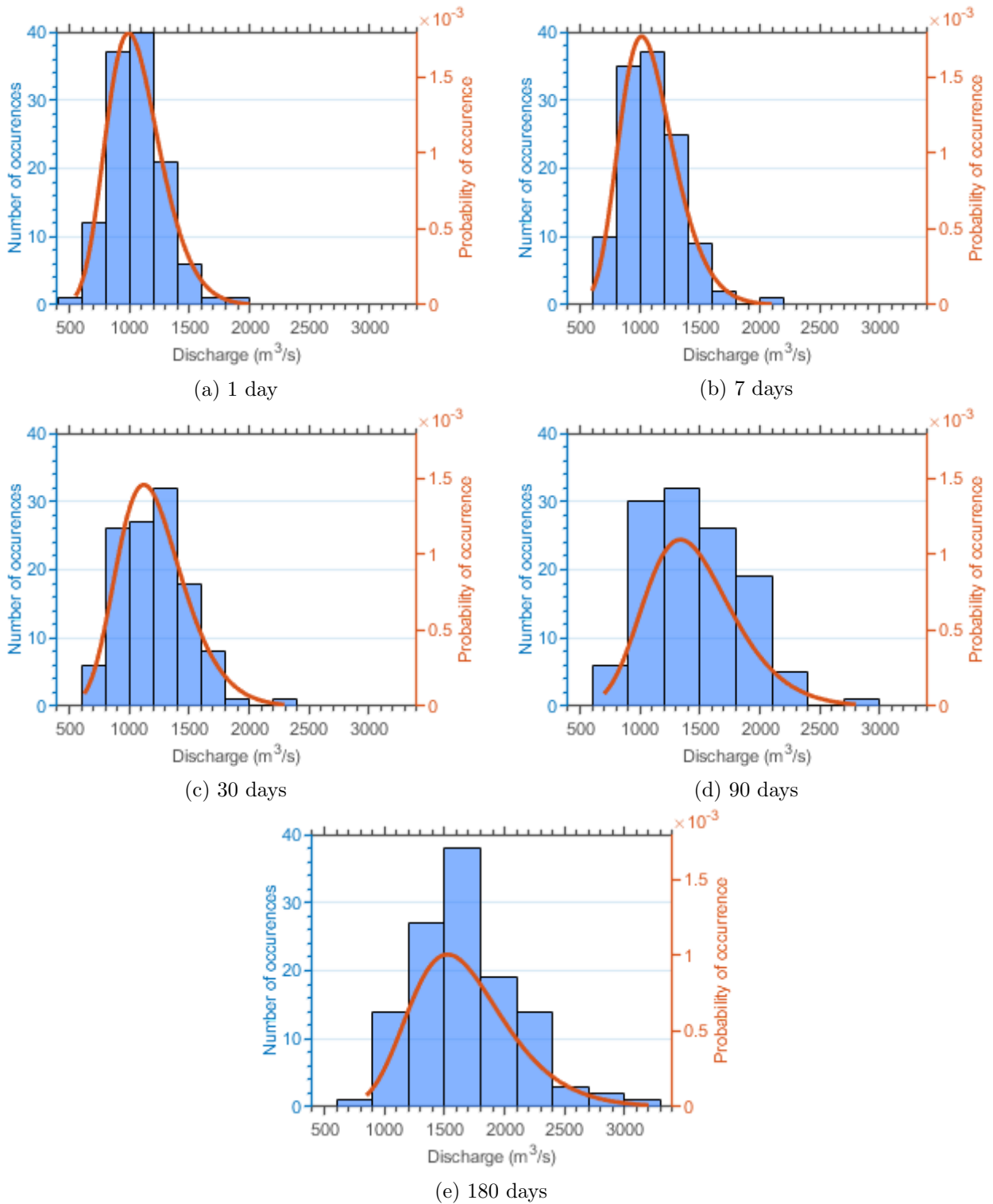
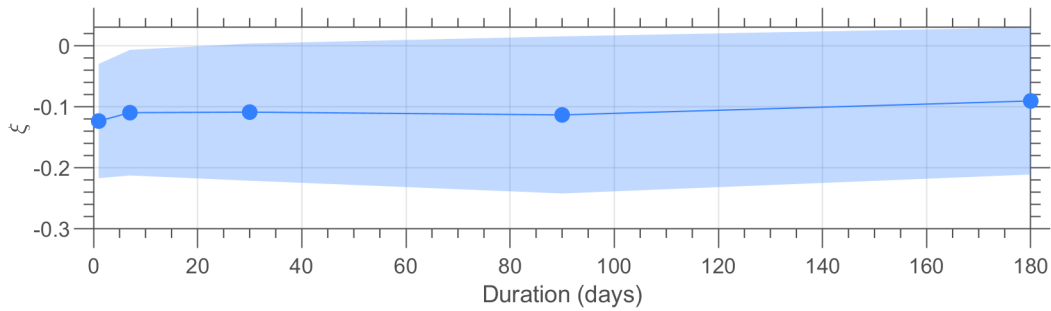


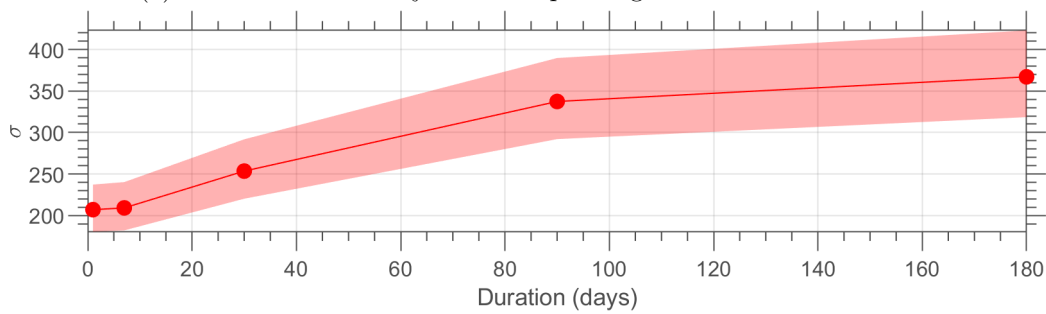
Figure D.1: Histogram and fitted probability density function of minimum annual discharges for different durations.



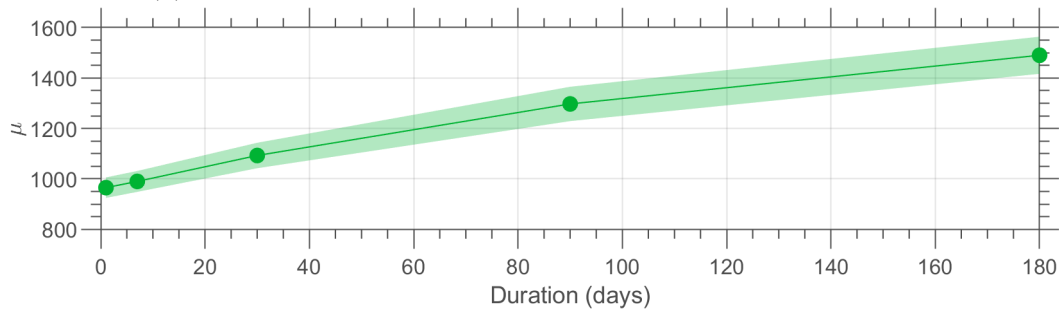
Waterinfo BM - parameter values



(a) Estimated value of ξ and corresponding 95% confidence interval.



(b) Estimated value of σ and corresponding 95% confidence interval.

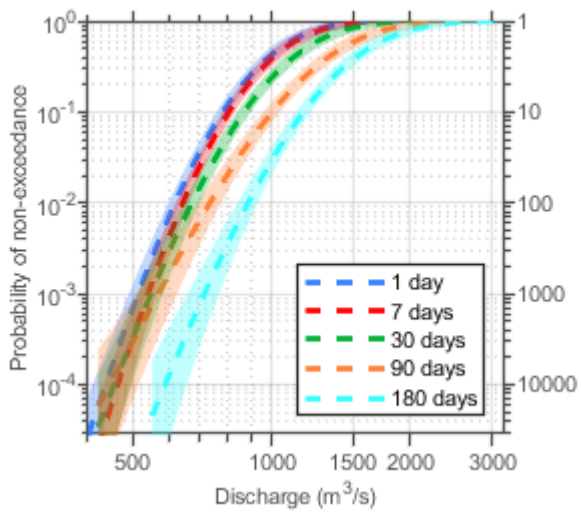


(c) Estimated value of μ and corresponding 95% confidence interval.

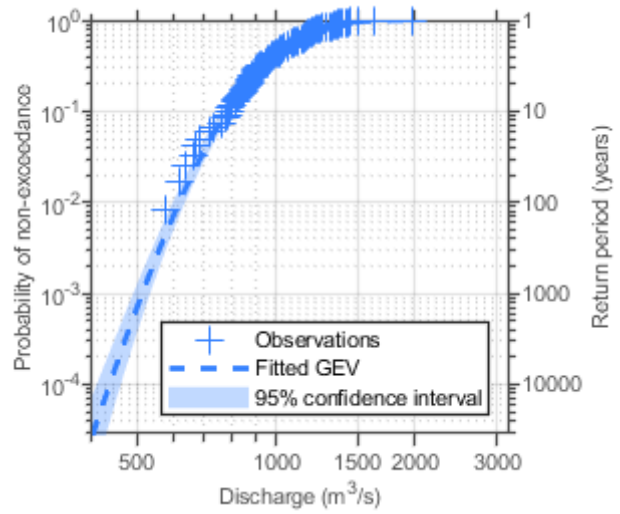
Figure E.1: Estimations of GEV parameters for all 5 durations and their corresponding 95% confidence interval.

F

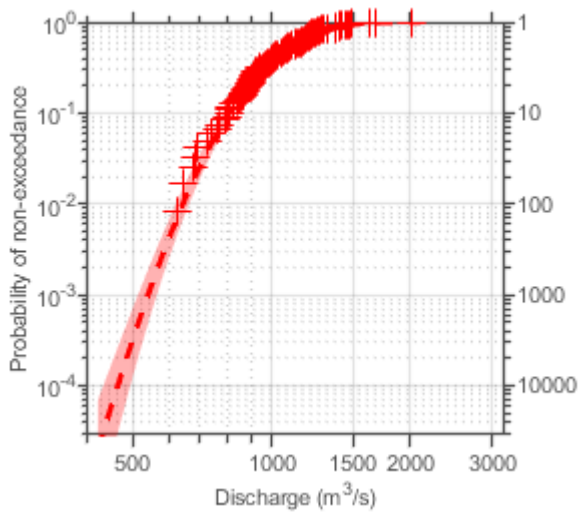
Waterinfo BM - extrapolated fit



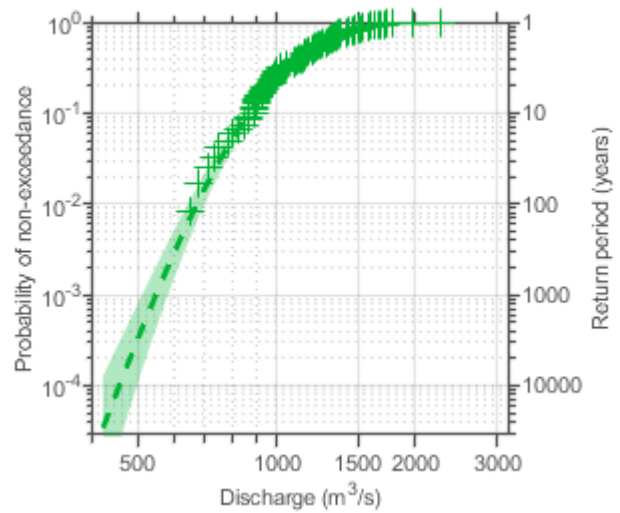
(a) 1, 7, 30, 90 and 180 days



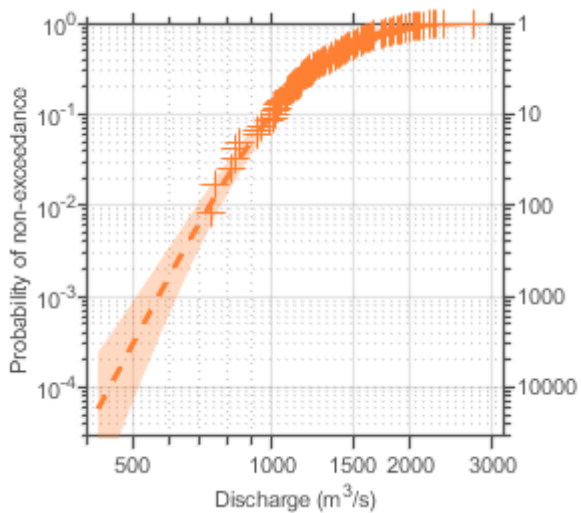
(b) 1 day



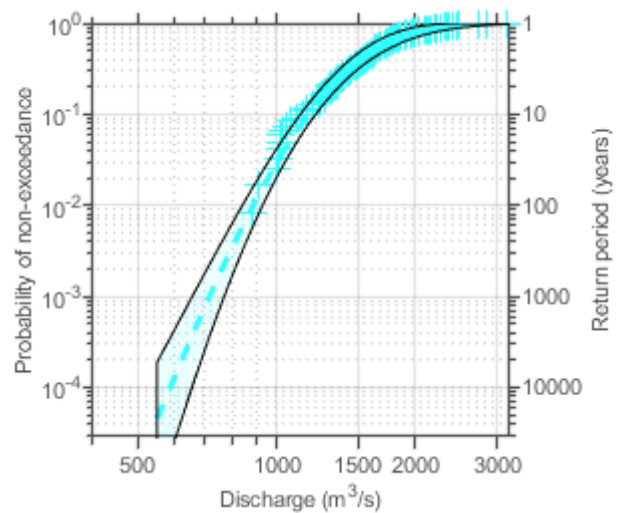
(c) 7 days



(d) 30 days



(e) 90 days



(f) 180 days

Figure F.1: Extrapolation of minimum annual discharges for different durations with corresponding observations and 95% confidence intervals.



Waterinfo PUT - annual minima

Figure G.1 shows the lowest discharges for separate events below a threshold of $1500 \text{ m}^3/\text{s}$ for different values of lag. Circled in black are examples of spots where an extra event will appear or disappear with respect to other lags. In Figure G.1b a black circle is shown, in which no event can be seen. In the same location in Figure G.1c an event of 180 days can be seen. This means that multiple events are combined into one event, which was earlier separated by a maximum of 4 days with discharges above the threshold of $1500 \text{ m}^3/\text{s}$.

The two connecting circles in Figure G.1c show a 1 day event in the upper circle and no event in the lower circle. In Figure G.1d the 1 day event has disappeared and a 90 day event has appeared. The 1 day event is connected into a longer event, of which only 1 minimum value will be selected and the joined series already contained a lower value. This results in the disappearance of an event. The 90 day event appears for the same reason as the already circled and explained 180 day event.

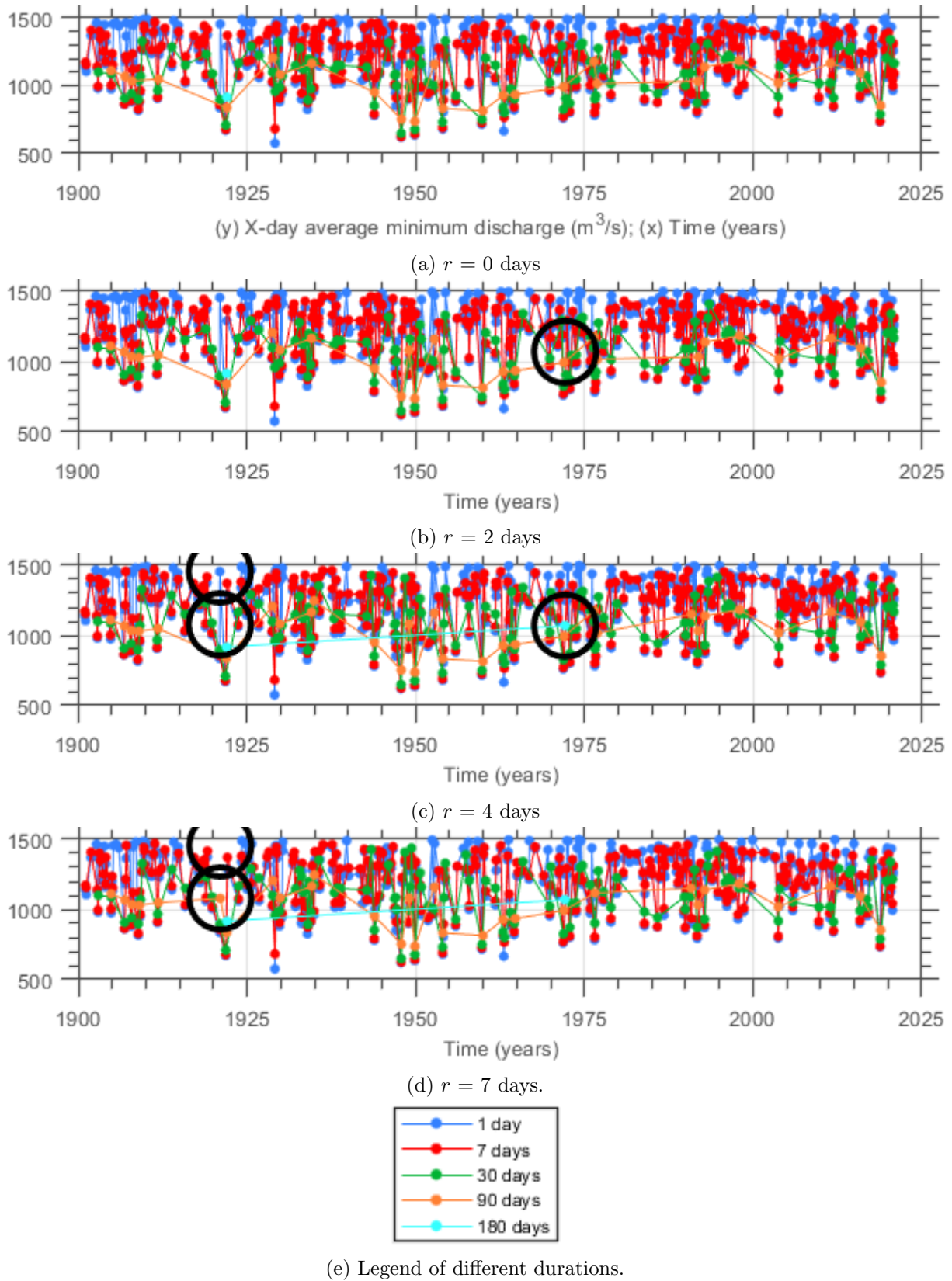


Figure G.1: Annual minimum average discharge for different durations using PUT method for $u = 1500 m^3/s$ for different r . The black circles are mentioned in the text and function as examples.

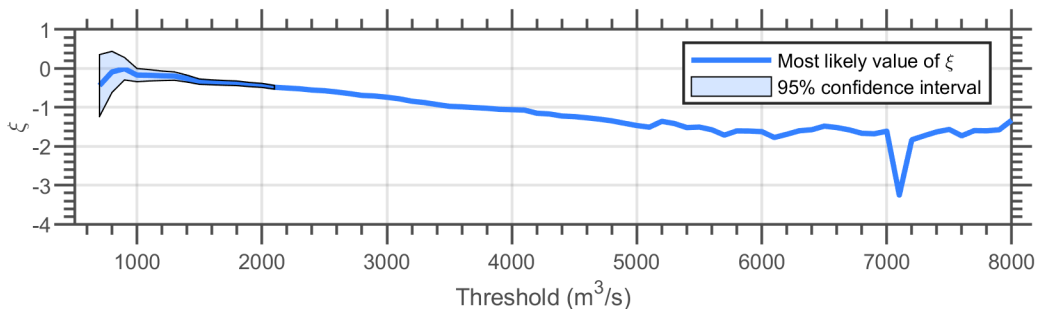
H

Waterinfo PUT - parameter values

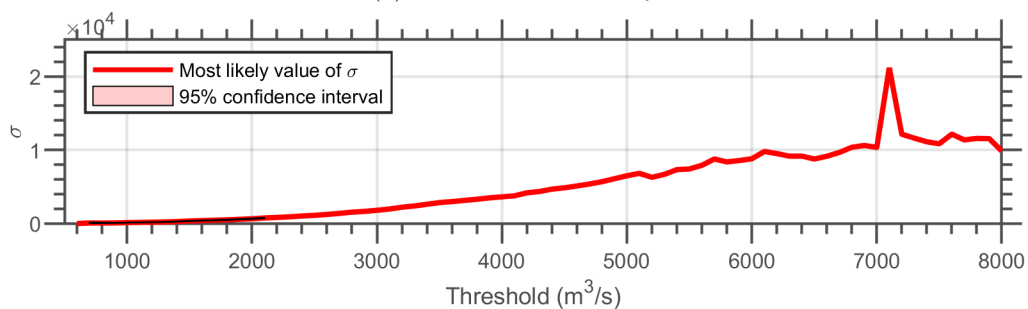
This Appendix shows the estimated ξ and σ value for the GP distribution for different durations and different thresholds. Linearity is visible for a range of threshold values with a duration of 1 or 7 days. This becomes less clear for the 30 day duration and is hardly visible for the 90 and 180 day duration. Besides the low amount of events mentioned in the last section, this is a sign the PUT method might not be suitable for the higher duration data.

The 1 and 7 day durations, Figure H.1 and H.2 are the only 2 figures with a 95% confidence interval. Even there, the confidence interval is not found for every threshold value. This has to do with the value of ξ . If the value of ξ is smaller than -0.5, the maximum likelihood estimators do not have standard asymptotic properties and become unlikely to be obtained [Coles, 2001]. This behaviour is the reason no 95% confidence interval is found by the software MatLab. The parameter values for a duration of 30, 90 and 180 days are given in Figure H.3 to H.5, but without any confidence interval.

As the PUT method did not result in a better fit than the block method, no further focus was put into finding out if another method would allow for a 95% interval with values of ξ below -0.5.

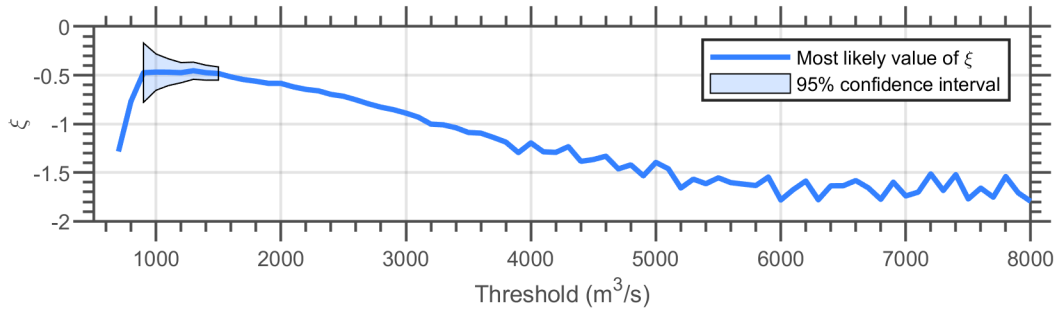


(a) Estimated value of ξ

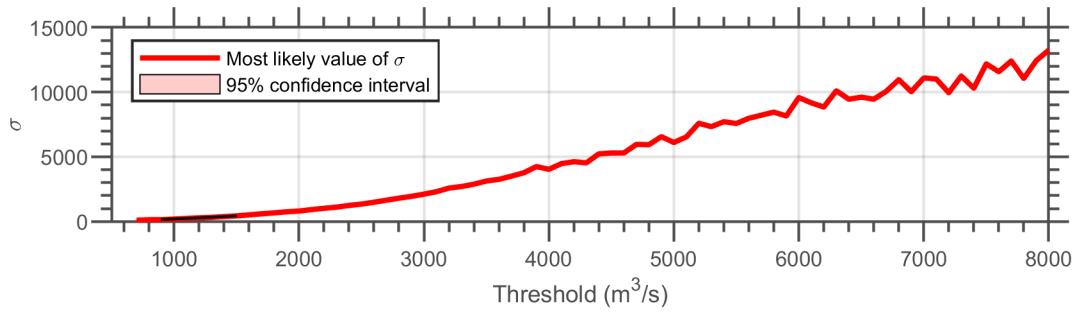


(b) Estimated value of σ

Figure H.1: Estimated value of GP parameters for a duration of 1 day.

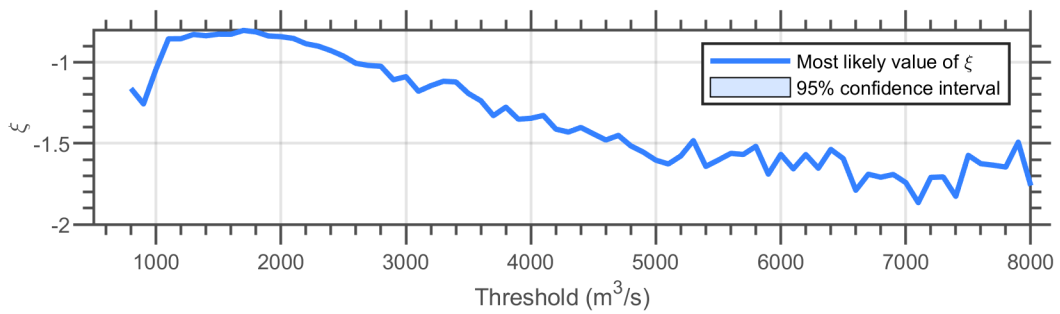


(a) Estimated value of ξ

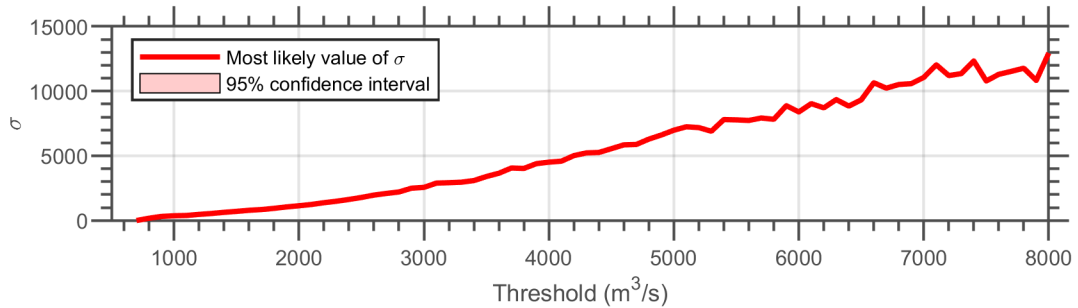


(b) Estimated value of σ

Figure H.2: Estimated value of GP parameters for a duration of 7 days.

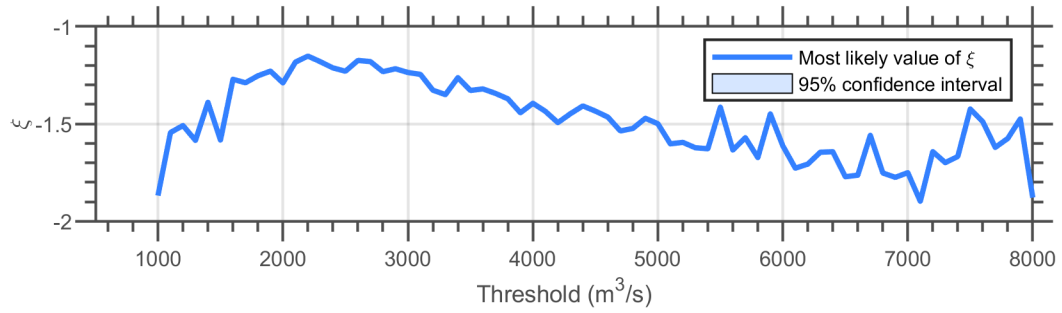


(a) Estimated value of ξ

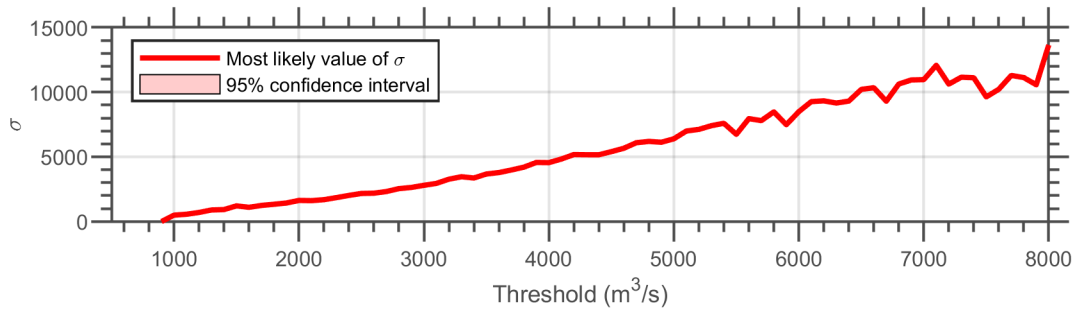


(b) Estimated value of σ

Figure H.3: Estimated value of GP parameters for a duration of 30 days.

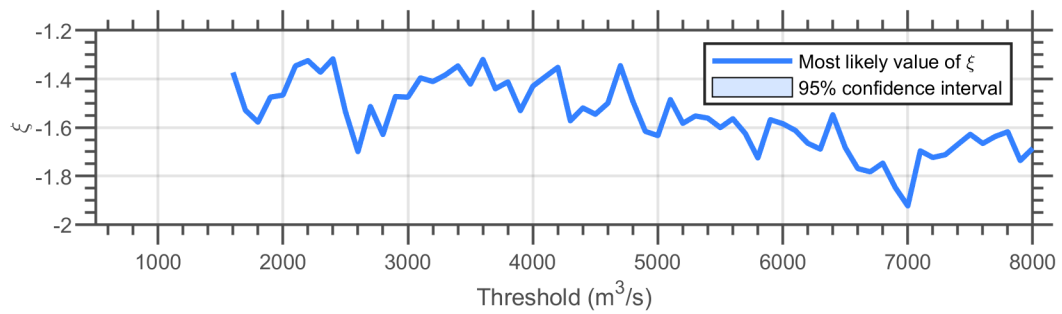


(a) Estimated value of ξ

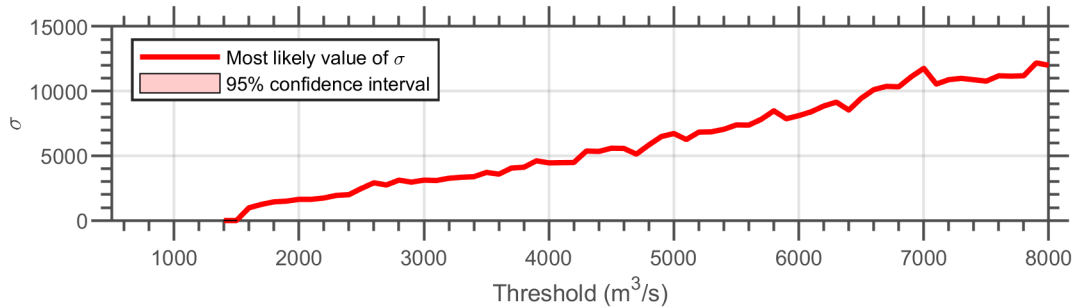


(b) Estimated value of σ

Figure H.4: Estimated value of GP parameters for a duration of 90 days.



(a) Estimated value of ξ



(b) Estimated value of σ

Figure H.5: Estimated value of GP parameters for a duration of 180 days.



Waterinfo PUT - observations and fit for all durations

The asymptotes for all durations are 483, 600, 648, 736 and 885 m^3/s for 1, 7, 30, 90 and 180 days respectively. This makes extrapolation to larger return periods not possible.

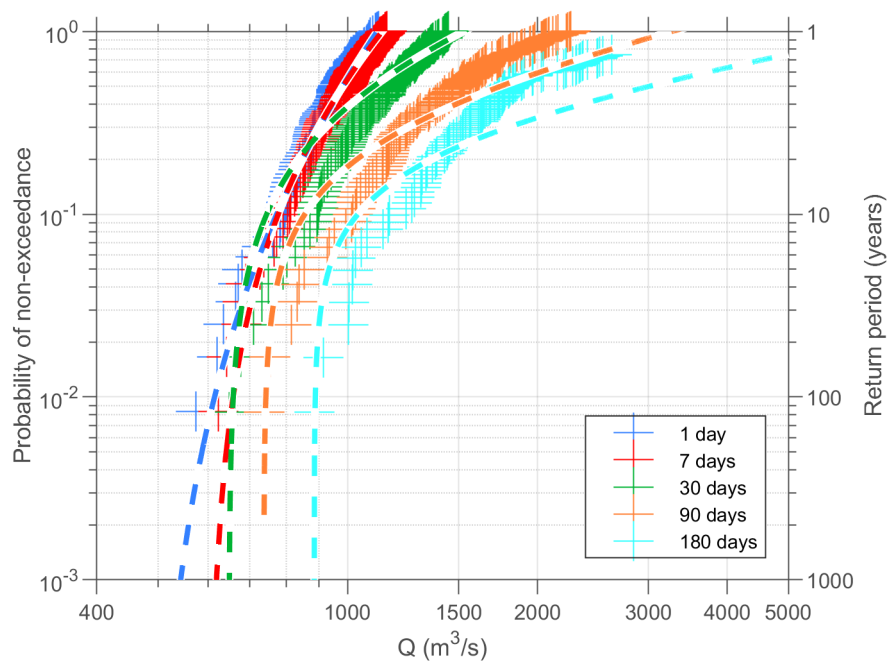


Figure I.1: Observed minimum discharges below a threshold for different durations and their estimated fit using the PUT method.

J

Fitted parameter values for all scenarios

Dataset		1 day	7 days	30 days	90 days	180 days
Waterinfo BM (GEV)	ξ	-0.12	-0.11	-0.11	-0.11	-0.09
	σ	207.0	209.2	253.5	337.3	367.0
	μ	965.1	989.8	1092.6	1297.0	1489.9
Waterinfo PUT (GP)	ξ	-0.34	-0.48			
	σ	345.4	434.5			
	u	1500	1500			
GRADE Reference	ξ	-0.14	-0.13	-0.12	-0.13	-0.15
	σ	192.6	199.1	232.8	285.1	309.6
	μ	820.1	838.5	939.0	1143.3	1342.4
2050 GL (2085 GL)	ξ	-0.15 (-0.15)	-0.15 (-0.15)	-0.14 (-0.14)	-0.15 (-0.14)	-0.15 (-0.15)
	σ	209.3 (209.1)	217.6 (217.1)	257.5 (256.6)	307.3 (307.6)	329.9 (334.4)
	μ	996.1 (991.6)	1021.2 (1016.0)	1153.4 (1145.4)	1402.3 (1391.7)	1636.0 (1642.3)
2050 GH (2085 GH)	ξ	-0.14 (-0.13)	-0.14 (-0.14)	-0.14 (-0.13)	-0.14 (-0.13)	-0.15 (-0.15)
	σ	193.8 (187.8)	201.2 (194.8)	237.5 (229.0)	285.4 (274.8)	311.8 (303.6)
	μ	947.6 (911.3)	969.9 (932.5)	1088.4 (1042.6)	1315.2 (1254.0)	1552.1 (1494.4)
2050 WL (2085 WL)	ξ	-0.14 (-0.13)	-0.14 (-0.13)	-0.14 (-0.12)	-0.14 (-0.13)	-0.14 (-0.15)
	σ	198.5 (184.4)	206.0 (190.9)	243.0 (223.6)	292.4 (267.1)	322.6 (309.7)
	μ	936.7 (905.8)	959.1 (925.4)	1077.4 (1030.9)	1304.9 (1238.8)	1549.3 (1536.1)
2050 WH (2085 WH)	ξ	-0.11 (-0.08)	-0.13 (-0.10)	-0.12 (-0.11)	-0.12 (-0.11)	-0.14 (-0.13)
	σ	182.9 (169.2)	190.2 (175.8)	223.5 (205.6)	267.9 (246.1)	298.9 (290.2)
	μ	884.1 (840.9)	905.0 (860.2)	1009.1 (954.7)	1211.6 (1137.9)	1464.7 (1419.3)

Table J.1: Values of fitted parameters for the Waterinfo data, both block method and PUT method, and the GRADE data, only block method, consisting of the reference data and the climate scenarios for 2050 and 2085.



Top 5's of the lowest flows for all scenarios

Data set	#1	#2	#3	#4	#5
Waterinfo					
1 day	575 (Feb 1929)	620 (Nov 1947)	635 (Nov 1949)	665 (Jan 1963)	670 (Nov 1921)
7 days	624 (Nov 1947)	644 (Nov 1949)	678 (Nov 1921)	681 (Feb 1929)	690 (Dec 1953)
30 days	648 (Nov 1947)	677 (Nov 1949)	709 (Nov 1921)	731 (Dec 1953)	749 (Nov 1959)
90 days	736 (Nov 1949)	752 (Nov 1947)	814 (Dec 1959)	832 (Jan 1954)	837 (Dec 1921)
180 days	885 (Dec 1949)	916 (Jan 1922)	1003 (Nov 1947)	1005 (Mar 1963)	1017 (Dec 2018)
GRADE					
1 day	254 (Apr 1*)	263 (Jul 3*)	273 (Mar 1*)	278 (May 4*)	288 (Mar 5*)
7 days	258 (Apr 1*)	268 (Jul 3*)	280 (May 4*)	283 (Mar 1*)	292 (Mar 5*)
30 days	276 (Apr 1*)	282 (Jul 3*)	311 (May 4*)	316 (Jan 2*)	316 (Dec 6*)
90 days	331 (Aug 3*)	353 (Feb 2*)	361 (May 1*)	364 (Apr 5*)	369 (Dec 6*)
180 days	390 (Jun 5*)	394 (Oct 3*)	436 (May 1*)	457 (Jan 6*)	462 (Jun 4*)
2050 GL					
1 day	346 (Mar 10*)	381 (Mar 16*)	393 (Feb 15*)	398 (Feb 7*)	408 (Jan 11*)
7 days	352 (Mar 10*)	384 (Mar 16*)	402 (Feb 15*)	403 (Feb 7*)	418 (Mar 17*)
30 days	366 (Mar 10*)	399 (Apr 10*)	416 (Mar 16*)	438 (Apr 16*)	439 (Feb 7*)
90 days	419 (Mar 10*)	420 (Apr 10*)	475 (Mar 16*)	523 (Apr 16*)	534 (Mar 15*)
180 days	547 (Apr 10*)	572 (Apr 16*)	629 (Mar 10*)	631 (Mar 16*)	642 (Apr 15*)
2050 WH					
1 day	341 (Feb 10*)	378 (Dec 14*)	383 (Jan 11*)	386 (Dec 9*)	390 (Dec 8*)
7 days	348 (Feb 10*)	386 (Dec 14*)	390 (Jan 11*)	394 (Dec 9*)	397 (Dec 8*)
30 days	364 (Mar 10*)	397 (Apr 10*)	417 (Jan 11*)	417 (Dec 14*)	423 (Dec 9*)
90 days	403 (Mar 10*)	405 (Apr 10*)	471 (Mar 16*)	474 (Apr 16*)	490 (Dec 8*)
180 days	506 (Apr 10*)	540 (Apr 16*)	552 (Mar 10*)	568 (Mar 16*)	606 (Mar 15*)
2085 GL					
1 day	352 (Mar 10*)	396 (Mar 16*)	400 (Feb 15*)	401 (Feb 7*)	402 (Jan 11*)
7 days	358 (Mar 10*)	400 (Mar 16*)	406 (Feb 7*)	410 (Feb 15*)	413 (Jan 11*)
30 days	366 (Mar 10*)	388 (Apr 10*)	427 (Mar 16*)	439 (Feb 7*)	444 (Mar 16*)
90 days	409 (Apr 10*)	414 (Mar 10*)	484 (Mar 16*)	486 (Apr 16*)	529 (Jan 14*+1)
180 days	529 (Apr 10*)	578 (Apr 16*)	609 (Mar 10*)	628 (Mar 16*)	638 (Apr 15*)
2085 WH					
1 day	354 (Feb 10*)	367 (Nov 12*)	368 (Dec 14*)	378 (Dec 8*)	384 (Dec 9*)
7 days	362 (Feb 10*)	374 (Nov 12*)	376 (Dec 14*)	384 (Dec 8*)	390 (Oct 13*)
30 days	378 (Mar 10*)	397 (Dec 14*)	414 (Apr 10*)	415 (Nov 12*)	417 (Dec 9*)
90 days	418 (Mar 10*)	421 (Apr 10*)	474 (Dec 8*)	484 (Dec 14*)	492 (Nov 13*)
180 days	516 (Apr 10*)	549 (Mar 10*)	585 (Apr 16*)	592 (Mar 16*)	592 (Jan 11*)

Table K.1: Top 5 lowest discharges (m^3/s) using the GRADE 2050GL, 2050WH, 2085GL and 2085WH data. Note that the numbers 1* until 17* represent different years, as the years from the simulation are not relevant.